Characterization of milk protein concentrate powders using powder rheometer and front-face fluorescence spectroscopy

by

Karthik Sajith Babu

B.Tech., Indian Institute of Food Processing Technology, 2015

A THESIS

submitted in partial fulfillment of the requirements for the degree

MASTER OF SCIENCE

Food Science

KANSAS STATE UNIVERSITY
Manhattan, Kansas

2018

Approved by:

Major Professor
Jayendra K. Amamcharla

Copyright

Abstract

Milk protein concentrate (MPC) powders are high-protein dairy ingredients obtained from membrane filtration processes and subsequent spray drying. MPC powders have extensive applications due to their nutritional, functional, and sensory properties. However, their flow properties, rehydration behavior, and morphological characteristics are affected by various factors such as processing, storage, particle size, and composition of the powder. Literature has shown that knowledge about the powder flowability characteristics is critical in their handling, processing, and subsequent storage. For this study, FT4 powder rheometer (FT4, Freeman Technologies, UK) was used to characterize the flowability of MPC powders during storage. This study investigated the flowability and morphological characteristics of commercial MPC powders with three different protein contents (70, 80, and 90%, w/w) after storage at 25ºC and 40ºC for 12 weeks. Powder flow properties (basic flowability energy (BFE), flow rate index (FRI), permeability, etc.) and shear properties (cohesion, flow function, etc.) were evaluated. After 12 weeks of storage at 40ºC, the BFE and FRI values significantly increased ($P < 0.05$) as the protein content increased from 70 to 90% (w/w). Dynamic flow tests indicated that MPC powders with high protein contents displayed higher permeability. Shear tests confirmed that samples stored at 40ºC were relatively less flowable than samples stored at 25ºC. Also, the lower protein content samples showed better shear flow behavior. The results indicated that MPC powders stored at 40ºC had more cohesiveness and poor flow characteristics than MPC powders stored at 25ºC. The circle equivalent diameter, circularity, and elongation of MPC powders increased as protein content and storage temperature increased, while the convexity decreased as protein content and storage temperature increased. Overall, the MPC powders evidently showed different flow properties and morphological characteristics due to their difference in composition

and storage temperature. Literature has shown various methods for determining the solubility of dairy powders, but it requires expensive instruments and skilled technicians. The front-face fluorescence spectroscopy (FFFS) coupled with chemometrics could be used as an efficient alternative, which is commonly used as fingerprints of the various food products. To evaluate FFFS as a useful tool for the non-destructive measurement of solubility in the MPC powders, commercially procured MPC powders were stored at two temperatures (25 and 40ºC) for 1, 2, 4, 8, and 12 weeks to produce powders with different rehydration properties, which subsequently influenced their fluorescence spectra. The spectra of tryptophan and Maillard products were recorded and analyzed with principal components analysis. The solubility index and the relative dissolution index (RDI) obtained from focused beam reflectance measurement was used to predict solubility and dissolution changes using fluorescence spectra of tryptophan and Maillard products. The solubility index and RDI showed that the MPC powders had decreased solubility as the storage time and temperature increased. The results suggest that FFFS has the potential to provide rapid, nondestructive, and accurate measurements of rehydration behavior in MPC powders. Overall, the results indicated that solubility and dissolution behavior of MPC powders were related to protein content and storage conditions that could be measured using FFFS.

Table of Contents

List of Figures viii
List of Tables xi
Acknowledgments xii
Chapter 1 - Introduction 1
References 2
Chapter 2 - Literature Review 4
Overview of milk protein concentrate powders 4
Flowability of dairy powders 7
Factors influencing powder flowability 9
Solubility of high-protein dairy powders 12
Overview of fluorescence spectroscopy 16
Basic principles of fluorescence spectroscopy 17
Fluorescence spectrometer 18
Fluorophore 19
Applications of fluorescence spectroscopy in dairy products 20
Processing-induced changes 20
Spectral data analysis 25
Descriptive techniques 26
Principal component analysis. 26
Predictive techniques 26
Coupling chemometrics with fluorescence spectroscopy 27
References 30
Chapter 3 - Research Objectives 37
Chapter 4 - Influence of protein content and storage temperature on the particle morphology and flowability characteristics of milk protein concentrate powders 38
Abstract 38
Introduction 39
Materials and methods 41
Experimental design 41

Microstructure 41
Morphological analysis 42
Flow properties 42
Basic flowability energy (BFE) 43
Stability index (SI) 43
Flow rate index (FRI) 43
Specific energy (SE) 43
Compressibility 44
Permeability 44
Wall friction test 44
Shear properties 45
Evaluation of solubility and dissolution behavior 45
Statistical analysis 46
Results and discussion 46
Microstructure 47
Morphology 48
Basic flow energy (BFE) 49
Stability index (SI), flow rate index (FRI), and specific energy (SE) 50
Compressibility 54
Permeability 55
Wall friction 56
Shear properties 58
Solubility index and dissolution behavior after storage 62
Acknowledgments 64
Conclusions 64
References 65
Chapter 5 - Application of front-face fluorescence spectroscopy as a tool for monitoring changes in milk protein concentrate powders during storage 69
Abstract 69
Introduction 70
Materials and methods 72

Milk protein concentrate powder samples 72
Color 73
Solubility index 73
Relative dissolution index (RDI) 73
FFFS 74
Spectral data analysis 75
Model development and performance evaluation 75
Results and discussion 76
Color 76
Solubility index 77
Relative dissolution index (RDI) 77
Front-face fluorescence spectra 83
Tryptophan emission spectra 83
Maillard emission spectra 84
Maillard exitation spectra 85
Multivariate analysis of MPC powders fluorescence spectra 88
Prediction of solubility index using PLSR 93
Prediction of relative dissolution index using PLSR 94
Acknowledgments 97
Conclusion 97
References 97
Chapter 6 - Conclusions 102
Appendix A – FT4 powder rheometer 104
Appendix B - SAS code for chapter 4 105

List of Figures

Figure 2.1. Process for manufacturing of milk protein concentrate (MPC) powders..... 5
Figure 2.2 Flow functions of dairy powders: high cohesive vs. less cohesive (adapted from Fitzpatrick et al., 2004a). 8
Figure 2.3 Schematic diagram of dissolution timeline for different types of food powder showing the overlaps between different phases with time (adapted from Fang et al., 2007)..... 12
Figure 2.4 Schematic illustration of rehydration mechanism for an agglomerated high-protein dairy powder (adapted from Crowley et al., 2016). 15
Figure 2.5 Jablonski diagram showing the fundamental principle in fluorescence spectroscopy (adapted from Karoui and Dufour, 2008). 18
Figure 2.6 The basic setup of a fluorescence spectrometer (adapted from Karoui, Mazerolles, and Dufour, 2003). 19
Figure 4.1 Scanning electron micrographs (× 500) of spray dried milk protein concentrate powder (MPC) particles: A) MPC70; B) MPC80; C) MPC90; and D) MPC90 (× 5000) after 12 weeks of storage at 40ºC. 48
Figure 4.2 Compressibility of the milk protein concentrate (MPC)70 (triangle), MPC80 (circle), and MPC90 (square) after 12 weeks of storage at 25ºC (solid) and 40ºC (open) after 12 weeks of storage. Values are the means of data from duplicate analysis. 55
Figure 4.3 Effect of applied normal stress on pressure drop across the milk protein concentrate (MPC) powders: MPC70 (triangle), MPC80 (circle), and MPC90 (square) after 12 weeks of storage at 25ºC (solid) and 40ºC (open). Values are the means of data from duplicate analysis. 56
Figure 4.4 Wall friction angle of the milk protein concentrate (MPC) powders after 12 weeks of storage at 25ºC (solid) and 40ºC (open) after 12 weeks of storage. Values are the means of data from duplicate analysis. Error bars indicate SD. 57
Figure 4.5 Changes in counts of fine particles (<10 μm) after 12 weeks of storage as obtained from focused beam reflectance measurement for the milk protein concentrate (MPC) powders: (a) MPC70, (b) MPC80, (c) MPC90 stored at 25ºC; (d) MPC70, (e) MPC80, (f) MPC90 stored at 40ºC..... 64

Figure 5.1 Solubility index (%) of selected (obtained from manufacturer M_1) milk protein concentrate (MPC) powders before and during storage at different temperatures (A) 25ºC (RT) and (B) 40ºC (HT) for control (C), 1, 2, 4, 8, and 12 weeks. The numbers in the legend represent the storage time in week. 80
Figure 5.2 Relative dissolution index (%) of selected (obtained from manufacturer M_1) milk protein concentrate (MPC) powders before and during storage at different temperatures (A) 25ºC (RT) and (B) 40ºC (HT) for control (C), 1, 2, 4, 8, and 12 weeks. The numbers in the legend represent the storage time in week. 81
Figure 5.3 Changes in fine (<10 μm) counts obtained from data collected with the focused beam reflectance measurement for milk protein concentrate (MPC) powders (obtained from manufacturer M_2): (A) MPC70; (B) MPC90 stored at 40ºC (HT) for control (C), 1, 2, 4, 8, and 12 weeks. The numbers in the legend represent the storage time in week. 82
Figure 5.4 Tryptophan emission spectra of (1) MPC70 and (2) MPC90 samples (same manufacturer) before storage and after storage at (A) 25ºC (RT) and (B) 40ºC (HT) of control (C), 1, 2, 4, 8, and 12 weeks. The numbers in the legend represent the storage time of the sample in weeks. 86
Figure 5.5 Maillard emission spectra of (1) MPC70 and (2) MPC90 samples (same manufacturer) before storage and after storage at (A) 25ºC (RT) and (B) 40ºC (HT) of control (C), 1, 2, 4, 8, and 12 weeks. The numbers in the legend represent the storage time of the sample in weeks. 87
Figure 5.6 Maillard excitation spectra of (1) MPC70 and (2) MPC90 samples (same manufacturer) before storage and after storage at (A) 25ºC (RT) and (B) 40ºC (HT) of control (C), 1, 2, 4, 8, and 12 weeks. The numbers in the legend represent the storage time of the sample in weeks. 88
Figure 5.7 Factor loadings of the first two principal components (A) and similarity map (B) of principal component analysis (PCA) made on tryptophan emission spectra of the MPC samples after storage. The solid line in (A) indicate PC-1 and dotted line in (A) indicate PC-2. The open circles in (B) represent samples stored at 25ºC (RT) and solid circles in (B) represent samples stored at 40ºC (HT). 90
Figure 5.8 Factor loadings of the first two principal components (A) and similarity map (B) of principal component analysis (PCA) made on Maillard emission spectra of the MPC

samples after storage. The solid line in (A) indicate PC-1 and dotted line in (A) indicate PC-2. The open circles in (B) represent samples stored at 25ºC (RT) and solid circles in (B) represent samples stored at 40ºC (HT). 92
Figure 5.9 Factor loadings of the first two principal components (A) and similarity map (B) of principal component analysis (PCA) made on Maillard excitation spectra of the MPC samples after storage. The solid line in (A) indicate PC-1 and dotted line in (A) indicate PC-2. The open circles in (B) represent samples stored at 25ºC (RT) and solid circles in (B) represent samples stored at 40ºC (HT). 93
Figure 5.10 Partial least squares prediction model: measured vs. predicted solubility index (%) values plot for a cross-validation prediction of (A) tryptophan fluorescence spectra, (B) Maillard emission spectra, and (C) Maillard excitation spectra for the 7-factor model for the entire data set (n=220). 95
Figure 5.11 Partial least squares prediction model: measured vs. predicted relative solubility index (%) values as obtained from the focused beam reflectance measurement plot for a cross-validation prediction of (A) tryptophan fluorescence spectra and (B) Maillard emission spectra. 96
Figure A.1 Test sequence of flow measurement. 104
Figure A.2 Test sequence of permeability measurement. 104
Figure A.3 Shear head for shear cell test. 104

List of Tables

Table 2.1 Composition of various MPC powders 4
Table 2.2 Jenike's classification of powder flowability based on flow index 9
Table 2.3 Powder and particle characteristics and factors influencing powder flowability[1] 10
Table 2.4 Comparison of various commercially available powder flow analyzers 11
Table 2.5 Overview of various techniques used for measuring the rehydration of high-protein dairy powders 15
Table 2.6 Fluorescence spectroscopy studies illustrating processing-induced changes in various dairy products 21
Table 2.7 Fluorescence spectroscopy studies illustrating effects of heat treatment on various dairy products 22
Table 4.1 Compositional analysis (%, w/w; means ± SD) of milk protein concentrate (MPC) powders used in this study 46
Table 4.2 Correlation coefficients between selected functional, morphological, and flowability of milk protein concentrate (MPC) powders 47
Table 4.3 Morphological characteristics of milk protein concentrate (MPC) powders after 12 weeks of storage at 25 and 40ºC 53
Table 4.4 Dynamic flow properties of milk protein concentrate (MPC) powders after 12 weeks of storage at 25 and 40ºC 53
Table 4.5 Shear flow properties of milk protein concentrate (MPC) powders after 12 weeks of storage at 25 and 40ºC 61
Table 5.1 Compositional analysis (%, w/w; mean values) of milk protein concentrate (MPC) powders used in this study. 79
Table 5.2 The mean values of L*, a*, and b* for the MPC samples received from one of the manufacturer before storage and samples stored at 25 and 40 ºC for 12 weeks[1] 79
Table 5.3 Summary of partial least squares (PLS) predictions for solubility index and relative solubility using front-face fluorescence spectroscopy. 96

Acknowledgments

I would like to express my sincere gratitude to my major advisor, Dr. Jayendra Amamcharla, for his guidance, care, and motivation throughout my master's program and during my research. I would like to thank Dr. Scott Smith and Dr. Umut Yucel for serving on my committee. I would like to extend my sincere thanks to Dr. Kingsly Ambrose, Dr. Kaliramesh Siliveru, and Dr. Praveen Vadlani for their guidance and help throughout this research. I am greatly thankful to my family, Food Science Institute faculty and staff, and other graduate students at K-State for their constant support. Finally, I would like to thank the Midwest Dairy Foods Research Center (St. Paul, MN) for their financial support.

Chapter 1 - Introduction

Milk protein concentrate (MPC) powder is a high-protein dairy ingredient manufactured from skim milk in which the major proteins in milk have been concentrated by membrane filtration process (Meena et al., 2017). MPC powders are generally classified according to their protein content, with MPC40 being a low-protein MPC (~42%protein), MPC85 representing a high-protein MPC (~85% protein), and milk protein isolate (MPI) stands for MPC powders with ~90% protein content (dry basis). Out of 3.457 billion pounds milk-based ingredients being produced, the production of MPC/MPI was estimated as 171 million pounds for the year 2016 (ADPI, 2017). High protein content, low lactose content, pleasant milk flavor profile, and functional properties have increased the application of MPC powders as ideal ingredients for a wide range of food formulations (Sharma et al., 2012, Agarwal et al., 2015). MPC powders are typically added to protein bars, beverages, processed cheese, Greek-style yogurts, ice-creams, and a variety of dairy and foods products to improve the nutritional, sensory, and functional properties of the finished product (Agarwal et al., 2015).

With the increased interest in using MPC powders in the food industry, knowledge of their functional properties such as rehydration characteristics, flow behavior, and particle morphology could be helpful in optimizing their storage, handling, and processing (Felix da Silva et al., 2018). However, flow properties and dissolution performance of MPC powders are influenced by powder properties, such as bulk composition and particle structure (morphology, the presence of pores and capillaries) (Crowley et al., 2014), and rehydration conditions (Crowley et al., 2015). Thus, improving powder functionality, particularly the rehydration characteristics and flowability, is becoming crucial. Changes in storage conditions (temperature and relative humidity), composition, capillary interactions within particles, and migration of

cohesive chemical components to the surface of powder particles impact the flowability of food powders (Teunou et al., 1999; Iqbal and Fitzpatrick, 2006). The flow properties of powders also depend on its physical characteristics, such as particle size distribution, particle morphology, surface structure, and bulk density (Crowley et al., 2014; Kim et al., 2005). However, there is a lack of fundamental understanding of the flow and shear characteristics of MPC powders, especially the influence of protein content and storage temperature during prolonged storage.

Various factors affect the rehydration behavior of MPC powders, and several methods are available to monitor their rehydration based on their rehydration stages and on definite phenomena related to powder rehydration. However, most of these methods are time-consuming, difficult to reproduce, subjective, involve expensive equipment, and skilled technicians. Literature has shown that front-face fluorescence spectroscopy (FFFS) can detect differences between various dairy products due to the presence of several intrinsic fluorophores.

Chapter 2 gives an overview of the MPC powders, flowability and solubility of dairy powders, and it gives an overview of FFFS, focusing primarily on its application in dairy products coupling with chemometrics. Chapter 3 outlines the research objectives. Chapter 4 is focused on studying the influence of protein content and storage temperature on the particle morphology and flowability characteristics of MPC powders. Whereas, Chapter 5 is focused on investigating the use of FFFS as a rapid non-destructive technique for monitoring storage changes and to predict solubility measurements in MPC powders.

References

Agarwal, S., R. L. W. Beausire, S. Patel, and H. Patel. 2015. Innovative uses of milk protein concentrates in product development. J. Food Sci. 80:23-A29.

Crowley, S. V., B. Desautel, I. Gazi, A. L. Kelly, T. Huppertz and J. A. O'Mahony. 2015. Rehydration characteristics of milk protein concentrate powders. J. Food Eng. 149:105-113.

Crowley, S. V., I. Gazi, A. L. Kelly, T. Huppertz and J. A. O'Mahony. 2014. Influence of protein concentration on the physical characteristics and flow properties of milk protein concentrate powders. J. Food Eng. 135:31-38.

Felix da Silva, D., L. Ahrné, R. Ipsen and A. B. Hougaard. 2018. Casein-Based powders: Characteristics and rehydration properties. Compr. Rev. Food Sci. Food Saf. 17:240-254.

Iqbal, T. and J. J. Fitzpatrick. 2006. Effect of storage conditions on the wall friction characteristics of three food powders. J. Food Eng. 72:273-280.

Kim, E. H., X. D. Chen and D. Pearce. 2005. Effect of surface composition on the flowability of industrial spray-dried dairy powders. Colloids and Surfaces B: Biointerfaces. 46:182-187.

Meena, G. S., A. K. Singh, N. R. Panjagari and S. Arora. 2017. Milk protein concentrates: Opportunities and challenges. J. Food Sci. Technol. 1-15.

Sharma, A., A. H. Jana and R. S. Chavan. 2012. Functionality of milk powders and milk-based powders for end use applications—a review. Compr. Rev. Food Sci. Food Saf. 11:518-528.

Teunou, E., J. J. Fitzpatrick and E. C. Synnott. 1999. Characterisation of food powder flowability. J. Food Eng. 39:31-37.

Chapter 2 - Literature Review

Overview of milk protein concentrate powders

Milk protein powders are systems that contain caseins, whey proteins, lactose, fat, and minerals in different proportions depending on the concentration process applied (Burgain et al., 2016). The use of casein-based dairy ingredients in food formulations is still growing (Felix da Silva et al., 2018). Casein-based dairy powders, such as milk protein concentrate (MPC), micellar casein isolate, sodium caseinate, and calcium caseinate have great value in various food formulations due to their protein functionality, and they are most often sold commercially as a spray dried powders (Felix da Silva et al., 2018). MPC powders are generally described as high-quality complete dairy protein complexes containing casein and whey proteins in the similar ratio as in milk. When compared to other dairy powders like whole milk powder (WMP) or non-fat dry milk (NFDM), MPC powders are higher in protein content and lower in lactose content, and they are available in protein concentrations ranging from 42% to 90% (Agarwal et al., 2015). This high protein/low lactose combination along with desirable functional, nutritional, and sensory attributes makes MPC powders an ideal ingredient for various food formulation. Table 2.1 compares the composition of various MPC powders with protein concentrations ranging from 42% to 90%.

Table 2.1 Composition of various MPC powders

Component (%)	NFDM	MPC42	MPC56	MPC70	MPC80	MPC85	MPC90
Protein	35	42	56	70	80	85	90
Lactose	53	46	31	16	6	4	1
Ash	4	6	7	7	7	7	6
Fat	1.5	1.5	1.5	1.5	1.5	1.5	1.5

Composition adapted from Agarwal et al. (2015)

Presently in the United States, there is no standard of identity for MPC powders. Furthermore, no countries in the world have laid down the compositional standards (minimum or maximum values for protein and lactose contents) for MPC powders. However, the American Dairy Products Institute and the U.S. Dairy Export Council have marked MPC powders as Generally Recognized as Safe (GRAS) and filed a notification showing MPC powders as food ingredients for various functional or nutritional applications in product development. Furthermore, the Food and Drug Administration has acknowledged the GRAS notification (Agarwal et al., 2015). Figure 2.1 illustrates the flowchart for manufacturing of MPC powders.

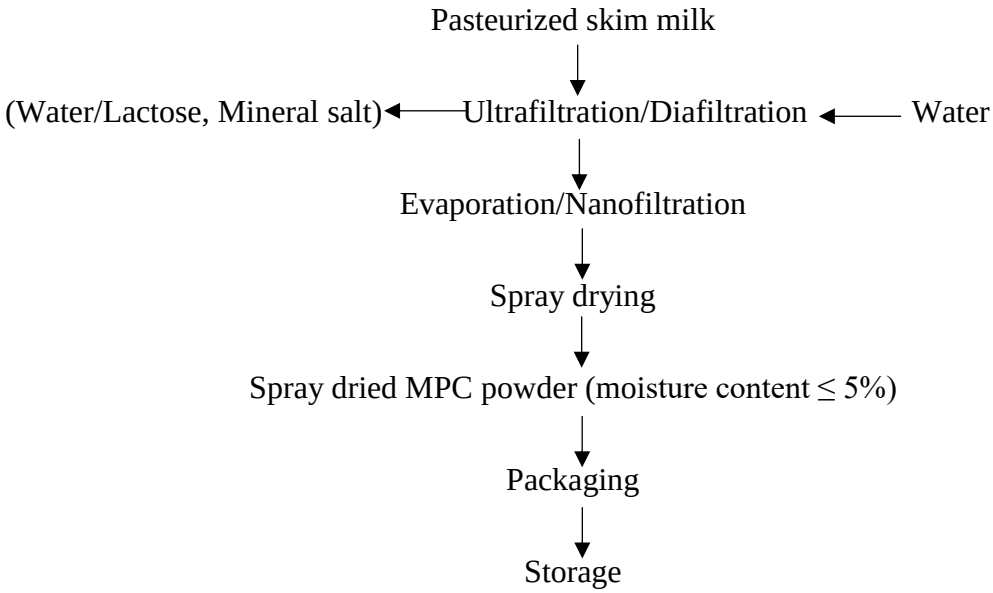

Figure 2.1. Process for manufacturing of milk protein concentrate (MPC) powders (adapted from Meena et al., 2017).

Membrane separation has revolutionized the dairy industry. Membrane technology is helpful in concentrating and fractionating valuable milk proteins. The liquid portion that can pass through the membrane is called as permeates and the portion of retained liquid is called as retentate or concentrate (Kumar et al., 2013). Manufacturing of MPC powders starts with skim milk as the base material. The very first step is the pasteurization of the procured skim milk to

meet the governing requirements to destroy potential pathogens and enzymes. Ultrafiltration (UF) or diafiltration (DF) is used to concentrate the skim milk. During the filtration step, whey proteins, caseins, micellar salts, and fat are in the retentate, whereas a portion of lactose, soluble salts, and nonprotein nitrogen are removed with the permeate (Agarwal et al., 2015; Meena et al., 2017). In high-protein MPC powders, UF alone is not sufficient to achieve the required protein-to-solids ratio in the retentate. Therefore, additional DF step is generally applied (Singh, 2007). Generally, MPC powders undergo comparatively less severe heat treatment and pH adjustments. Better heat stability and excellent solubility are prime concerns of MPC manufacturers (Felix da Silva et al., 2018).

Dairy powders are widely used for convenience in applications for transportation, handling, processing, and for food product formulations (Sharma et al., 2012). However, complete rehydration is typically a major criterion for MPC powder's primary functionality. Due to the poor reconstitution of MPC powders, the end-users are subjected to modify existing unit operations and product formulations in order to accelerate powder rehydration (Crowley et al., 2015). Previously, Anema et al. (2006) recognized caseins as the major components for the poor dispersion in MPC85 powder particles. The rate-limiting step in the rehydration of MPC powders was the dispersion of inter-linked casein micelles (Mimouni et al., 2010). Numerous studies have established that slow dispersion of primary particles is accountable for the longer rehydration times of casein-based powders (Schuck et al., 2007; Fang et al., 2012; Richard et al., 2013). However, Bouvier et al. (2013) proved that increasing the size and number of pores in MPC powder particles through extrusion-porosification noticeably enhanced their rehydration behavior. Therefore, as the dissolution of MPC powders are generally a prerequisite for their good performance, and it is viewed as a critical property for their selection in food various food

formulations (Mimouni et al. 2010b). Furthermore, prior to their processing for various food formulations, MPC powders will be stored, and it is essential to understand, predict, and control their behavior during storage, handling, and processing (Fitzpatrick et al. 2004a; Felix da Silva et al., 2018). Therefore, properties such as rehydration characteristic and flow behavior will influence the performance of several unit operations in the handling and processing of MPC powders. Some of the functional properties of significance to dairy powders are outlined below.

Flowability of dairy powders

Characterization of flowability in food powders is essential for predicting the powder flow from hoppers in small-scale systems or at the industries such as from storage silos or bins dispensing into powder mixing systems (Juliano and Barbosa-Cnovas, 2010). Currently, a large variety of dairy ingredients are produced industrially in powder form, and the knowledge about the powder flowability characteristics is critical in their handling, processing, and subsequent storage. Powder flowability can be defined as the relative movement of a bulk of powder particles among adjacent particles/along the container wall surface (Peleg, 1978). Food powder flow properties are important in handling and processing operations, such as flow from hoppers and silos, transportation, mixing, compression and packaging (Peleg, 1978). Obtaining reliable and consistent flow out of hoppers and feeders without excessive spillage and dust generation is of great concern in the food industry. Flow properties characterize the behavior of powders during hopper flow, conveying through feeders, and other handling equipment. Flow behavior is also crucial for the design of bins or hoppers especially to maximize the use of discharge units to their design capacity in order to prevent costly downstream handling problems. The flowability tests can be broadly divided into uncompacted conditions (e.g., the angle of repose), tapped or vibrated (Hausner ratio and compressibility index), and consolidated (shear tests). Jenike (1964)

pioneered the methods for determining the diameter of hopper outlet and minimum hopper angle (required for mass flow) using shear cell techniques and has developed a standard for the design and development of bins which is regarded as a first standard method to characterize flowability in food powders. The major flow related properties widely studied are flow function, the angle of internal friction, and angle of wall friction. The flow function plot in Figure 2.2 (unconfined yield stress vs. major consolidating stress) represents the cohesion developed in powder when consolidated. This must be overcome to initiate the flow of powders.

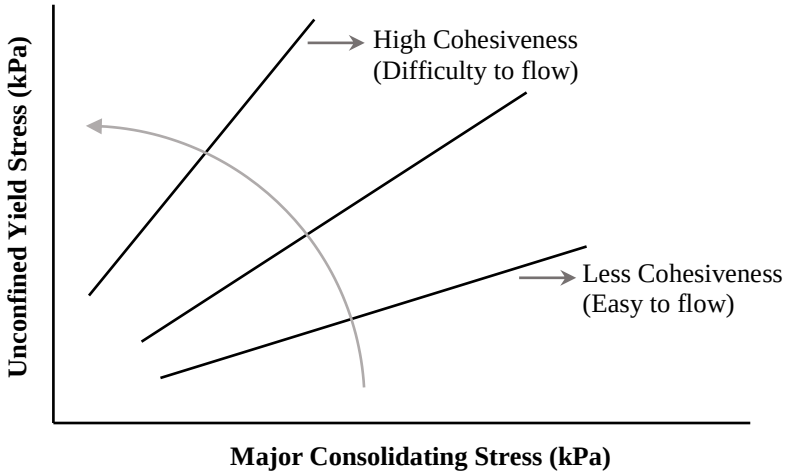

Figure 2.2 Flow functions of dairy powders: high cohesive vs. less cohesive (adapted from Fitzpatrick et al., 2004a).

Flowability can be affected by the amount of free and associated moisture inside each particle. Other components such as fats, sugars, proteins, and fibers also determine the flowability of a powder. Additionally, surface properties such as friction, ductility, and interlocking capacity may depend on the powder composition and structural distribution on the surface (Juliano and Barbosa-Cnovas, 2010). Moreover, examining the effect of factors such as moisture content, temperature, storage time, particle composition, particle morphology, and size distribution, is highly essential for the characterization of food powders (Juliano and Barbosa-Cnovas, 2010). Previously, Merrow (1988) reported that critical issues in food powder

processing plants occurred during the handling and transportation of powders. Flow characterization is necessary for equipment design and development, storage of bulk solids, and transporting/handling of solids, additionally, its required for quality control and for process modeling (Fitzpatrick et al., 2004a; Juliano and Barbosa-Cnovas, 2010). Moreover, before the processing steps for the manufacture of dairy products, such powders will be stored in silos and bags, and it is important to be able to understand, predict and control their behavior during storage, handling, and processing (Fitzpatrick et al. 2004b). Therefore, properties such as flow and shear properties will impact the performance of unit operations in the handling and utilization of milk protein powders (Silva et al. 2016). In Jenike's classification of powder, Jenike used the flow index to classify food powder flowability with higher values representing easy or free-flowing (Table 2.2).

Table 2.2 Jenike's classification of powder flowability based on flow index

Flowability	Flow index[1]
Hardened	<1
Very cohesive	<2
Cohesive	<4
Easy flow	<10
Free flowing	>10

[1]Adapted from Fitzpatrick et al. (2004a).

Factors influencing powder flowability

The flow of powders is a complex phenomenon in which both the powder/particle and physiochemical characteristics govern the powder flow behavior (Juliano and Barbosa-Cnovas, 2010). The bulk properties like moisture content, density, composition, shape, and particle size are directly associated with powder flowability. The forces opposing flow are friction, the attraction between particles (cohesion), the attraction between the particles and system walls (adhesion), and mechanical resistance due to particle interlocking (Peleg, 1978). Many studies

have shown the effects of different conditions on the flow properties (Peleg et al., 1973; Teunou et al., 1999). Table 2.3 illustrates various powder and particle characteristics that influence powder flowability. Surface roughness or surface mechanical characteristics of particles profoundly influences physical interlocking of the particles, thereby hindering the consistent and reliable flow of powders (Juliano and Barbosa-Cnovas, 2010). Physical characteristics that affect the flowability of powders include particle surface properties, particle shape, and particle size distribution, and overall morphology of the particles (Bian et al., 2015; Siliveru et al., 2017). Additionally, surface properties and powder composition affect the degree of mechanical interlocking. When particles become smaller, they provide a greater surface area for surface cohesive forces to interact to increase friction to resist flow (Fitzpatrick et al. 2004a).

Table 2.3 Powder and particle characteristics and factors influencing powder flowability[1]

Type	Factors influencing powder flowability
Powder properties	Size distribution
	Bulk density
	Homogeneity
	Powder compressibility
	Cohesiveness
	Internal friction
	Wall friction
Particle properties	Composition
	Density
	Particle size
	Particle shape
	Surface roughness
	Particle compressibility
	Surface friction

[1]Adapted from Juliano and Barbosa-Cnovas (2010).

In the last decade, the Freeman FT4 powder rheometer has emerged as a novel powder flow testing device. FT4 was designed to establish the flow patterns formed in nonconfined materials by forces exerted by a twisted blade moving along a helical path through the powder bed. These flow patterns are determined by the combination of axial and rotational speeds. The

flow resistance is characterized by the flow energy; the summation of the rotational and translational work required to drive a rotating impeller a certain distance into a powder bed. It has been shown to be able to differentiate the flowability of powders that otherwise exhibit similar behavior under shear testing (Freeman, 2007). Free flowing powders will exhibit very little resistance to force, or torque, transferred through the powder bed in either the downward or the upward direction. In contrast, poor flowing powders displays a substantial amount of torque in either direction. The wave of powder displacement is virtually in steady state, allowing flow to be observed, and generally resulting in smooth, linear, or logarithmic profiles of the measured forces. The FT4 rheometer is capable of measuring a range of additional powder properties like aeration, wall friction, as well as bulk properties like permeability, compressibility, and density. A very brief comparison of FT4 powder rheometer with the other commercially available flow testing devices is provided in Table 2.4.

Table 2.4 Comparison of various commercially available powder flow analyzers

Powder flow analyzers		
FT4 Powder Rheometer (Freeman Technology Ltd. Worcestershire, UK)	Powder Flow Tester (PFT) (Brookfield Engineering Laboratories, Inc., Middleboro, MA, USA)	Revolution Powder Analyzer (Mercury Scientific Inc., Newtown, CT, USA)
Bulk properties: Density, compressibility, permeability. *Dynamic flow properties*: Basic flowability, aeration, stability index, consolidation, flow rate, specific energy. *Shear properties*: Major principle stress, unconfined yield stress, cohesion, angle of internal friction, flow function coefficient. *Typical applications*: Give potential insights on segregation, attrition, caking, moisture, agglomeration, electrostatics, design of new hoppers/silos, etc.	*Bulk properties*: Density *Shear properties*: Unconfined failure strength, major principal, consolidating stress, tensile strength, angle of internal friction, angle of wall friction, cohesive strength *Typical applications*: Certifying material quality before shipping of powders, benchmarking (determining differences in flow-ability, reverse engineering, design of new hoppers/silos, etc.	Measures various flow parameters including avalanche energy, break energy, surface fractal, sample density, avalanche angle, etc. *Typical applications*: Measure powder's ability to flow, consolidate, granulate, cake, pack, and fluidize.

Solubility of high-protein dairy powders

Reconstitution or dissolution of food powder generally consists of four phases: wetting of powder particles, sinking, dispersing, and particles completely dissolving in solution (Fang et al., 2007). Figure 2.3 shows a schematic diagram of dissolution timeline for different types of powder displaying the overlaps between different phases with time. An overall rehydration mechanism for an agglomerated high-protein dairy powder is illustrated in Figure 2.4. Milk protein concentrate with >80% protein content has been reported to display poor dissolution behaviors (Mimouni et al., 2009). The low solubility index indicated a higher insoluble material (Anema et al., 2006; Havea, 2006). The higher insoluble material can cause filters and pipes to clog, sedimentation layer development and the product will face processing constraints leading to not achieving desired functional and nutritional properties (Chandan and Kilara, 2011).

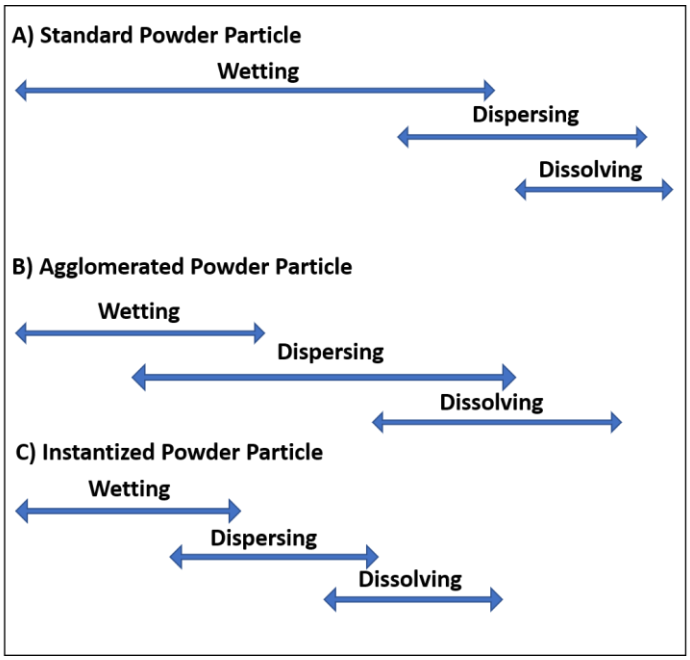

Figure 2.3 Schematic diagram of dissolution timeline for different types of food powder showing the overlaps between different phases with time (adapted from Fang et al., 2007).

The solubility of MPC powders depends on factors such as processing, storage, dissolution conditions, and the composition of powder (Hauser and Amamcharla, 2016a). Fang et al. (2012) reported that increasing the inlet air temperature during spray-drying led to a decrease in solubility. During thermal processing, the high temperature denatures the protein, resulting in aggregation and interactions between whey and casein. When the proteins denature, they begin to unfold and expose the hydrophobic bonds, resulting in inadequate rehydration of the MPC powders. Mimouni et al. (2010a) reported that the release of casein micelles from powder particles is the rate-limiting step in the rehydration process of MPC powders, as this slow-dissolving material consisted almost entirely of caseins and colloidal salts, whereas the whey proteins, lactose, and non-micellar minerals (sodium and potassium) showed to dissolve nearly immediately into the water. Additional processing steps like reducing calcium, adding salt during diafiltration (Gazi and Huppertz, 2015), high-pressure treatment (Udabage et al., 2012), and adding lactose solution during processing (Schuck et al., 2007) can enhance the solubility of MPC powders. MPC powders have the best possible solubility immediately after production (Fang et al., 2012; Gazi and Huppertz, 2015).

The solubility of MPC powder changes over the storage period. Storage time, temperature, and relative humidity affect the solubility of high-protein dairy powders. Increasing the storage temperature decreases the solubility of MPC (Anema et al., 2006; Fyfe et al., 2011; Gazzi and Huppetz, 2015; Hauser and Amamcharla, 2016b). Anema et al. (2006) investigated the effect of storage time and temperature on the solubility of MPC85 using solubility tests. They have concluded that, at a given temperature, the solubility of MPC85 decreased with storage time. Anema et al. (2006) suggested that the poor solubility of the MPC85 is possibly due to the cross-linking of the proteins by hydrophobic and/or hydrogen bonding. Fang et al. (2011) also

demonstrated that the storage time increases the changes that arise due to increased storage temperature. Additionally, the powder composition also determines the solubility of the MPC powders. Casein, calcium, magnesium, and phosphorus are the slowest-dissolving portions of MPC (Mimouni et al., 2010b; Sikand et al., 2011). Previous studies reported that casein typically decreased the solubility of MPC powders and attempts were made to identify the possible reasons by studying the surface properties of the powder particles and the interactions between the proteins. However, the interactions between the caseins changed with the powder composition (Mimouni et al., 2010a; Gazi and Huppertz, 2015). Studies have shown that increasing the amount of lactose during production led to an increase in solubility (Schuck et al., 2007; Richard et al., 2013).

Previous studies reported that a crust or skin formed during storage of the MPC powders, further reducing the water transfer rate to casein. (Fyfe et al., 2011; Crowley et al., 2015; Gazi and Huppertz, 2015). Mimouni et al. (2009) reported that with or without a skin or crust, the rate of water transfer decreased the solubility of powder. Likewise, increasing the agitation or rehydration time has been revealed to entirely or partially remove the skin (Mimouni et al., 2010a). It is well known that the structure and morphology of spray-dried powder particles may depend on the composition of the retentate as well as the spray drying conditions. Additionally, it is very important to note that powder morphology strongly influences the rehydration behavior (Felix da Silva et al., 2018). Various methods are available for monitoring the rehydration of high-protein dairy powders based on rehydration stages (Figure 2.4), and not all methods give information on specific phenomena related to powder rehydration. Applications of various methods for measuring rehydration of high-protein dairy powders are shown in Table 2.5.

Table 2.5 Overview of various techniques used for measuring the rehydration of high-protein dairy powders

Technique	Rehydration stage	In-line	Off/at-line	Reference
Solubility test	Dissolution	-	✓	(Anema et al., 2006)
Light scattering	Swelling, dispersion, and dissolution	-	✓	(Mimouni et al., 2009)
Ultrasound device	Final stage	✓	✓	(Hauser and Amamcharla, 2016a)
FBRM[1]	Dispersion	✓	✓	(Hauser and Amamcharla, 2016b)
NMR[2] relaxometry	Dissolution and water penetration	-	✓	(Shuck et al., 2007)
Turbidimetry	All stages	✓	✓	(Gaiani et al., 2005)
Rheology	All stages, except swelling	✓	✓	(Gaiani et al., 2006)
Microscopy	All stages	-	✓	(Mimouni et al., 2009)

[1]FBRM-focused-bean reflectance measurement, [2]NMR-nuclear magnetic resonance

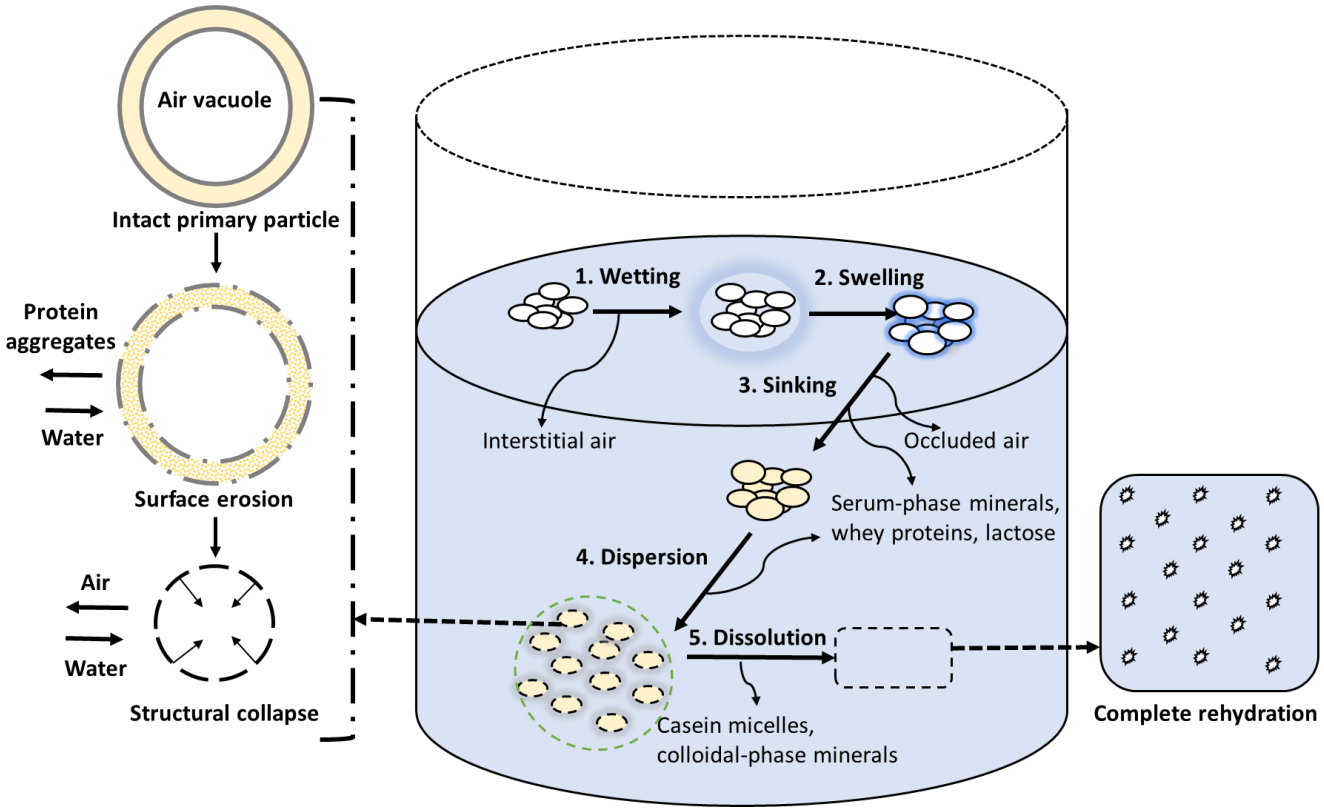

Figure 2.4 Schematic illustration of rehydration mechanism for an agglomerated high-protein dairy powder (adapted from Crowley et al., 2016).

Overview of fluorescence spectroscopy

The mandate for high quality and safety in foods clearly demands high standards for quality and process control, which in turn requires rapid technologies for sampling methods and data analysis (Christensen et al., 2006). In recent years, it has become increasingly notable that the application of rapid spectroscopic methods to food analysis can alleviate major problems in the production and storage of food products. Indeed, the traditional analytical methods for analyzing foods are slow, relatively expensive, time-consuming, require highly skilled operators, and could not be easily adapted for in-line monitoring. The traditional chemical methods are not efficient enough to shelter the growing demands of the food industries. Thus, a significant number of non-destructive instrumental techniques such as fluorescence spectroscopy and infrared spectroscopy have been developed for the determination of product composition and functionality. These new rapid techniques are relatively low-cost and can be applied to both fundamental types of research and in the food industry, as on-line sensors for monitoring the dairy food products (Shaikh and O'Donnell, 2017).

During the last two decades, fluorescence spectroscopy has provided valuable information about the chemical, physical, and sensory properties in several types of compound food products (Novales et al., 1996; Karoui and Blecker, 2011). The increased use of fluorescence spectroscopy has been facilitated by improved instrumentation and new data analytical techniques such as multivariate and chemometric data analysis (Karoui, Mazerolles, and Dufour, 2003). Fluorescence spectroscopy is a rapid technique whose theory and methodology have been extensively used for studying molecular structure and function in the area of food chemistry (Strasburg and Ludescher, 1995). Even though fluorescence is one of the oldest methods used, it has recently become quite popular as a rapid and nondestructive tool in

dairy applications (Shaikh and O'Donnell, 2017). An indication of this wide popularity and acceptance is the increasing number of research publications about fluorescence as well as the introduction of new commercial instruments (such as Amaltheys analyzer) for fluorescence examination (Lacotte et al., 2015), mainly, focusing on front-face fluorescence spectroscopy (FFFS). Fluorescence spectrum is obtained when emission spectra are measured at several excitation wavelengths. Such fluorescence spectrum can, ideally, be decomposed and analyzed by chemometric data analysis, enabling identification of the underlying fluorescent phenomena as studied from unique fingerprints of the fluorophores. Other advantages of the fluorescence spectroscopy are that it is fast, nondestructive, selective, and sensitive (Karoui and Blecker, 2011).

Basic principles of fluorescence spectroscopy

Fluorescence is the emission of light after absorption of ultraviolet (UV) or visible light of a fluorescent molecule or substructure called a fluorophore. The fluorophore absorbs energy in the form of light at a specific wavelength and releases energy in the form of emission of light (higher wavelength). Fundamental principles can be illustrated by a Jablonski diagram (Zude, 2008), as depicted in Figure 2.5. The first step is excitation; it is the absorption of light by the fluorophore, which is subsequently shifted to an electronically excited state, meaning that an electron goes from the ground singlet state, S_0, to an excited singlet state, S_1. This is followed by a vibrational relaxation, where the molecule transfers from a higher electronically excited state to a lower one (with no radiation). The final step is the emission, where the electron returns to its more stable ground state, S_0, emitting light at a wavelength according to the difference in energy between the two electronic states. In the ground state, almost all molecules occupy the lowest vibrational level. By excitation with UV or visible light, it is possible to promote the molecule of

interest to one of the several vibrational levels for the given electronically excited level. This implies that absorption and fluorescence emission does not only occur at one single wavelength but rather over the distribution of wavelengths corresponding to several vibrational transitions as components of a single electronic transition. In fact, fluorescence is characterized by two wavelength parameters that significantly improve the specificity of the method, compared to other spectroscopic techniques based only on absorption (Zude, 2008).

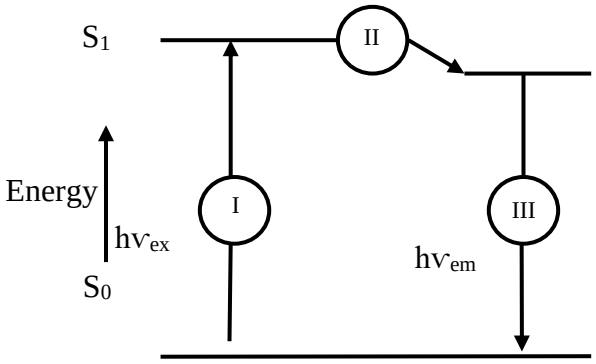

Figure 2.5 Jablonski diagram showing the fundamental principle in fluorescence spectroscopy (adapted from Karoui and Dufour, 2008).

Fluorescence spectrometer

The basic setup for an instrument for measuring fluorescence is shown in Figure 2.6. The fluorescence spectrometer consists of a light source; a monochromator and filters for selecting the excitation wavelengths; a sample compartment; a monochromator and filters for selecting the emission wavelengths; a detector, which converts the emitted light into an electric signal; and a unit for data acquisition and analysis (Karoui and Blecker, 2011). The sampling can have a considerable effect on the obtained fluorescence signal. If absorbance is less than 0.1, the intensity of the emitted light is proportional to the fluorophore concentration, and excitation and emission spectra are accurately recorded by a standard right-angle fluorescence device. In this case, the excitation light travels through the sample from one side, and the detector is positioned at right angles to the center of the sample. When the absorbance of the sample exceeds 0.1, the

intensity of emission and excitation spectra decreases, and excitation spectra are distorted. In addition, the dilution may change the concentration of other relevant fluorescent species below or close to the detection limit of fluorescence (Karoui and Blecker, 2011). By using FFFS, it is possible to measure more turbid or opaque samples, since the signal becomes more independent of the penetration of the light through the sample.

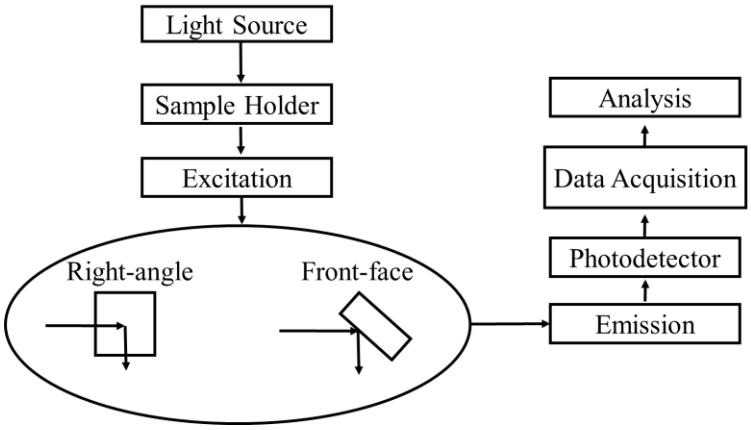

Figure 2.6 The basic setup of a fluorescence spectrometer (adapted from Karoui, Mazerolles, and Dufour, 2003).

Fluorophore

When measuring fluorescence on food samples, chemical compounds occurring naturally within the sample matrix induce fluorescence emission. A fluorophore is a fluorescent chemical compound that can re-emit light upon light excitation. In dairy products, primarily aromatic amino acids, Maillard reaction products, riboflavin, porphyrins, and lipid oxidation products are the fluorophores that lead to fluorescence emission (Shaikh and O'Donnell, 2017). Each fluorophore has a characteristic excitation and emission spectrum, which can be used to separate and identify molecules as well as to differentiate between substitutions and conformations of the same molecule. Traditionally, fluorescence has been applied to clear solutions with known fluorophores. The measurements are carried out using an angle of 90º between the sample and

the excitation light. In such situations, and when the concentration is below a certain level, the measured intensity is proportional to the concentration and follows Lambert-Beer's law. However, scattering, quenching, and inner filter effects destroy this relationship when the concentration is high or when the sample is turbid or solid. Instead, FFFS could be a great alternative. FFFS measures fluorescence emitted only from the sample surface, which reduces the influence of non-fluorescence disturbances. In FFFS, the angle between the sample and the light beam could be changed.

Applications of fluorescence spectroscopy in dairy products

Recently, the application of fluorescence spectroscopy coupled with multivariate statistical techniques for the evaluation of dairy products has increased (Shaikh and O'Donnell, 2017). In most of the research papers, the obtained fluorescence signal was chosen to specific fluorophores (aromatic amino acids and nucleic acids, tryptophan, tyrosine and phenylalanine in proteins; vitamins A and B_2, and nicotinamide adenine dinucleotide (NADH)) after fixing the excitation or the emission wavelength.

Processing-induced changes

Table 2.6 summarizes the literature describing processing-induced changes. Several studies used emission spectra from 305 to 400 nm to explain changes in protein structure as an effect of chemical composition (Dufour et al., 2001; Granger et al., 2006), processing conditions (Karoui et al., 2007), and geographical origin and time of season (Karoui et al., 2005). Depending on the experimental parameters, the spectra showed variations in peak maximum and wavelength position. Various studies proved that fluorescence spectroscopy could distinguish between cheeses with different structures at the molecular level (Herbert et al., 2000; Karoui and Dufour, 2003). A shift in the peak maximum toward lower wavelengths shows the exposure of

tryptophan to more hydrophobic surroundings. Whereas, a shift toward longer wavelengths suggests relatively increased exposure of tryptophan to more hydrophilic surroundings (Lakowicz, 2006). Herbert et al. (1999) also have illustrated examples of these shifts. They observed that emission maximum of tryptophan changed to lower wavelengths during coagulation of milk. This change in the emission spectra was explained by changes in casein micelle structure induced by decreased pH. Schamberger and Labuza (2006) determined that FFFS could be considered a very promising method for measuring Maillard browning in milk and could also be implemented as an on-line instrument and can oversee the thermal processing of milk. Liu and Metzger (2007) applied FFFS for monitoring storage changes in NFDM. They collected NFDM samples from three different manufacturers and stored at four different temperatures (4, 22, 35, and 50ºC) for 8 weeks. Fluorescence of Maillard reaction products (FMRP), riboflavin, and tryptophan was investigated. The obtained spectral data sets allowed good discrimination of the NFDM samples stored at 50ºC from the others. Moreover, good discrimination of samples as a function of the storage time was observed.

Table 2.6 Fluorescence spectroscopy studies illustrating processing-induced changes in various dairy products

Product	Processing Parameters	Wavelengths[a]	Reference
Milk	Milk coagulated with rennet was used	ex at 290 nm and em at 305-400 nm	(Herbert et al., 1999)
Emmental cheese	Cheeses of different ages and geographic origin made from raw milk and thermally treated milk	ex at 290 nm and em at 305-400 nm	(Karoui et al., 2005b)
Soft cheese	Cheeses with variation in dry matter and fat produced with milk were analyzed before salting and after 30 days of ripening	ex at 290 nm with em at 305-400 nm and ex at 250-350 nm with em at 410 nm	(Kulmyrzaev et al., 2005)
Ice cream	Produced from different types of fat, emulsifier, and protein content	ex at 290 nm and em at 310-360 nm	(Granger et al., 2006)

Soft cheese	Samples from the different zone of three cheese products were selected.	ex at 290 nm and em at 305-400 nm, ex at 380 nm and em at 400-640 nm, ex at 250-350 nm and em at 410nm	(Karoui et al., 2007b)
Nonfat dry milk	Samples from three manufacturers exposed to different storage temperatures for up to 8 weeks.	ex at 290 nm and em at 305-450 nm, ex at 360 nm and em at 380-480 nm, ex at 380 nm and em at 400-590 nm, ex at 250-350 nm and em at 410 nm	(Liu and Metzger, 2007)
Cream cheese	Designed experiment with variation in fat, salt, and pH	ex from 260 to 360 nm and em from 280 to 600 nm	(Andersen et al., 2010)

[a] em and ex denote the emission and excitation wavelengths measured, respectively.

Thermal treatment is an essential step in the manufacturing of dairy products which safeguards the microbiological safety and increases shelf life. However, heat treatment induces undesirable changes in dairy products including decreased sensory, functional, and nutritional properties (Shaikh and O'Donnell, 2017). Several fluorescence indicators have been shown to give information about the degree of heat treatment such as advanced Maillard reaction products and tryptophan fluorescence. Table 2.7 summarizes the literature on effects of heat treatment changes on various dairy products.

Table 2.7 Fluorescence spectroscopy studies illustrating effects of heat treatment on various dairy products

Product	Parameters	Wavelengths[a]	Reference
Milk	Raw milk exposed to different heat treatments for different time periods	ex at 340 nm and em at 415 nm	(Morales and Van Boekel, 1997)
Milk	Overheated and normally heated half-cream ultra-high treated milk and pasteurized milk mixed to give a range of heat treatments	ex at 290 and 360 nm with em at 305-450 and 380-600 nm, respectively, and ex at 250-420 nm with em at 440 nm	(Kulmyrzaev and Dufour, 2002)
Milk	Milk with two fat levels exposed to different heat	ex at 290 nm and em at 340 nm, ex at 330 nm and em at 420 nm	(Birlouez-Aragon et al., 2002)

	treatments for two different heating periods		
Milk	Milk exposed to different heat treatments	ex at 250 and 380 nm with em at 280-480 and 380-600 nm, respectively, and ex at 290-490 nm with em at 518 nm	(Kulmyrzaev et al., 2005b)
Milk	Raw skim milk exposed to different heat treatments	ex at 290 nm and em at 305-450 nm, ex at 360 nm and em at 380-600 nm	(Schamberger and Labuza, 2006)
Milk	Exposed to different heat treatments	ex at 340 nm with em at 440 nm, ex at 290 nm with em at 340 nm	(Feinberg et al., 2006)
Skim milk powder	Predict lactulose content	ex at 315 nm with em at 377 nm	(Ayala et al., 2017)
Infant formula	Microwave heating impact on infant formula	ex at 290 nm with em at 340 nm	(Desic and Birlouez-Aragon, 2011)
Liquid and condensed milk	Assess nutritional quality of heat treated milk	ex at 330 nm with em at 420 nm	(Birlouez-Aragon et al., 2001)

[a] em and ex denote the emission and excitation wavelengths measured, respectively.

The development of advanced Maillard reaction products in milk and model systems were previously measured by fluorescence spectroscopy using excitations at 340, 350, or 360 nm and emissions at 415 or 440 nm (Morales et al., 1996; Birlouez-Aragon et al., 2002;). It was clear that the fluorescence intensity increased with more severe heat treatment, illustrating the formation of Maillard reaction products. The possibility of measuring the fluorescence of advanced Maillard products led to the introduction of the fluorescence of Maillard products and soluble tryptophan (FAST) index. It is a measurement of the fluorescence of advanced Maillard products (ex 330 nm/em 420 nm) divided by the tryptophan fluorescence (ex 290 nm/em 340 nm) of the pH 4.6 soluble supernatant (Birlouez-Aragon et al., 1998). Other studies have used model systems to show that the fluorescence measurements depend on the chemical composition (Matiacevich et al., 2006). The actual fluorescence signal is influenced by parameters such as

polarity, pH, and temperature (Lakowicz, 2006). In a similar line, Feinberg et al. (2006) also used fluorescence spectroscopy to identify various heat treatments (pasteurization, high pasteurization, direct UHT, indirect UHT, and sterilization) of commercial milk samples (n=200) stored at 25 and 35°C for 90 days. By applying factorial discriminant analysis (FDA), they found that tryptophan spectra could be used to discriminate sterilized milk and pasteurized milk from the other milk samples. However, tryptophan spectra were unsuccessful in discriminating the other types of milk. A possible explanation could be that fluorescence spectra were collected in the pH 4.6 soluble fraction of the milk sample, resulting in a loss of information.

It is interesting to note that the maximum of peak intensities while measuring heat treatment varies depending on the sample materials and instrument. However, the usage of measurements as a general tool for measuring heat treatment should be researched further. This is also supported by Feinberg et al. (2006), who showed that the use of the fluorescence measurements did not give a precise measurement of the heat treatment of commercial milk samples. Therefore, the fluorescence measurements should be combined with other chemically analyzed tracers to give an appropriate measurement of the degree of heat treatment. Tryptophan fluorescence of milk was found to decrease with increasing heat treatment (Birlouez-Aragon et al., 2002). This is supported by the finding that fluorescence emission at 340 nm was correlated to the content of native β-lactoglobulin (Elshereef et al., 2006). However, solutions of β-lactoglobulin showed both increasing and decreasing intensities with heat treatment (Renard et al., 1998; Elshereef et al., 2006), illustrating the need for further research to understand the actual effect of heat on dairy proteins. In a study of milk heat treatment, Kulmyrzaev and Dufour (2002) found high correlations between lactulose, furosine, and tryptophan spectra. For pasteurized milk, there was no correlation between the lactulose or furosine content. The

different results may be due to variation in sample preparation and measurement method between these experiments. Lactulose and furosine are non-fluorescent and are not measured by fluorescence. Indeed, the high correlations found are due to an indirect relationship because the lactulose concentration changes together with the change in tryptophan fluorescence. Lactulose and furosine are often used as indicators of heat treatment of milk (Mendoza et al., 2005). In contrast, correlation of the concentration of these compounds to fluorescence spectroscopic data gave contradictory results. The high sensitivity of fluorescence towards small compositional changes and product environment is definitely an essential advantage of fluorescence spectroscopy (Shaikh and O'Donnell, 2017). In summary, the experiments and studies discussed above demonstrate that fluorescence spectroscopy has the potential to monitor the chemical modifications that occur in dairy products during processing and subsequent storage.

Spectral data analysis

The chemical information from fluorescence spectroscopy contained in the spectra is hidden in the band position, the band intensities, and the bandwidths. Whereas, the band positions give evidence about the presence and the structure of specific chemical compounds in a blend of the food matrix, the intensities of the spectra are related to the yield of these compounds via the Beer-Lambert law. The easy way to determine the content of a chemical compound is to measure the change of the intensity of a well-resolved band that clearly belongs to this compound. This is possible for a pure component. But dairy products retain numerous components giving complex spectra with overlapping bands. The most effective way to evaluate the fluorescence data is to use chemometric tools to extract quantitative, qualitative or structural information from the fluorescence spectra. These methods encompass descriptive techniques such as the principal component analysis (PCA), canonical correlation analysis (CCA), and

common components specific weights analysis (CCSWA); predictive techniques such as factorial discriminant analysis (FDA), principal component regression (PCR), and partial least square regression (PLSR).

Descriptive techniques

Principal component analysis.

The most commonly used descriptive technique with chemometrics is PCA. The purpose of this technique is to obtain an overview of all the information in the dataset. In PCA, a new set of fewer coordinate axes called principal components (PCs) is created. PCA allows the use of the entire spectrum for the quantitative analysis, and it offers a synthetic portrayal of large datasets with minimum loss of valuable spectral information (Karoui et al., 2003). The factors associated with the PCs can be directly related to properties of the investigated systems, such as concentrations, protein-protein interactions, and can also be interpreted as a spectrum. Chemometric tools such as PCA make it possible to extract information related to the structural changes in dairy products. For example, the PCA similarity map defined by the first principal component (PC1) and the second principal component (PC2) of the PCA performed on tryptophan emission spectra of different kinds of milk showed that PC2 accounted for 98.5% of the total variance and PC1 accounted for 89.1% of the total variance. Thus, discrimination of the samples as a function of homogenization was observed, and discrimination of samples as a function of heat treatment was observed according to PC2 (Dufour and Riaublanc, 1997).

Predictive techniques

Partial least square regression is a common technique in chemistry and other applied sciences. It uses the two-block predictive PLS to model the relationship between two matrices, X (the input matrix) and Y (desired output matrix). PLS converts the variables of X into a reduced

set of variables, termed as latent variables (LVs). The LVs are mutually linearly independent and have a high covariance with Y, and they establish a reasonable approximation of the full input dataset X (Amamcharla and Metzger, 2015).

Principal component regression method is a multiple regression applied from the PCs rather than from the raw data. Indeed, when the variables of spectra are numerous and are strongly correlated between them, it is preferable to carry out the prediction starting from the PCs. All the PCs are not introduced in the regression model, and the last components with small variances are discarded. Dufour et al. (2001) applied PCR to predict the sensory variables from the tryptophan fluorescence spectra in soft cheeses. The results showed that a good prediction was obtained for several sensory attributes: surface (R^2 =0.65), moisture content (R^2 =0.66), texture (R^2 =0.69), and pastiness (R^2 =0.86). These results using PCR highlighted the relationship between the organization of the protein network as evaluated using fluorescence spectroscopy and textural attributes of cheeses.

Coupling chemometrics with fluorescence spectroscopy

Dufour and Riaublanc (1997) investigated the potential of FFFS to discriminate between raw, heated (70ºC for 20 min), homogenized, and homogenized and heated milk. The authors applied PCA to the tryptophan and vitamin A fluorescence spectra, and proper differentiation between milk samples as a function of homogenization and heat treatment applied to milk samples was observed. They concluded that the treatments applied to milk induced specific modifications in the shape of the fluorescence spectra. The PCA applied to the normalized spectra allowed good discrimination of milk samples subjected to different temperatures and times. Herbert et al. (1999) used FFFS to monitor milk coagulation at the molecular level. Emission fluorescence spectra of the tryptophan were recorded for each system during the milk

coagulation kinetics. By applying the PCA to normalized fluorescence spectra data sets of the three systems, detection of structural changes in casein micelles in coagulation and discrimination of different dynamics of the three coagulation systems was achieved. Another study investigated the potential of FFFS to discriminate between milk samples (n=40) according to their geographical origin (Karoui et al., 2005). Fluorescence spectra of tryptophan and riboflavin were recorded directly on milk, with excitation wavelengths set at 290 and 380 nm, respectively. By applying FDA to the spectral collection, a trend to a good separation between milk as a function of their origins was observed.

Dufour et al. (2000) and Mazerolles et al. (2001) used FFFS to monitor semi-hard cheese (n=16). By applying PCA to the normalized tryptophan fluorescence spectra, good discrimination of cheeses presenting a ripening time of 21, 51, and 81 days were observed. Dufour et al. (2000) have studied fluorescence spectra of vitamin A and observed two shoulders located at 295 and 305 nm and a maximum located at 322 nm. By applying PCA to the normalized vitamin A spectra, better discrimination of cheeses aged 21, 51, and 81 days from that aged 1 day was observed. Karoui et al. (2006) investigated tryptophan, vitamin A, and riboflavin spectra of semi-hard cheeses (n=12) of four different brands, which were produced during summer. By applying CCSWA to the spectral data sets and physicochemical measurements, good discrimination of the four brands was observed.

In another study, FFFS has been used for the authentication of different varieties of soft, semi-hard, and hard cheeses during ripening at the local stage (Herbert et al., 2000; Karoui and Dufour, 2003). To test the accuracy of FFFS in differentiating between the eight soft kinds of cheese, the authors applied FDA to the most relevant PCs, and good discrimination of cheeses was observed, with better results obtained with vitamin A spectra than with tryptophan spectra.

Karoui et al. (2005) attempted to classify cheeses. Emission spectra were scanned following excitation at 250 and 290 nm, and excitation spectra the following emission at 410 nm. By applying FDA, 100% correct classification was obtained from the emission and excitation spectra, suggesting the use of FFFS as an accurate technique for the determination of the geographic origin of cheeses.

Boubellouta et al. (2011) investigated if the FFFS can provide information about molecular changes that occur in the micelle structure. The results demonstrated changes in emission spectra of vitamin A and riboflavin at 322 nm and 482 nm, respectively. The gelation time determined by fluorescence spectroscopy as well as rheology increased with increasing milk heat treatment. The PCA analysis of fluorescence spectra discriminated samples according to their heat treatment and temperature at which milk samples were renneted (Blecker et al., 2012).

Overall, FFFS has a potential for on-line industrial quality and process control, as it is possible to measure compounds related to the quality and process conditions fast and nondestructively. Most likely, FFFS can be used for several other parameters in product development, process control, raw material determination, etc., but research is still required before it can be used for routine measurements within the industry. Furthermore, fluorescence gives information about more than one parameter in one measurement, whereas traditional analytical chemical measurements typically provide information about only one parameter at a time. Previous studies suggested that FFFS could provide valuable information about several parameters such as product structure, heat treatment, milk coagulation, storage changes, and changes during ripening. The scientific accomplishments in combination with the fact that equipment prices are dropping as well as the commercialization of portable, highly sensitive fluorescence spectrophotometers make FFFS a promising tool for future quality determination

and process control as well an efficient and versatile research tool with respect to a wide range of dairy products. As illustrated in the above sections, the environment of intrinsic fluorophores recorded on dairy products contains valuable information regarding the composition and nutritional values of dairy products. The considerable potential for the application of FFFS combined with multivariate statistical analysis for the evaluation of quality in dairy products has also been demonstrated.

Although fluorescence spectroscopy technique has been extensively exploited for studies of food chemistry, the utility of this technique for molecular studies has not yet been fully recognized in dairy product, especially in the casein-based protein ingredients. Fluorescence spectroscopy has the same potential to address molecular problems in dairy ingredients as in other fields of food science because the scientific questions that need to be answered are closely related. One drawback of fluorescence spectroscopy is that the measurement conditions and method should be optimized and calibrated for each individual product and application. Standardized protocols for these calibrations are also required.

References

Agarwal, S., R. L. W. Beausire, S. Patel, and H. Patel. 2015. Innovative uses of milk protein concentrates in product development. J. Food Sci. 80:23-A29.

Amamcharla, J. K. and L. E. Metzger. 2015. Prediction of process cheese instrumental texture and melting characteristics using dielectric spectroscopy and chemometrics. J. Dairy Sci. 98:6004-6013.

Andersen, C. M., and Mortensen, G. 2008. Fluorescence spectroscopy: A rapid tool for analyzing dairy products. J. Agric. Food Chem. 56:720-729.

Andersen, C. M., M. B. Frst and N. Viereck. 2010. Spectroscopic characterization of low-and non-fat cream cheeses. Int. Dairy J. 20:32-39.

Anema, S. G., D. N. Pinder, R. J. Hunter and Y. Hemar. 2006. Effects of storage temperature on the solubility of milk protein concentrate (MPC85). Food Hydrocoll. 20:386-393.

Ayala, N., A. Zamora, C. Gonzalez, J. Saldo and M. Castillo. 2017. Predicting lactulose concentration in heat-treated reconstituted skim milk powder using front-face fluorescence. Food Control. 73:110-116.

Bian, Q., R. P. K. Ambrose and Bh. Subramanyam. 2015. Effect of chaff on bulk flow properties of wheat. J. Stored Prod. Res. 64:21-26.

Birlouez-Aragon, I., M. Nicolas, A. Metais, N. Marchond, J. Grenier and D. Calvo. 1998. A rapid fluorimetric method to estimate the heat treatment of liquid milk. Int. Dairy J. 8:771-777.

Birlouez-Aragon, I., P. Sabat and N. Gouti. 2002. A new method for discriminating milk heat treatment. Int. Dairy J. 12:59-67.

Blecker, C., J. Habib-Jiwan and R. Karoui. 2012. Effect of heat treatment of rennet skim milk induced coagulation on the rheological properties and molecular structure determined by synchronous fluorescence spectroscopy and turbiscan. Food Chem. 135:1809-1817.

Boubellouta, T., V. Galtier and E. Dufour. 2011. Structural changes of milk components during acid-induced coagulation kinetics as studied by synchronous fluorescence and mid-infrared spectroscopy. Appl. Spectrosc. 65:284-292.

Bouvier, J., M. Collado, D. Gardiner, M. Scott and P. Schuck. 2013. Physical and rehydration properties of milk protein concentrates: Comparison of spray-dried and extrusion-porosified powders. Dairy Sci. Technol. 93:387-399.

Burgain, J., J. Scher, J. Petit, G. Francius and C. Gaiani. 2016. Links between particle surface hardening and rehydration impairment during micellar casein powder storage. Food Hydrocoll. 61:277-285.

Chandan, R. C. and A. Kilara. 2011. Dairy Ingredients for Food Processing. Amex, Iowa: Wiley-Blackwell, Amex, Iowa.

Christensen, J., L. Norgaard, R. Bro and S. B. Engelsen. 2006. Multivariate autofluorescence of intact food systems. Chem. Rev. 106:1979-1994.

Crowley, S. V., A. L. Kelly, P. Schuck, R. Jeantet and J. A. O'mahony. 2016. Rehydration and solubility characteristics of high-protein dairy powders. Advanced Dairy Chemistry. Springer. 99-131

Crowley, S. V., B. Desautel, I. Gazi, A. L. Kelly, T. Huppertz and J. A. O'Mahony. 2015. Rehydration characteristics of milk protein concentrate powders. J. Food Eng. 149:105-113.

Crowley, S. V., I. Gazi, A. L. Kelly, T. Huppertz and J. A. O'Mahony. 2014. Influence of protein concentration on the physical characteristics and flow properties of milk protein concentrate powders. J. Food Eng. 135:31-38.

Desic, S. D. and I. Birlouez-Aragon. 2011. The FAST index–A highly sensitive indicator of the heat impact on infant formula model. Food Chem. 124:1043-1049.

Dufour, E. and A. Riaublanc. 1997. Potentiality of spectroscopic methods for the characterisation of dairy products. I. front-face fluorescence study of raw, heated and homogenised milks. Le Lait. 77:657-670.

Dufour, E., G. Mazerolles, M. F. Devaux, G. Duboz, M. H. Duployer and N. M. Riou. 2000. Phase transition of triglycerides during semi-hard cheese ripening. Int. Dairy J. 10:81-93.

Dufour, E., M. F. Devaux, P. Fortier and S. Herbert. 2001. Delineation of the structure of soft cheeses at the molecular level by fluorescence spectroscopy—relationship with texture. Int. Dairy J. 11:465-473.

Elshereef, R., H. Budman, C. Moresoli and R. L. Legge. 2006. Fluorescence spectroscopy as a tool for monitoring solubility and aggregation behavior of β-lactoglobulin after heat treatment. Biotechnol. Bioeng. 95:863-874.

Fang, Y., C. Selomulya and X. D. Chen. 2007. On measurement of food powder reconstitution properties. Drying Technol. 26:3-14.

Fang, Y., S. Rogers, C. Selomulya and X. D. Chen. 2012. Functionality of milk protein concentrate: Effect of spray drying temperature. Biochem. Eng. J. 62:101-105.

Feinberg, M., D. Dupont, T. Efstathiou, V. Loupre and J. Guyonnet. 2006. Evaluation of tracers for the authentication of thermal treatments of milks. Food Chem. 98:188-194.

Felix da Silva, D., L. Ahrné, R. Ipsen and A. B. Hougaard. 2018. Casein-Based powders: Characteristics and rehydration properties. Compr. Rev. Food Sci. Food Saf. 17:240-254.

Fitzpatrick, J. J., S. A. Barringer and T. Iqbal. 2004a. Flow property measurement of food powders and sensitivity of jenike's hopper design methodology to the measured values. J. Food Eng. 61:399-405.

Fitzpatrick, J. J., T. Iqbal, C. Delaney, T. Twomey and M. K. Keogh. 2004b. Effect of powder properties and storage conditions on the flowability of milk powders with different fat contents. J. Food Eng. 64:435-444.

Freeman, R. 2007. Measuring the flow properties of consolidated, conditioned and aerated powders—a comparative study using a powder rheometer and a rotational shear cell. Powder Technol. 174:25-33.

Fyfe, K. N., O. Kravchuk, T. Le, H. C. Deeth, A. V. Nguyen and B. Bhandari. 2011. Storage induced changes to high protein powders: Influence on surface properties and solubility. J. Sci. Food Agric. 91:2566-2575.

Gaiani, C., J. Scher, P. Schuck, J. Hardy, S. Desobry and S. Banon. 2006. The dissolution behaviour of native phosphocaseinate as a function of concentration and temperature using a rheological approach. Int. Dairy J. 16:1427-1434.

Gaiani, C., S. Banon, J. Scher, P. Schuck and J. Hardy. 2005. Use of a turbidity sensor to characterize micellar casein powder rehydration: Influence of some technological effects. J. Dairy Sci. 88:2700-2706.

Gazi, I. and T. Huppertz. 2015. Influence of protein content and storage conditions on the solubility of caseins and whey proteins in milk protein concentrates. Int. Dairy J. 46:22-30.

Granger, C., J. Da Costa, J. Toutain, P. Barey and M. Cansell. 2006. Mapping of ice cream formulation using front-face fluorescence spectroscopy. Int. Dairy J. 16:489-496.

Hauser, M. and J. K. Amamcharla. 2016a. Development of a method to characterize high-protein dairy powders using an ultrasonic flaw detector. J. Dairy Sci. 99:1056-1064.

Hauser, M. and J. K. Amamcharla. 2016b. Novel methods to study the effect of protein content and dissolution temperature on the solubility of milk protein concentrate: Focused beam reflectance and ultrasonic flaw detector-based methods. J. Dairy Sci. 99:3334-3344.

Havea, P. 2006. Protein interactions in milk protein concentrate powders. Int. Dairy J. 16: 415–422.

Herbert, S., A. Riaublanc, B. Bouchet, D. J. Gallant and E. Dufour. 1999. Fluorescence spectroscopy investigation of acid-or rennet-induced coagulation of milk. J. Dairy Sci. 82:2056-2062.

Herbert, S., N. M. Riou, M. F. Devaux, A. Riaublanc, B. Bouchet, D. J. Gallant and E. Dufour. 2000. Monitoring the identity and the structure of soft cheeses by fluorescence spectroscopy. Le Lait. 80:621-634.

Jenike, A. W. 1976. Storage and Flow of Solids, Bulletin No. 123 (Utah Engineering Station, Salt Lake City, Utah)

Juliano, P. and G. V. Barbosa-Cnovas. 2010. Food powders flowability characterization: Theory, methods, and applications. Annu. Rev. Food Sci. Technol. 1:211-239.

Karoui, R. and C. Blecker. 2011. Fluorescence spectroscopy measurement for quality assessment of food systems—A review. Food Bioproc. Tech. 4:364-386.

Karoui, R. and R. Dufour. 2006. Prediction of the rheology parameters of ripened semi-hard cheeses using fluorescence spectra in the UV and visible ranges recorded at a young stage. Int. Dairy J. 16:1490-1497.

Karoui, R., A. M. Mouazen, E. Dufour, R. Schoonheydt and J. De Baerdemaeker. 2006b. Utilisation of front-face fluorescence spectroscopy for the determination of some selected chemical parameters in soft cheeses. Le Lait. 86:155-169.

Karoui, R., E. Dufour, R. Schoonheydt and J. De Baerdemaeker. 2007a. Characterisation of soft cheese by front face fluorescence spectroscopy coupled with chemometric tools: Effect of the manufacturing process and sampling zone. Food Chem. 100:632-642.

Karoui, R., G. Mazerolles and r. Dufour. 2003. Spectroscopic techniques coupled with chemometric tools for structure and texture determinations in dairy products. Int. Dairy J. 13:607-620.

Karoui, R., R. Dufour and J. De Baerdemaeker. 2007b. Front face fluorescence spectroscopy coupled with chemometric tools for monitoring the oxidation of semi-hard cheeses throughout ripening. Food Chem. 101:1305-1314.

Karoui, R., R. Dufour, L. Pillonel, E. Schaller, D. Picque, T. Cattenoz and J. Bosset. 2005. The potential of combined infrared and fluorescence spectroscopies as a method of determination of the geographic origin of emmental cheeses. Int. Dairy J. 15:287-298.

Kulmyrzaev, A. A., D. Levieux and r. Dufour. 2005c. Front-face fluorescence spectroscopy allows the characterization of mild heat treatments applied to milk. relations with the denaturation of milk proteins. J. Agric. Food Chem. 53:502-507.

Kulmyrzaev, A. and R. Dufour. 2002. Determination of lactulose and furosine in milk using front-face fluorescence spectroscopy. Le Lait. 82:725-735.

Kulmyrzaev, A., E. Dufour, Y. Noël, M. Hanafi, R. Karoui, E. M. Qannari and G. Mazerolles. 2005. Investigation at the molecular level of soft cheese quality and ripening by infrared and fluorescence spectroscopies and chemometrics—relationships with rheology properties. Int. Dairy J. 15:669-678.

Kumar, P., N. Sharma, R. Ranjan, S. Kumar, Z. F. Bhat and D. K. Jeong. 2013. Perspective of membrane technology in dairy industry: A review. Asian-Australas. J. Anim. Sci. 26:1347.

Lacotte, P., F. Gomez, F. Bardeau, S. Muller, A. Acharid, X. Quervel, P. Trossat, and I. Birlouez-Aragon. 2015. Amaltheys: A fluorescence-based analyzer to assess cheese milk denatured whey proteins. J. Dairy Sci. 98:6668–6677.

Lakowicz, J. R. 2006. Principles of Fluorescence Spectroscopy. Third Edition. Springer, New York.

Liu, X. and L. E. Metzger. 2007. Application of fluorescence spectroscopy for monitoring changes in nonfat dry milk during storage. J. Dairy Sci. 90:24-37.

Matiacevich, S. B. and M. P. Buera. 2006. A critical evaluation of fluorescence as a potential marker for the maillard reaction. Food Chem. 95:423-430.

Meena, G. S., A. K. Singh, N. R. Panjagari and S. Arora. 2017. Milk protein concentrates: Opportunities and challenges. J. Food Sci. Technol. 1-15.

Mendoza, M. R., A. Olano and M. Villamiel. 2005. Chemical indicators of heat treatment in fortified and special milks. J. Agric. Food Chem. 53:2995-2999.

Merrow EW. 1988. Estimating startup times for solids-processing plants. Chem. Eng. Prog. 95:89-92.

Mimouni, A., H. C. Deeth, A. K. Whittaker, M. J. Gidley and B. R. Bhandari. 2009. Rehydration process of milk protein concentrate powder monitored by static light scattering. Food Hydrocoll. 23:1958-1965.

Mimouni, A., H. C. Deeth, A. K. Whittaker, M. J. Gidley and B. R. Bhandari. 2010b. Rehydration of high-protein-containing dairy powder: Slow- and fast-dissolving components and storage effects. Dairy Science & Technology. 90:335-344.

Mimouni, A., H. C. Deeth, A. Whittaker, M. Gidley and B. Bhandari. 2010a. Investigation of the microstructure of milk protein concentrate powders during rehydration: Alterations during storage. J. Dairy Sci. 93:463-472.

Morales, F. J. and M. Van Boekel. 1997. A study on advanced maillard reaction in heated casein/sugar solutions: Fluorescence accumulation. Int. Dairy J. 7:675-683.

Morales, F. J., C. Romero and S. Jimnez-Prez. 1996. Fluorescence associated with maillard reaction in milk and milk-resembling systems. Food Chem. 57:423-428.

Peleg M, Mannheim CH, Passy N. 1973. Flow properties of some food powders. J. Food Sci. 38:959-64

Peleg M. 1978. Flowability of food powders and methods for its evaluation—a review. J. Food Proc. Eng. 1:303-328.

Renard, D., J. Lefebvre, M. Griffin and W. G. Griffin. 1998. Effects of pH and salt environment on the association of β-lactoglobulin revealed by intrinsic fluorescence studies. Int. J. Biol. Macromol. 22:41-49.

Richard, B., J. F. Le Page, P. Schuck, C. Andre, R. Jeantet and G. Delaplace. 2013. Towards a better control of dairy powder rehydration processes. Int. Dairy J. 31:18-28.

Schamberger, G. P. and T. P. Labuza. 2006. Evaluation of front-face fluorescence for assessing thermal processing of milk. J. Food Sci. 71:69-74.

Schuck, P., S. Mejean, A. Dolivet, C. Gaiani, S. Banon, J. Scher and R. Jeantet. 2007. Water transfer during rehydration of micellar casein powders. Lait; Lait. 87:425-432.

Shaikh, S. and C. O'Donnell. 2017. Applications of fluorescence spectroscopy in dairy processing: A review. Curr. Opin. Food Sci. 17:16-24.

Sharma, A., A. H. Jana and R. S. Chavan. 2012. Functionality of milk powders and milk-based powders for end use applications—a review. Compr. Rev. Food Sci. Food Saf. 11:518-528.

Sikand, V., P. S. Tong, S. Roy, L. Rodriguez-Saona and B. A. Murray. 2011. Solubility of commercial milk protein concentrates and milk protein isolates. J. Dairy Sci. 94:6194-6202.

Siliveru, K., C. G. Jange, J. W. Kwek and R. P. K. Ambrose. 2017. Granular bond number model to predict the flow of fine flour powders using particle properties. J. Food Eng. 208:11-18.

Silva, J. V. and J. A. O'Mahony. 2017. Flowability and wetting behaviour of milk protein ingredients as influenced by powder composition, particle size and microstructure. Int. J. of Dairy Technol. 70:277-286.

Singh, H. 2007. Interactions of milk proteins during the manufacture of milk powders. Le Lait. 87:413-423.

Strasburg, G. M. and R. D. Ludescher. 1995. Theory and applications of fluorescence spectroscopy in food research. Trends Food Sci. Technol. 6:69-75.

Teunou, E., J. J. Fitzpatrick and E. C. Synnott. 1999. Characterisation of food powder flowability. J. Food Eng. 39:31-37.

Udabage, P., A. Puvanenthiran, J. A. Yoo, C. Versteeg and M. A. Augustin. 2012. Modified water solubility of milk protein concentrate powders through the application of static high pressure treatment. J. Dairy Res. 79:76-83.

Zude, M. 2008. Optical Monitoring of Fresh and Processed Agricultural Crops. CRC Press.

Chapter 3 - Research Objectives

This study focused on evaluating the influence of protein content and storage temperature on the flow and shear behavior, morphology, and functional characteristics of milk protein concentrate (MPC) powders. Another focus of the study was to develop and evaluate front-face florescence spectroscopy (FFFS) as a rapid method to monitor and predict the functional characteristics of milk protein concentrate (MPC) powders. The specific objectives of the study are:

1. To determine the influence of protein content and storage temperature on the flowability, morphology, and functional characteristics of MPC powders.
2. To use the proposed FFFS as a tool for monitoring changes in MPC powders during storage.
3. To develop and evaluate partial least square regression (PLSR) model for prediction of solubility index and relative dissolution index of MPC powders using FFFS.

Chapter 4 - Influence of protein content and storage temperature on the particle morphology and flowability characteristics of milk protein concentrate powders

Abstract

Milk protein concentrate (MPC) powders are widely used as ingredients for food product formulations due to its nutritional profile and sensory attributes. Processing parameters, storage conditions, and composition influences the flow properties of MPC powders. This study investigated the bulk and shear flow properties of MPC70 (70.3), MPC80 (81.5), and MPC90 (88.1) % (w/w, protein content) after storage for 12 weeks at 25 and 40ºC. Additionally, the morphological and functional changes of the MPC powders were investigated and correlated with flowability. After 12 weeks of storage at 25ºC, the basic flow energy values significantly increased ($P < 0.05$) from 510 mJ to 930 mJ as the protein content increased from 70 to 90% (w/w). Flow rate index was significantly higher ($P < 0.05$) for samples with high protein contents. Dynamic flow tests indicated that MPC powders with high protein content displayed higher permeability. Shear tests confirmed that the samples stored at 25ºC were more flowable than samples stored at 40ºC. Also, the higher protein content samples showed poor shear flow behavior. The results indicated that MPC powders stored at 25ºC had lesser cohesiveness and better flow characteristics than MPC powders stored at 40ºC. Overall, the MPC powders had markedly different flow properties due to their difference in composition and morphology. This study delivers insights on the particle morphology and flow behavior of MPC powders.

Keywords: High-protein dairy powders, flow properties, and powder rheology

---

[1]Accepted for publication: Journal of Dairy Science

Introduction

Milk protein concentrate (MPC) powders are high-protein dairy ingredients which are added to a variety of food product formulations to improve their nutritional, functional, and sensory properties. MPC powders contain higher protein content compared to nonfat dry milk (NFDM) and lower in serum phase components like lactose and soluble minerals. The MPC powders are manufactured using membrane separation techniques such as ultrafiltration or microfiltration and are combined with diafiltration to achieve higher protein contents (Agarwal et al., 2015). Subsequently, unit operations like reverse-osmosis/evaporation and spray drying are employed to manufacture MPC in powder forms. High protein content, low lactose content, high buffering capacity, pleasant milk flavor profile, and functional properties such as water binding have increased the usage of MPC powders as ideal ingredients for a wide range of applications, such as in beverages, yogurt, cheeses, nutritional formulations, and protein bars (Huffman and Harper, 1999; Agarwal et al., 2015). However, rehydration and flowability characteristics in MPC powders are influenced by intrinsic powder properties, such as surface and bulk composition (Crowley et al., 2014), particle structure (presence of pores and capillaries), and rehydration conditions (Crowley et al., 2015).

Changes in storage conditions (temperature and relative humidity), composition, capillary interactions within particles, and migration of cohesive chemical components to the surface of powder particles impact the flowability of food powders (Teunou et al., 1999; Iqbal and Fitzpatrick, 2006; Siliveru et al., 2016b). Additionally, prior to processing, dairy powders will be stored in silos and bags, and thus it is important to understand, predict, and control their flow behavior during storage, handling, and processing (Fitzpatrick et al. 2004b). The flow properties of powders also depend on its physical characteristics, such as particle size distribution, particle

shape, surface structure, and bulk density (Crowley et al., 2014; Kim et al., 2005). Rennie et al. (1999) have studied the effect of composition, particle size, moisture, and temperature on the cohesion of whole milk powder (WMP) and skim milk powder (SMP). They have noted that WMP was more cohesive than SMP with increasing temperature, indicating the influence of fat and formation of liquid bridges in the cohesive mechanism. The flow properties of milk powders with different fat contents (Fitzpatrick, 2004b), infant milk powders (Szulc et al., 2017), and NFDM (Abdalla et al., 2017) have been studied previously. Since the MPC powders are widely used in different food product formulations, the need for quality of the final product has motivated researchers to carry out studies on its functional properties, such as solubility (Anema et al., 2006; Fyfe et al., 2011; Hauser and Amamcharla, 2016a), improving solubility on storage (Bansal et al., 2017), and heat stability (Eshpari et al., 2014). Most of these studies focused on the technological aspects of MPC powders and their application in food product formulations. However, there is a lack of fundamental understanding of the bulk flow and shear characteristics of MPC powders, especially its impacts during storage. Also, there is a need for more insight on the bulk flow and shear characteristics of MPC powders because these properties are important for handling, formulation, mixing, processing, storage, and packaging (Fitzpatrick et al., 2004a). Moreover, investigating the flow behavior of powders is crucial in process equipment designing to ensure a reliable flow of powders and to avoid the formation of clogs/rat-holes (Fitzpatrick, 2004a). Very few researchers investigated the effect of protein content on the flowability (Crowley et al., 2014; Silva and O'Mahony, 2017) and morphology/microstructure (Mimouni et al., 2010; Fang et al., 2012; Ji et al., 2017; Nasser et al., 2017) of high-protein milk powders. Also, no published information is available on the dynamic and shear properties of stored MPC powders.

The Freeman FT4 powder rheometer (Freeman Technology, Worcestershire, UK) is extensively used to characterize powder flow behavior by measuring the resistance offered by a powder bed to a helical blade (Krantz et al., 2009; Bharadwaj et al., 2010; Juliano and Barbosa-Canovas, 2010). The Freeman FT4 powder rheometer consists of blades, pistons, and shear heads that could be rotated and simultaneously moved transversely down into a powder bed while axial force and rotational force are measured (Freeman, 2007). The objective of this research was to measure and compare the flow, dynamic, and shear flow properties of MPC70, MPC80, and MPC90 after storage for 12 weeks at 25 and 40ºC.

Materials and methods

Experimental design

MPC powders (one lot each) with three different protein contents 70, 80, and 90% (w/w), were collected from a commercial manufacturer within the United States. The MPC powders were sealed in Whirl-Pak bags (Nasco, CA, USA) and were stored at two different temperatures (25 and 40ºC) in an incubator (Percival Scientific, Perry, IA) for 12 weeks. Each measurement was carried out in duplicate. To evidently mark and correlate the storage changes with morphology and flow measurements, the MPC powders were analyzed for microstructure, solubility index, and dissolution characteristics.

Microstructure

The microstructure of MPC powders were examined using a scanning electron microscope (SEM) according to the method described by Mimouni et al. (2010). The MPC powders were directly mounted onto a carbon double-sided adhesive tape on microscopy stubs and sputter coated with palladium using a Denton Vacuum Desk II sputter coater (Denton Vacuum, Moorestown, NJ, USA) for 15 min to avoid the charge buildup under the electron

beam. The imaging was conducted using a S-3500N (Hitachi Science Systems Ltd., Tokyo, Japan) and examined by a secondary electron detector (SED) operating at 10 kV.

Morphological analysis

Morphological characteristics of MPC powders were analyzed by Malvern Morphologi G3ID (Malvern Instruments, Worcestershire, UK). The circle equivalent diameter (CED), high sensitivity circularity (HSC), elongation, and convexity were calculated from the 2-D images. Circularity (range 0 to1) describes how close the shape of the particle to a perfect circle. Whereas, convexity (range 0 to1) is a measure of the surface roughness of a particle. A smooth particle has a convexity of 1 while an irregularly shaped particle or very 'spiky' has a convexity closer to 0. Circle or square, has an elongation value of 0. Whereas, shapes with large aspect ratios have an elongation closer to 1 (Li et al., 2016). For each MPC sample, the measurements were carried out in triplicates, and the mean values were obtained.

Flow properties

The FT4 powder rheometer was used to evaluate the flow properties of the stored MPC powders. A detailed description of FT4 and its application methods in powder characterization could be obtained from the FT4 instruction manual (Freemans Technology, Tewkesbury, UK) and were previously reported by Freeman (2007) and Leturia et al. (2014). The FT4 powder rheometer comprises a vertical glass sample container (120 mm height and 50 mm internal diameter) and a rotating blade (10 mm height and 48 mm diameter), which navigates across the sample bed. Flow measurements using FT4 were calculated by continuously recording the forces causing deformation and flow of the powder particles executed by moving blade (Leturia et al., 2014). The FT4 rheometer has an in-built pre-conditioning step that helps uniformly pack the powder particles before the flow property measurement and is followed by splitting (to remove

excess powder particles), and the mass of the MPC powders were automatically recorded. Splitting the conditioning run performed on powders helped to decrease variability between trials due to filling (Bharadwaj et al., 2010). The properties of MPC powders measured using FT4 powder rheometer are described below:

Basic flowability energy (BFE)

The BFE is the basic essential energy required to start a specific flow pattern for an exact volume of conditioned MPC powders during the downward movement of the blade (Leturia et al., 2014). During downward displacement through the MPC powders, the BFE was calculated from work done in the downward traverse of the blade at a constant tip speed of 100 mm/s.

Stability index (SI)

Agglomeration and segregation of MPC powders were evaluated by a stability test. The test cycles were conducted at 100 mm/s blade tip speed with the blade traversing through the MPC powder bed (Leturia et al., 2014). The SI was calculated by using Equation 4.1.

$$\text{SI} = \frac{\text{Total energy consumed at test number 7 (mJ)}}{\text{Total energy consumed at test number 1 (mJ)}} \qquad (4.1)$$

Flow rate index (FRI)

To evaluate the flow rates of MPC powders, the flow energy was measured at four different blade tip speeds (100, 70, 40, and 10 mm/s) during downward traversing of the blade (Freeman, 2007; Leturia et al., 2014). Equation 4.2 was used to calculate the FRI.

$$\text{FRI} = \frac{\text{Flow energy at test 4}}{\text{Flow energy at test 1}} \qquad (4.2)$$

Specific energy (SE)

The specific energy was estimated during the upward navigation of the blade through the MPC powder bed using a very slight shearing and elevating mode of displacement. It gives an

indication of the flow properties of the MPC powder in a loosely packed and unconfined state (Mitra et al., 2017). The value of SE was then determined using Equation 4.3.

$$\mathrm{SE} = \frac{(\text{Upward energy at cycle six} + \text{Upward energy at cycle 7})}{2 \times \text{Split mass}} \qquad (4.3)$$

Compressibility

Compressibility evaluates the change in density as a function of applied normal stress. The MPC powder bed was conditioned and subsequently, after splitting, the vented piston assembly was used to compress the MPC powder samples under increasing normal stress from 0.5 to 15 kPa (0.5, 1, 2, 4, 6, 8, 10, 12, 15 kPa). After reaching equilibrium at the target stress, the distance traveled by the vented piston was measured, and the compressibility was calculated as a percent change in volume (Freeman, 2007; Bian et al., 2015c).

Permeability

A vented piston assembly was used to measure the resistance to air flow across the powder bed and was quantified as the air pressure drop at each applied normal stress from 0.5 to 15 kPa (0.5, 1, 2, 4, 6, 8, 10, 12, 15 kPa). The air flow velocity through the MPC powder bed was maintained at 2 mm/s throughout the test period (Freeman, 2007; Bian et al., 2015c).

Wall friction test

This test measures the ability of MPC powders to flow continuously (steady-state flow) across a container wall material. In this study, wall friction of MPC powders were measured against stainless steel considering its use as the common processing equipment material. The rotational wall friction module used to analyze the MPC samples, it consisted of a serrated base assembly and a wall friction head to induce both normal and shear stresses for wall friction angle (WFA, ϕ) measurement (Freeman, 2007). As the powder bed resisted the rotation of the wall friction head, the torque increased until the resistance was overcome. The torque required to

maintain this rotational momentum was measured as the shear stress. Equation 4 was used to calculate the WFA using the relationship between shear stress (τ_w) and normal stress (σ_w) (Leturia et al., 2014).

$$\phi = \tan^{-1}\left(\frac{\tau_w}{\sigma_w}\right) \qquad (4.4)$$

Shear properties

The shear tests were carried out using the rotational shear cell accessory of the FT4 powder rheometer. The shear properties provide information on the flow of powders at rest and are commonly used to evaluate the flowability of powders during discharge in a process line (Mitra et al., 2017). Shear flow property data is important to design hoppers and select hopper construction material. The rotational shear cell part of the FT4 powder rheometer consists of a vessel with a serrated base with a column containing the MPC sample and a FT4 shear head to achieve both vertical and rotational stresses. The powder shear properties such as unconfined yield strength (UYS), cohesion, angle of internal friction (AIF), and flow function (FF) were measured using the standard shear testing program of the FT4 rheometer. The normal stress was maintained constant at 9 kPa throughout the measurements.

Evaluation of solubility and dissolution behavior

MPC powders were reconstituted at 5% (w/w) powder concentration in distilled water and the solubility of the MPC powders stored at 25 and 40ºC for 12 weeks were estimated based on the total solids in the supernatant obtained by centrifugation at 700 × g for 10 min at 25°C as described by Anema et al. (2006). The amount of soluble material (σ) in the MPC was calculated using Equation 5.

$$\sigma = \frac{weight\ of\ dry\ material}{weight\ of\ solution} \times 100 \qquad (4.5)$$

The dissolution characteristics of the MPC powders stored at 25 and 40ºC were evaluated using focused beam reflectance measurement (FBRM) method described by Hauser and Amamcharla (2016b).

Statistical analysis

The flow and morphological characteristics were analyzed using PROC MIXED in SAS (version 9.4, SAS Institute Inc., Cary, NC) by Tukey's test at a significance P-value of 0.05. The Pearson correlation analysis that summarizes the strength of linear relationships between selected variables were also performed.

Results and discussion

As per the certificate of analysis provided by the manufacturer, the composition of MPC powders used in this study is shown in Table 4.1. As expected, the protein and lactose contents were significantly different ($P < 0.05$) for all the MPC powders used in this study. As the protein content increased from 70.3 to 88.1% (w/w), the lactose content decreased from 16.1 to 0.5% (w/w). On the other hand, the fat content in the MPC powders did not exhibit any significant difference ($P > 0.05$). Differences in physical properties, as influenced by the storage temperature and protein content, were the key factors evaluated in this study. The strength of linear relationships between selected variables is provided in Table 4.2.

Table 4.1 Compositional analysis (%, w/w; means ± SD) of milk protein concentrate (MPC) powders used in this study

Type	Protein (%, w/w)	Fat (%, w/w)	Moisture (%, w/w)	Lactose (%, w/w)	Ash (%)
MPC70	70.3 ± 0.25	1.3 ± 0.05	4.7 ± 0.13	16.1 ± 0.51	6.4 ± 0.06
MPC80	81.5 ± 0.41	1.1 ± 0.06	4.9 ± 0.11	6.6 ± 0.62	6.3 ± 0.13
MPC90	88.1 ± 0.52	1.1 ± 0.07	4.6 ± 0.14	0.5 ± 0.66	6.3 ± 0.11

Table 4.2 Correlation coefficients between selected functional, morphological, and flowability of milk protein concentrate (MPC) powders

Variable	σ	CED	BFE	SI	FRI	SE	UYS	Ch	AIF	FF
Sol	1.00									
CED	-0.27	1.00								
BFE	-0.18	0.97*	1.00							
SI	0.23	-0.86*	-0.92*	1.00						
FRI	-0.42*	0.93*	0.89*	-0.88*	1.00					
SE	-0.18	0.83*	0.86*	-0.97*	0.83*	1.00				
UYS	-0.78*	0.73*	0.65*	-0.65*	0.88*	0.58*	1.00			
Ch	-0.72*	0.74*	0.67*	-0.74*	0.91*	0.71*	0.97*	1.00		
AIF	-0.73*	0.79*	0.70*	-0.64*	0.90*	0.59*	0.99*	0.95*	1.00	
FF	0.86*	-0.59*	-0.53*	0.60*	-0.79*	-0.54*	-0.97*	-0.96*	-0.93*	1.00

σ = solubility index, CED = circle equivalent diameter, BFE = basic flow energy, SI = stability index, FRI = flow rate index, SE = specific energy, UYS = unconfined yield strength, Ch = cohesion, AIF = angle of internal friction, FF = flow function coefficient.
*Pearson's r values (+ve or −ve) are found to be significant ($P < 0.05$).

Microstructure

Figure 4.1 illustrates the SEM micrographs of MPC powders after 12 weeks of storage at 40ºC. The SEM micrograph of MPC70 (stored for 12 weeks at 40ºC) revealed smoother surfaces of milk protein particles when compared to MPC90 and MPC80 stored at the same temperature. Additionally, no major microstructural changes were observed in the state of lactose (due to the collapse of the particle structure) in the MPC powders, demonstrating that higher lactose contents can only cause such structural changes (Fyfe et al., 2011). Figure 4.1B and Figure 4.1C illustrate that MPC80 and MPC90 after 12 weeks of storage at 40ºC had resulted in size alterations in powder particles, indicating more wrinkled particle surfaces. A similar surface appearance (MPC85) was demonstrated in a previous study (Fang et al., 2012) and such surfaces indicated shrinkage of the protein material (Mimouni et al., 2010). After 12 weeks of storage at 40ºC (Figure 4.1D), MPC90 exhibited more holes, broken particles, and roughness on the surface of the particles. These findings agreed with previous studies in MPC powders stored for 30 days

(Fang et al., 2012) and 60 days (Gaiani et al., 2006). Overall, the results from SEM micrographs suggested that MPC powder particles were affected by the protein content.

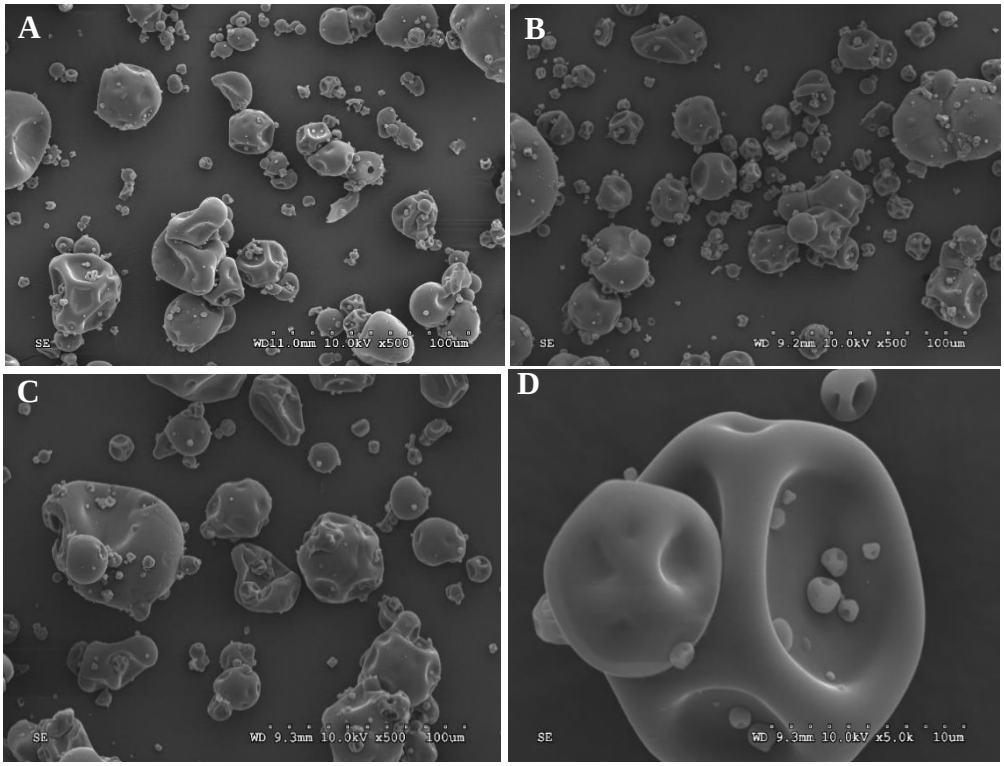

Figure 4.1 Scanning electron micrographs (× 500) of spray dried milk protein concentrate powder (MPC) particles: A) MPC70; B) MPC80; C) MPC90; and D) MPC90 (× 5000) after 12 weeks of storage at 40ºC.

Morphology

The morphological properties of MPC powders after 12 weeks of storage at 25 and 40ºC were investigated, and the results are summarized in Table 4.3. The CED of MPC powder particles increased with the increase in protein content at both storage temperatures (Table 4.3). HSC results confirmed that morphology of MPC90 powder particles after storage at 25ºC exhibited less round-shaped or more irregularly-shaped particles (Table 4.3) when compared to the MPC70 and MPC80. For all the MPC powders HSC increased as the storage temperature increased. At both storage temperatures, the elongation was higher in MPC90 when compared to MPC70, indicating more irregular shaped particles. Interestingly, after storage for 12 weeks at

40ºC, the CED and elongation of MPC90 was ~16% and ~25% lower when compared to MPC90 stored at 25ºC. At both storage temperatures, the convexity was higher in MPC70 when compared to MPC90, indicating higher regular shaped particles in the MPC70. Previously, Li et al. (2016) studied different lactose/milk protein isolate model systems produced in a pilot scale spray dryer and reported that as the protein content increased the circularity and convexity increased, whereas elongation decreased for the resultant powders. However, in the present study, when comparing MPC powders stored at 25°C, circularity, convexity and elongation did not follow the trend reported by Li et al. (2016) and could be attributed to the variations in the spray dryer configurations between the two studies.

Basic flow energy (BFE)

The BFE of MPC powders ranged from 510 to 930 mJ (Table 4.4). For the powders stored at 25ºC, the BFE increased significantly ($P < 0.05$) with an increase in protein content from 70 to 90%. This indicated that the energy required to initiate the flow for MPC70 is less compared to the MPC80 and MPC90. A lower BFE requirement for MPC70 at both storage temperatures could be attributed to its particle morphology in terms of lower CED, higher HSC (less irregular shaped particles), and higher convexity. In addition to the morphological characteristics, chemical characteristics such as protein-protein interactions are less in MPC70 compared to MPC80 and MPC90 and consequently resulted in a lower BFE in MPC70. Moreover, the lactose content of MPC70 was 16.1% and lactose can act as a molecular spacer and can potentially limit the protein-protein interactions, thus improving flowability. On the other hand, higher BFE requirement in MPC80 and MPC90 is attributed to morphology (CED, HSC, and convexity) of its powder particles and greater protein-protein interactions on the surface of the powder particles in MPC80 and MPC90. The MPC80 and MPC90 contained 6.6

and 0.5% lactose, respectively and consequently more protein-protein interactions on the surface of the powder particles (Havea, 2006). The Pearson correlation (Table 4.2) revealed a positive correlation between CED and BFE (r = 0.97).

MPC90 stored at 25ºC showed a BFE of 930 mJ, whereas MPC90 stored at 40ºC had a BFE of 722 mJ, which was ~22% lower when compared to MPC90 stored at 25ºC. Similarly, MPC80 stored at 25ºC had a BFE of 695 mJ, which was ~11% higher when compared to MPC80 stored at 40ºC. Therefore, after storage for 12 weeks at 40ºC, only less energy was required to initiate the flow in MPC80 and MPC90. This could be due to the fact that coarse powders in general have better flow properties than fine powders (Li et al., 2017). Lapčík et al. (2015) reported low BFE values ranging from 127 mJ to 157 mJ for SMP, demineralized whey powder, and whey powders. Whereas, BFE >750 mJ was observed by Mitra et al. (2017) for *basundi* (heat-desiccated Indian dairy sweet) dry mix. Overall, the results indicated that MPC80 and MPC90 required more energy to initiate the flow when compared to MPC70 and may require more energy during bulk handling of MPC powders.

Stability index (SI), flow rate index (FRI), and specific energy (SE)

SI showed no significant differences (P > 0.05) with an increase in protein content and storage temperature (Table 4.4). Bian et al. (2015a) defined that the powder is stable if the SI values fall in the range of 0.9 to 1.1, indicating no segregation and disintegration during flow. On the other hand, the powders with SI values less than 0.9 and more than 1.1 would be considered unstable (Bian et al., 2015a). After storage for 12 weeks at 25ºC, SI value was highest for MPC70 (1.04), suggesting MPC70 is a stable powder (better flowability) with less segregation during flow. At both the storage temperature (25 and 40ºC) the MPC powders were found to be stable and did not agglomerate during flow testing.

The FRI values were less than 1.73, indicating the MPC powders have exhibited average flow rate sensitivities indicating less cohesiveness (Leturia et al., 2014). The FRI of MPC90 and MPC80 were significantly ($P < 0.05$) higher than that of MPC70 (Table 4.4). As expected, the MPC70 had the lowest FRI value because of its low cohesiveness (Table 4.5). The low FRI values in MPC70 compared to MPC80 and MPC90 indicated less interlocking of the powder particles (Jan et al., 2017) and suggested less irregular shaped particles (Table 4.3). The increase in storage temperature showed no significant difference ($P > 0.05$) on the FRI of MPC powders. Indeed, in MPC powders, due to the presence of entrapped air, the powders were slightly influenced by flow rate (Mitra et al., 2017).

SE indicated how easily MPC powders will flow in an unconfined environment, signifying relative cohesion of the MPC powders under low-stress conditions and SE demonstrates the energy needed to establish a specific flow pattern in a pre-conditioned and precise volume of MPC powders (Freeman, 2007; Freeman and Fu, 2008; Jan et al., 2017). The SE increased significantly ($P < 0.05$) with the increase in protein content (Table 4.4). SE values ranged from 18 to 24 mJ/g and higher values indicated that MPC80 and MPC90 were less flowable when compared to MPC70. Morphological results showed that MPC90 has higher CED, and therefore higher particle interlocking could occur during the transition of the blade through the MPC powder bed (Bharadwaj et al., 2010). MPC70 had the lowest SE value, indicating that it was the least cohesive sample at controlled condition state and suggested that it flows readily in a low stress and conditioned state. The lower SE values in MPC70 could be further explained with less particle interlocking because of comparatively smoother surfaces in MPC70. However, MPC90 showed highest (24.4 mJ/g) SE value, indicating it to be more cohesive.

Overall, the bulk flow results were correlated (Table 4.2) with the CED, indicating that MPC powders comprised of more regular shaped particles (high HSC) flow better than those with irregularly shaped particles. The increment of BFE and SE with increasing protein content and storage temperature could be attributed to the lower flowability, higher cohesion, and increased packing of finer particles in void spaces (Mitra et al., 2017). SEM micrographs (Figure 1D) confirmed the presence and packing of such smaller particles in the MPC90 samples stored at 40ºC.

Table 4.3 Morphological characteristics of milk protein concentrate (MPC) powders after 12 weeks of storage at 25 and 40ºC

Type	Circle Equivalent Diameter (μm)		High Sensitivity Circularity[1]		Elongation[2]		Convexity[3]	
	25ºC	40ºC	25ºC	40ºC	25ºC	40ºC	25ºC	40ºC
MPC70	$13.51 \pm 0.06^{a,x}$	$14.12 \pm 0.01^{a,y}$	$0.874 \pm 0.002^{a,x}$	$0.890 \pm 0.002^{a,y}$	$0.196 \pm 0.004^{a,x}$	$0.177 \pm 0.001^{a,y}$	$0.992 \pm 0.001^{a,x}$	$0.991 \pm 0.000^{a,y}$
MPC80	$17.06 \pm 0.12^{b,x}$	$15.06 \pm 0.35^{b,y}$	$0.874 \pm 0.001^{a,x}$	$0.892 \pm 0.001^{a,y}$	$0.186 \pm 0.001^{b,x}$	$0.171 \pm 0.001^{b,y}$	$0.988 \pm 0.000^{b,x}$	$0.991 \pm 0.001^{a,y}$
MPC90	$22.85 \pm 0.02^{c,x}$	$19.68 \pm 0.05^{c,y}$	$0.831 \pm 0.001^{b,x}$	$0.879 \pm 0.002^{b,y}$	$0.227 \pm 0.001^{c,x}$	$0.181 \pm 0.003^{c,y}$	$0.981 \pm 0.000^{c,x}$	$0.988 \pm 0.000^{b,y}$

[a-c]Mean values for different protein contents within a column with different superscript differ ($P < 0.05$).

[x, y]Mean values for the storage temperatures within a morphological parameter with a different letter differ ($P < 0.05$).

[1]High sensitivity circularity or HSC (range 0-1; a powder particle with perfect circle has a circularity of 1 whereas an irregularly shaped powder particle has a circularity value closer to 0).

[2]Elongation (range 0-1; shapes with large aspect ratios have an elongation closer to 1 whereas a circle or square-shaped powder particle have an elongation value of 0).

[3]Convexity (range 0-1; a smooth-shaped powder particle has a convexity of 1 whereas an irregularly shaped powder particle has a convexity closer to 0).

Table 4.4 Dynamic flow properties of milk protein concentrate (MPC) powders after 12 weeks of storage at 25 and 40ºC

Type	Basic flow energy (BFE; mJ)		Stability index (SI)		Flow rate index (FRI)		Specific energy (SE; mJ/g)	
	25ºC	40ºC	25ºC	40ºC	25ºC	40ºC	25ºC	40ºC
MPC70	$510.09 \pm 12.32^{a,x}$	$512.53 \pm 9.60^{a,x}$	$1.04 \pm 0.02^{a,x}$	$1.05 \pm 0.02^{a,x}$	$1.52 \pm 0.01^{a,x}$	$1.49 \pm 0.05^{a,x}$	$18.92 \pm 0.01^{a,x}$	$18.34 \pm 0.05^{a,x}$
MPC80	$695.09 \pm 5.01^{b,x}$	$617.37 \pm 10.01^{b,y}$	$0.97 \pm 0.01^{a,x}$	$0.98 \pm 0.02^{a,x}$	$1.57 \pm 0.04^{b,x}$	$1.60 \pm 0.02^{b,x}$	$24.14 \pm 0.04^{b,x}$	$22.01 \pm 0.02^{b,x}$
MPC90	$930.75 \pm 1.54^{c,x}$	$722.46 \pm 2.15^{c,y}$	$0.94 \pm 0.01^{a,x}$	$0.97 \pm 0.01^{a,x}$	$1.73 \pm 0.01^{c,x}$	$1.71 \pm 0.01^{c,x}$	$24.43 \pm 0.03^{b,x}$	$23.92 \pm 0.04^{b,x}$

[a-c]Mean values for different protein contents within a column with different superscript differ ($P < 0.05$).

[x, y]Mean values for the storage temperatures within a dynamic flow parameter with a different letter differ ($P < 0.05$).

Compressibility

Compressibility results showed that the percent change in volume increased with normal stress applied to all the MPC powders (Figure 4.2). Indeed, the increase in percent change in volume with increase in normal stress applied for the MPC powders would be due to the closer particle packing and increase in interparticle surface contact (Bian et al, 2015b; Jan et al., 2017). The difference in protein contents and storage temperatures did not exhibit any noticeable effect on the compressibility. Compressibility at 15 kPa pressure suggested that MPC90 (both at 25 and 40ºC) when compared to MPC70 and MPC80 were less compressible, indicating coarser and irregular particles. Compressibility results could be related to the difference in composition, particle morphology, particle interlocking, and interparticle interactions in MPC powders after storage. Furthermore, fine particles exhibit higher compressibility than the coarser ones because of the greater surface area and fewer voids (Jan et al., 2017). Overall, particle morphology and particle interlocking after storage for 12 weeks at 20 and 40ºC have marginally influenced the compressibility, indicating less compressibility related constraints in the handling of stored MPC powders.

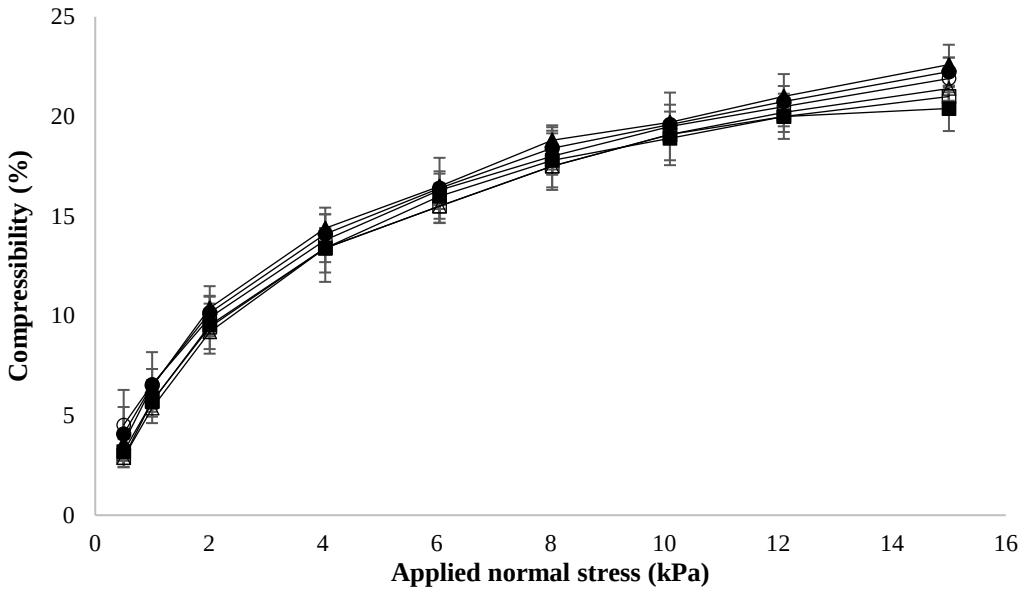

Figure 4.2 Compressibility of the milk protein concentrate (MPC)70 (triangle), MPC80 (circle), and MPC90 (square) after 12 weeks of storage at 25ºC (solid) and 40ºC (open) after 12 weeks of storage. Values are the means of data from duplicate analysis.

Permeability

Permeability is a measure of the powder particles resistance to air flow. Evaluating permeability of MPC powders is important to understand their flow during handling and processing. Knowledge of powder permeability is also important in developing efficient unloading strategies (Bian et al., 2015c). MPC90 showed the lowest pressure drop, indicating higher permeability (Figure 4.3). Above normal stress of 8 kPa, the increase in pressure drop for MPC80 and MPC70 stored at 40ºC was low when compared with MPC80 and MPC70 stored at 25ºC, indicating higher permeability for the powders stored at 40ºC. Higher permeability of MPC90 could be related to its higher CED and irregular shape (lower HSC), indicating a larger void structure. However, in MPC70 after storage for 12 weeks, the rearrangement of particles might have reduced the interparticle void spaces (Bian et al., 2016c), resulting in an increased pressure drop and reduced permeability. Compared to MPC80, MPC90 has a lower pressure drop and is therefore more permeable (regardless of its comparable compressibility results), indicating

the influence of particle shape on packing structure when particle size distributions of the powders are similar (Siliveru et al., 2016a; Siliveru et al., 2016b).

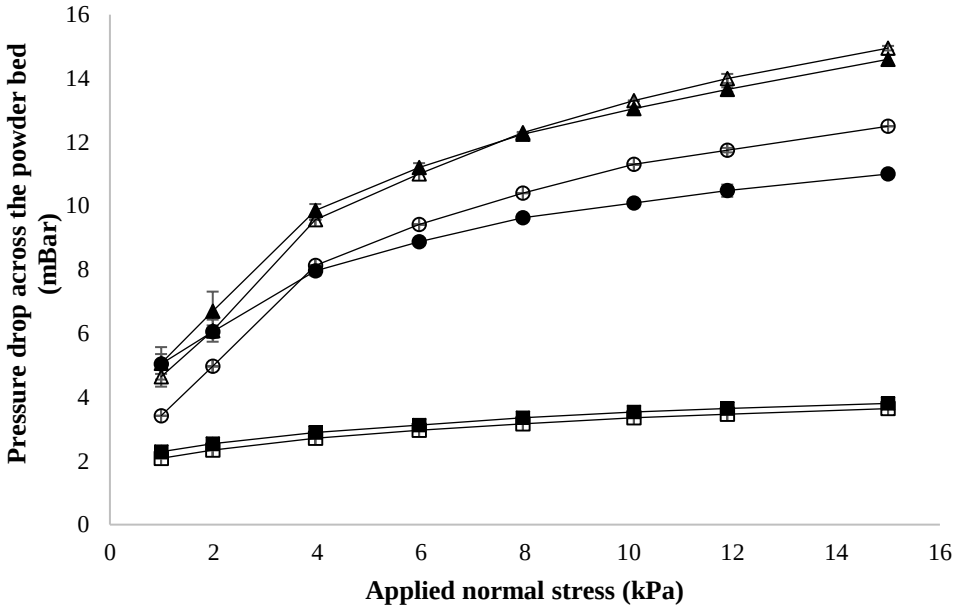

Figure 4.3 Effect of applied normal stress on pressure drop across the milk protein concentrate (MPC) powders: MPC70 (triangle), MPC80 (circle), and MPC90 (square) after 12 weeks of storage at 25ºC (solid) and 40ºC (open). Values are the means of data from duplicate analysis.

Wall friction

Figure 4.4shows the WFA values of MPC powders stored at 25 and 40ºC for 12 weeks and illustrates possible flow constraints due to frictional resistance in MPC powder particles on bin or hopper wall material. The influence of protein content and storage temperature on WFA was notable as observed from Figure 4. The increase in storage temperature had a significant effect on the WFA ($P < 0.05$) in MPC powders, indicating an associated increase in wall-particle interactions. There exists a difficulty in interpreting the exact reasons for the observed increase in wall friction with temperature and protein content for some powders and a decrease for other powders. Iqbal and Fitzpatrick (2006) also reported the effect of storage conditions on the wall friction characteristics of whey permeate powder and concluded that it is difficult to interpret why wall friction increases with temperature for some powders and decreases for other. Higher

values of WFA in MPC90 stored (12 weeks) at 25 and 40ºC were in accordance with increasing cohesivity (Table 4.5), which was within the range of values (11.8 to 27.3º) reported by Fitzpatrick et al. (2004a) for various food powders. The larger WFA in MPC powders indicated higher wall friction and greater deposition or segregation on the wall (Iqbal and Fitzpatrick, 2006; Crowley et al., 2014). WFA was higher in MPC90 when compared to MPC80, suggesting particle shape influenced WFA. Higher WFA values indicated that MPC90 have a greater chance of adhesion in a hopper/bin wall material, suggesting that steeper hopper angle is required to obtain consistent and reliable bulk flow in MPC90. Previously, Fitzpatrick et al. (2007) found that whey permeate powder stored at 30ºC had less WFA when compared to the powder stored at 15ºC. For comparison, Crowley et al. (2014) reported lower WFA values (18º) for MPC70 and comparatively higher WFA values (19.6º) for MPC90.

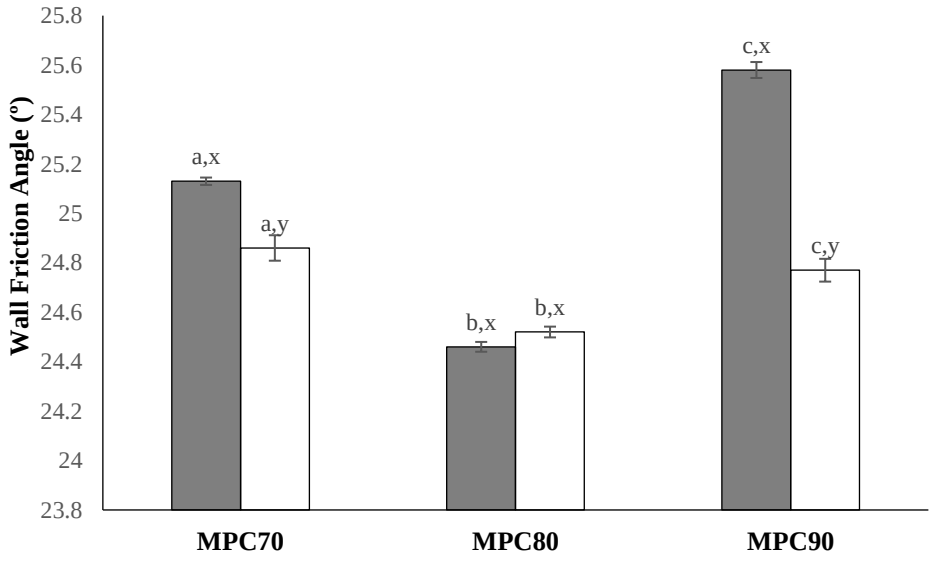

Figure 4.4 Wall friction angle of the milk protein concentrate (MPC) powders after 12 weeks of storage at 25ºC (solid) and 40ºC (open) after 12 weeks of storage. Values are the means of data from duplicate analysis. Error bars indicate SD.

[a,b]Mean values for different protein content with different alphabets differ ($P < 0.05$).
[x,y]Mean values for the storage temperature with a different letter differ ($P < 0.05$).

Shear properties

Protein content and storage temperature have influenced the shear flow properties and the results are shown in Table 4.5. The UYS values of the MPC powders increased with the increase in protein content and storage temperature (Table 4.5), indicating that more cohesive interactions between the particles of MPC powders. The UYS increased from 2.57 to 3.12 kPa with an increase in protein content from 70 to 90% for samples stored for 12 weeks at 25ºC. For MPC70, the UYS has significantly increased ($P < 0.05$) from 2.57 to 2.73 kPa with an increase in storage temperature from 25 to 40ºC. At both storage temperatures, the particles of MPC90 powders were more resistant to flow than MPC70 powder particles. Irregular particle shape could be a possible reason for the higher UYS values of MPC90 than MPC70. Teunou et al. (1999) reported that for whey permeate powders, the UYS increased after storage for 1 week at 20ºC at a maximum consolidating stress of 40 kPa. Previously, Lapčík et al. (2015) observed the UYS of SMP and whey powders to be 4.48 and 4.69 kPa, respectively.

A significant increase ($P < 0.05$) in cohesion values were observed with the increase in protein content and storage temperature. Possible reasons for this could be differences in particle arrangement and particle interlocking in MPC powders after storage for 12 weeks at 25 and 40ºC. Although the lactose content was higher in MPC70, the increased storage temperature did not increase the cohesion because the glass transition temperature of MPC was higher than the storage temperatures used in this study (Li et al., 2016). There was a positive correlation (Table 4.2) of cohesion to FRI ($r = 0.91$), indicating cohesive powders were more sensitive to flow rate because of the presence of entrained air (Mitra et al., 2017). There was a positive correlation (Table 2) of CED to cohesion ($r = 0.74$). This suggests that particle morphology imparts significant flow changes. MPC90 showed cohesion values ~34% higher than MPC70 due to

larger CED in MPC90. Similarly, MPC80 showed cohesion values ~15% higher than MPC70, suggesting less particle-particle interlocking and resistance to flow in MPC70. The higher cohesion in MPC90 could be due to its higher protein content, differences in particle shape, particle interlocking, packing of smaller particles in void spaces, and surface irregularity (Figure 1D) enabling higher cohesive interactions (Teunou and Fitzpatrick, 2000; Siliveru et al., 2016b, Siliveru et al., 2017). The poor flow of MPC80 and MPC90 was probably due to high CED (Table 4.3), which may be due to increased particle-particle interactions and particle interlocking. Previously, Fitzpatrick et al. (2007) reported that rennet casein and sodium caseinate powders were also cohesive. Although the flowability of MPC powders after storage has not been previously characterized, Crowley et al. (2014) reported that more cohesive interactions occurred between particles in high-protein MPC powders.

Significant increase ($P < 0.05$) in AIF values were observed with the increase in protein content and storage temperature, indicating flow constraints (Table 4.5). The AIF values increased from 40.38º to 41.35º and 34.55º to 36.28º with an increase in temperature from 25 to 40ºC for MPC90 and MPC70, respectively. In comparison, Lapčík et al. (2015) have observed the AIF of 26.5, 36.4 and 40.4º for whey, DPW, and SMP, respectively. SEM micrographs and morphology of MPC powder particles evidently showed that elevated storage temperature increased the particle to particle interlocking due to higher intermolecular attractions among MPC powder particles (Scoville and Peleg, 1981; Anema et al., 2006; Nasser et al., 2017).

According to the Jenike's flow classification (Jenike, 1964), a powder is cohesive if its flow function is < 4 and easy flowing if its flow function is within 4-10. All the MPC powders stored at 25 and 40ºC storage temperature showed a flow function of > 4. A significant decrease ($P < 0.05$) in FF values were observed with the increase in protein content and storage

temperature, indicating potential flow issues. Significantly higher ($P < 0.05$) FF values were observed for MPC70 compared to MPC80 and MPC90, indicating that the powders will tend to become comparatively more cohesive with the increase in the protein content. However, with an increase in storage temperature, the FF values slightly decreased, indicating that the MPC powders tend to become cohesive at higher temperature. Furthermore, the microstructure and morphological results showed that MP70 had a higher proportion of regularly shaped particles and a comparatively smoother surface (Table 4.3), which confirms that MPC70 was more easy-flowing or less cohesive than MPC80 and MPC90.

Table 4.5 Shear flow properties of milk protein concentrate (MPC) powders after 12 weeks of storage at 25 and 40ºC

Type	Unconfined yield stress (kPa)		Cohesion (kPa)		Angle of internal friction (º)		Flow function coefficient	
	25ºC	40ºC	25ºC	40ºC	25ºC	40ºC	25ºC	40ºC
MPC70	$2.57 \pm 0.01^{a,x}$	$2.73 \pm 0.05^{a,y}$	$0.58 \pm 0.02^{a,x}$	$0.61 \pm 0.01^{a,y}$	$34.55 \pm 0.04^{a,x}$	$36.28 \pm 0.01^{a,y}$	$6.06 \pm 0.01^{a,x}$	$5.72 \pm 0.01^{a,y}$
MPC80	$2.61 \pm 0.07^{a,x}$	$2.97 \pm 0.01^{a,y}$	$0.63 \pm 0.02^{b,x}$	$0.72 \pm 0.01^{b,y}$	$34.96 \pm 0.01^{b,x}$	$37.63 \pm 0.01^{b,y}$	$5.92 \pm 0.01^{b,x}$	$5.15 \pm 0.01^{b,y}$
MPC90	$3.12 \pm 0.01^{b,x}$	$3.24 \pm 0.11^{b,y}$	$0.75 \pm 0.03^{c,x}$	$0.82 \pm 0.01^{c,y}$	$40.38 \pm 0.01^{c,x}$	$41.35 \pm 0.01^{c,y}$	$5.24 \pm 0.05^{c,x}$	$4.91 \pm 0.02^{c,y}$

[a-c]Mean values for different protein contents within a column with different superscript differ ($P < 0.05$).

[x, y]Mean values for the storage temperatures within a shear flow parameter with a different letter differ ($P < 0.05$).

Solubility index and dissolution behavior after storage

The solubility index of MPC70, MPC80, and MPC90 after storage for 12 weeks at 25ºC was 88.2, 78.2, and 51.3%, respectively. Whereas, after storage for 12 weeks at 40ºC, the solubility index of MPC70, MPC80, and MPC90 was 38.8, 31.6, and 24.6%, respectively. The MPC powders stored at 25ºC exhibited a higher solubility index as compared to powders stored at 40ºC. Additionally, the solubility decreased with the increase in the protein content from 70 to 90%. Previous studies reported that the solubility of MPC powders is higher immediately after production and decreases with the increase in storage time and temperature (Anema et al., 2006; Fyfe et al., 2011), which were in agreement with the results from this study. Also, the increase in protein content negatively impacted the solubility (Gazi and Huppertz, 2015). In addition to solubility index, the dissolution characteristics observed from FBRM results also confirmed that the solubility of MPC powder was influenced by the protein content and storage temperature. The changes in the fine particle counts (<10 µm chord length) for the MPC powders obtained from the FBRM are provided in Figure 4.5. It was observed that fine particle counts (Figure 5) increased at a higher rate for MPC powders stored at 25ºC compared to the MPC powders stored at 40ºC. Additionally, the slow disintegration of large powder particles into fine particles for the powders stored at 40ºC further confirms the negative effect of storage temperature on the MPC powders. Similar observations were obtained in previous studies (Hauser and Amamcharla, 2016b; Gandhi et al., 2017). Storing the MPC powders for 12 weeks at 40ºC resulted in crosslinking networks at the surface of the MPC powders (Anema et al., 2006). These crosslinking networks include interactions between hydrophobic caseins and whey proteins, which hinders the hydration in the MPC powders (Anema et al., 2006; Uluko et al., 2016). As the protein content increased in MPC powders from 70 to 90% (w/w), the MPC90 showed more

primary particle aggregates and exhibited more resistance to dispersing in water (Crowley et al., 2015). Also, with the increase in storage temperature, the protein-protein aggregation/association increased, as shown by lesser counts of fine particles as observed using the FBRM.

Compared to MPC90 and MPC80, MPC70 had a better solubility, indicating the powder particles were less closely packed and thereby decreasing the chances for intermolecular reactions (Anema et al., 2006). Indeed, higher protein contents and higher storage temperature increased these intermolecular interactions leading to higher protein linkages which consequently adversely affected the shear behavior of MPC powders. Interestingly, we have observed that changes in solubility index could be correlated decently with the shear test results (Table 4.2). There was a positive correlation of UYS, cohesion, and FF to solubility index ($r = 0.78$, 0.72, and 0.86, respectively). The MPC powders with poor dissolution characteristics also exhibited poor shear behavior. Moreover, storage for 12 weeks has induced a substantial rearrangement at the MPC powder particle surface (Nasser et al., 2017). SEM micrographs (Figure 1) also showed the presence of surface roughness and packing of smaller particles in void spaces in the powder with 90% (w/w) protein content, corresponding to storage for 12 weeks at 40ºC. Overall, cohesion, AIF, and FF were significantly different ($P < 0.05$) for MPC70, MPC80, and MPC90 (after storage at both 25 and 40ºC) samples and results indicated that under consolidation the flow behavior of MPC70 would be better than MPC80 and MPC90. Thus, on prolonged storage, the cohesion forces developed between the MPC powder particles subsequently lead to a higher bulk cohesion (Fitzpatrick et al., 2007). The results also suggested that modification of MPC powder particle shape could improve the flow of MPC powders.

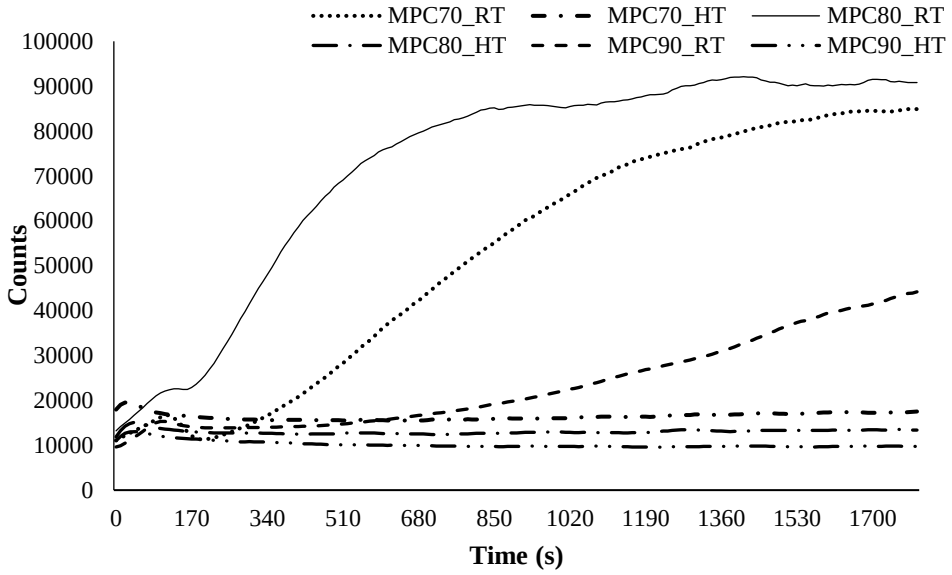

Figure 4.5 Changes in counts of fine particles (<10 μm) after 12 weeks of storage as obtained from focused beam reflectance measurement for the milk protein concentrate (MPC) powders: (a) MPC70, (b) MPC80, (c) MPC90 stored at 25ºC; (d) MPC70, (e) MPC80, (f) MPC90 stored at 40ºC.

Acknowledgments

Technical assistance from Dr. Kingsly Ambrose (Department of Agricultural and Biological Engineering, Purdue University) with the powder flow experiments and morphology characterization; Dr. Kaliramesh Siliveru and Dr. Praveen Vadlani (Department of Grain Science and Industry, Kansas State University) with the flowability experiments, is greatly appreciated.

Conclusions

This study investigated the effect of protein content and storage temperature on particle morphology and flow properties of stored MPC powders (12 weeks). Processing and subsequent storage resulted in MPC powders with varying physical and functional characteristics which sequentially influenced the flowability. The BFE and SE of the MPC powders increased with an increase in protein content, indicating bulk flow challenges and higher energy requirement for making the powder flow at unconfined conditions. The interparticle interactions and particle interlocking have influenced the flow behavior of MPC powders after prolonged storage at 25

and 40ºC. Shear tests showed that the MPC powders were more cohesive with the increase in protein content and storage temperature. The shear flow properties of MPC powders were influenced by particle morphology and particle interlocking. Overall, the results indicated that differences in protein content and storage temperature affected the particle morphology and flow behavior of stored MPC powders.

References

Abdalla, A. K., K. Smith and J. Lucey. 2017. Bulk density and flowability of nonfat dry milk and skim milk powder. Egyptian Journal of Dairy Science. 45:17-24.

Agarwal, S., R. L. W. Beausire, S. Patel, and H. Patel. 2015. Innovative uses of milk protein concentrates in product development. J. Food Sci. 80:A23–A29.

Anema, S. G., D. N. Pinder, R. J. Hunter and Y. Hemar. 2006. Effects of storage temperature on the solubility of milk protein concentrate (MPC85). Food Hydrocoll. 20:386-393.

Bansal, N., T. Truong and B. Bhandari. 2017. Feasibility study of lecithin nanovesicles as spacers to improve the solubility of milk protein concentrate powder during storage. Dairy Sci. Technol. 96:861-872.

Bharadwaj, R, W. R. Ketterhagen, B. C. Hancock. 2010. Discrete element simulation study of a Freeman powder rheometer. Chemical Engineering Science 65(21):5747-56.

Bian, Q., R. P. K. Ambrose and Bh. Subramanyam. 2015a. Effect of chaff on bulk flow properties of wheat. J. Stored Prod. Res. 64:21-26.

Bian, Q., R. P. K. Ambrose and Bh. Subramanyam. 2015b. Effects of insect-infested kernels on bulk flow properties of wheat. J. Stored Prod. Res. 63:51-56.

Bian, Q., S. Sittipod, A. Garg and R. P. K. Ambrose. 2015c. Bulk flow properties of hard and soft wheat flours. J. Cereal Sci. 63:88-94.

Crowley, S. V., I. Gazi, A. L. Kelly, T. Huppertz and J. A. O'Mahony. 2014. Influence of protein concentration on the physical characteristics and flow properties of milk protein concentrate powders. J. Food Eng. 135:31-38.

Crowley, S. V., B. Desautel, I. Gazi, A. L. Kelly, T. Huppertz and J. A. O'Mahony. 2015. Rehydration characteristics of milk protein concentrate powders. J. Food Eng. 149:105-113.

Eshpari, H., P. S. Tong and M. Corredig. 2014a. Changes in the physical properties, solubility, and heat stability of milk protein concentrates prepared from partially acidified milk. J. Dairy Sci. 97:7394-7401.

Fang, Y., S. Rogers, C. Selomulya and X. D. Chen. 2012. Functionality of milk protein concentrate: Effect of spray drying temperature. Biochem. Eng. J. 62:101-105.

Fitzpatrick, J.J., K. Barry, P.S.M. Cerqueira, T. Iqbal, J. O'Neill, and Y.H. Roos. 2007. Effect of composition and storage conditions on the flowability of dairy powders. Int. Dairy J.17:383–392.

Fitzpatrick, J. J., S. A. Barringer and T. Iqbal. 2004a. Flow property measurement of food powders and sensitivity of jenike's hopper design methodology to the measured values. J. Food Eng. 61:399-405.

Fitzpatrick, J. J., T. Iqbal, C. Delaney, T. Twomey and M. K. Keogh. 2004b. Effect of powder properties and storage conditions on the flowability of milk powders with different fat contents. J. Food Eng. 64:435-444.

Freeman, R. 2007. Measuring the flow properties of consolidated, conditioned and aerated powders—a comparative study using a powder rheometer and a rotational shear cell. Powder Technol. 174:25-33.

Freeman, R., and X. Fu. 2008. Characterisation of powder bulk, dynamic flow and shear properties in relation to die filling. Powder Metallurgy 51:196–201.

Fyfe, K. N., O. Kravchuk, T. Le, H. C. Deeth, A. V. Nguyen and B. Bhandari. 2011. Storage induced changes to high protein powders: Influence on surface properties and solubility. J. Sci. Food Agric. 91:2566-2575.

Gaiani, C., J. J. Ehrhardt, J. Scher, J. Hardy, S. Desobry and S. Banon. 2006. Surface composition of dairy powders observed by X-ray photoelectron spectroscopy and effects on their rehydration properties. Colloids and Surfaces B: Biointerfaces. 49:71-78.

Gandhi, G., J. K. Amamcharla and D. Boyle. 2017. Effect of milk protein concentrate (MPC80) quality on susceptibility to fouling during thermal processing. LWT-Food Science and Technology. 81:170-179.

Gazi, I. and T. Huppertz. 2015. Influence of protein content and storage conditions on the solubility of caseins and whey proteins in milk protein concentrates. Int. Dairy J. 46:22-30.

Hauser, M. and J. K. Amamcharla. 2016a. Development of a method to characterize high-protein dairy powders using an ultrasonic flaw detector. J. Dairy Sci. 99:1056-1064.

Hauser, M. and J. K. Amamcharla. 2016b. Novel methods to study the effect of protein content and dissolution temperature on the solubility of milk protein concentrate: Focused beam reflectance and ultrasonic flaw detector-based methods. J. Dairy Sci. 99:3334-3344.

Havea, P. 2006. Protein interactions in milk protein concentrate powders. Int. Dairy J. 16: 415–422.

Huffman, L.M., and W. James Harper. 1999. Maximizing the Value of Milk Through Separation Technologies. J. Dairy Sci. 82(10):2238–2244.

Iqbal, T. and J. J. Fitzpatrick. 2006. Effect of storage conditions on the wall friction characteristics of three food powders. J. Food Eng. 72:273-280.

Jan, S., C. Ghoroi and D. C. Saxena. 2017. A comparative study of flow properties of basmati and non-basmati rice flour from two different mills. J. Cereal Sci. 76:165-172.

Jenike, A. W. 1976. Storage and Flow of Solids, Bulletin No. 123 (Utah Engineering Station, Salt Lake City, Utah)

Ji, J., J. Fitzpatrick, K. Cronin, M. A. Fenelon and S. Miao. 2017. The effects of fluidised bed and high shear mixer granulation processes on water adsorption and flow properties of milk protein isolate powder. J. Food Eng. 192:19-27.

Juliano, P. and G. V. Barbosa-Canovas. 2010. Food powders flowability characterization: Theory, methods, and applications. Annu. Rev. Food Sci. Technol. 1:211-239.

Kim, E. H., X. D. Chen and D. Pearce. 2005. Effect of surface composition on the flowability of industrial spray-dried dairy powders. Colloids and Surfaces B: Biointerfaces. 46:182-187.

Krantz, M., H. Zhang and J. Zhu. 2009. Characterization of powder flow: Static and dynamic testing. Powder Technol. 194:239-245.

Lapčík, L., B. Lapčíková, E. Otyepková, M. Otyepka, J. Vlček, F. Buňka and R. N. Salek. 2015. Surface energy analysis (SEA) and rheology of powder milk dairy products. Food Chem. 174:25-30.

Leturia, M., M. Benali, S. Lagarde, I. Ronga and K. Saleh. 2014. Characterization of flow properties of cohesive powders: A comparative study of traditional and new testing methods. Powder Technol. 253:406-423.

Li, R., Y. H. Roos and S. Miao. 2016. The effect of water plasticization and lactose content on flow properties of dairy model solids. J. Food Eng. 170:50-57.

Mimouni, A., H. C. Deeth, A. K. Whittaker, M. J. Gidley and B. R. Bhandari. 2010. Investigation of the microstructure of milk protein concentrate powders during rehydration: Alterations during storage. Journal of Dairy Science. 93:463-472.

Mitra, H., H. A. Pushpadass, M. E. E. Franklin, R. P. K. Ambrose, C. Ghoroi and S. N. Battula. 2017. Influence of moisture content on the flow properties of basundi mix. Powder Technol. 312:133-143.

Nasser, S., R. Jeantet, P. De-Sa-Peixoto, G. Ronse, N. Nuns, F. Pourpoint, J. Burgain, C. Gaiani, A. Hdoux and G. Delaplace. 2017. Microstructure evolution of micellar casein powder upon ageing: Consequences on rehydration dynamics. J. Food Eng. 206:57-66.

Rennie, P. R., X. D. Chen, C. Hargreaves and A. R. Mackereth. 1999. A study of the cohesion of dairy powders. J. Food Eng. 39:277-284.

Scoville, E. and M. Peleg. 1981. Evaluation of the effects of liquid bridges on the bulk properties of model powders. J. Food Sci. 46:174-177.

Siliveru, K., C. G. Jange, J. W. Kwek and R. P. K. Ambrose. 2017. Granular bond number model to predict the flow of fine flour powders using particle properties. J. Food Eng. 208:11-18.

Siliveru, K., R. P. K. Ambrose and P. V. Vadlani. 2016b. Significance of composition and particle size on the shear flow properties of wheat flour. J. Sci. Food Agric. 97:2300-2306.

Siliveru, K., J. W. Kwek, G. M. Lau and R. P. K. Ambrose. 2016a. An image analysis approach to understand the differences in flour particle surface and shape characteristics. Cereal Chem. 93:234-241.

Silva, J. V. and J. A. O'Mahony. 2017. Flowability and wetting behaviour of milk protein ingredients as influenced by powder composition, particle size and microstructure. Int. J. of Dairy Technol. 70:277-286.

Szulc, K., J. Estkowski, A. Tuwalski and A. Lenart. 2017. Effect of water activity on flowability of infant milk powders of various raw material composition. Issues. 2016:2014.

Teunou, E., J. J. Fitzpatrick and E. C. Synnott. 1999. Characterisation of food powder flowability. J. Food Eng. 39:31-37.

Teunou, E. and J. J. Fitzpatrick. 2000. Effect of storage time and consolidation on food powder flowability. J. Food Eng. 43:97-101.

Uluko, H., L. Liu, J. Lv and S. Zhang. 2016. Functional characteristics of milk protein concentrates and their modification. Crit. Rev. Food Sci. Nutr. 56:1193-1208.

Chapter 5 - Application of front-face fluorescence spectroscopy as a tool for monitoring changes in milk protein concentrate powders during storage

Abstract

This study investigated the feasibility of front-face fluorescence spectroscopy (FFFS) to predict the solubility index and relative dissolution index (RDI) of milk protein concentrate (MPC) powders during storage. Twenty MPC powders with varying protein contents from 4 different commercial manufacturers were used in this study. MPC powders were stored at 2 temperatures (25 and 40ºC) for 0, 1, 2, 4, 8, and 12 weeks. The front-face fluorescence spectra of tryptophan and Maillard products were recorded and analyzed with chemometrics to predict the solubility index and RDI of MPC powders. The similarity maps showed clear discrimination of the MPC samples stored at 25 and 40ºC. Partial least square regression (PLSR) models were developed using the fluorescence spectra of tryptophan and Maillard products to predict the solubility index and RDI measurements of MPC powders and the prediction models were validated using the full cross-validation method. A correlation coefficient (R^2) of 0.78, 0.83, and 0.76 were obtained between fluorescence spectra (tryptophan emission, Maillard emission, and Maillard excitation, respectively) and solubility index. The R^2 value for the RDI predictions were 0.74 and 0.71 for the dataset of tryptophan emission and Maillard emission, respectively. The ratio of prediction error to standard deviation was >2 and ~2 for reference solubility index and RDI measurements, respectively. The results indicated that the solubility and dissolution behavior of MPC powders were related to their protein content and storage conditions that could

[1]Submitted for publication: Journal of Dairy Science

be monitored and measured using FFFS. Hence, FFFS can be used as a rapid and nondestructive analytical technique to predict the solubility and dissolution charecteristics of MPC powders.

Keywords: High-protein dairy powder, storage, focused beam reflectance measurement, solubility

Introduction

Milk protein concentrate (MPC) powders are high in protein and low in lactose content and are added as ingredients in food product formulations to enhance the nutritional, functional, and sensory properties (Agarwal et al., 2015). The consistent and proper solubility of MPC powders are critical in delivering the desired physical and functional characteristics in the finished products. Processing conditions, powder composition, storage conditions, and dissolution conditions affect the overall solubility of MPC powders (Hauser and Amamcharla, 2016a). Thermal processing steps can result in structural alterations in proteins due to denaturation, aggregation of whey proteins, and formation of protein complexes between whey protein and caseins (Corredig and Dalgleish, 1999; Fang et al., 2012). Subsequent storage conditions further impact the protein interactions leading to a reduction in solubility of the MPC powders (Anema et al., 2006). Mimouni et al., (2010) observed that poor dispersible casein fractions are responsible for the high rehydration time in the MPC powders (>80% protein content) and slow rehydration is intensified during prolonged storage at elevated temperature and relative humidity (Crowley et al., 2015). According to Richard et al. (2012), the poor rehydration behavior of casein-dominant powders is due to slow penetration of water into primary particles. Therefore, MPC powders have the best possible solubility immediately after production and the solubility reduces as the storage time and temperature increases (Augustin et al., 2012; Fang et al., 2012; Gazi and Huppertz, 2015).

Application of rapid spectroscopic methods in dairy food analysis can alleviate critical problems in the production, storage, and distribution of dairy products (Karoui et al., 2003). Recently, Shaikh and O'Donnell (2017) reviewed the potential of the fluorescence spectroscopy as a rapid, nondestructive tool for evaluating the quality and safety attributes of dairy products. The traditional analytical methods in food analysis are time-consuming, relatively expensive, labor-intensive and these methods have limited applications for on-line/in-line monitoring (Karoui et al., 2003). Therefore, traditional methods alone are not adequate to shelter the growing demands of the dairy industry. Thus, several non-destructive techniques have been developed to rapidly determine product quality parameters. These new rapid techniques are relatively low-cost and can be applied in both fundamental researches and in the dairy industry, as on-line sensors for monitoring dairy foods production (Kamal and Karoui, 2015).

During the last two decades, fluorescence spectroscopy has proved to provide essential insights on the chemical, physical, and sensory properties of several complex food products (Karoui and Blecker, 2011). Front-face fluorescence spectroscopy (FFFS) is a rapid non-destructive method, comparatively inexpensive, and provides an extensive amount of information when coupled with multivariate statistical analysis. Coupling FFFS with chemometrics is a sensitive, reliable technique which provides unique information on the presence of fluorophores and has great potential to monitor and predict physical, chemical, and functional properties of dairy products (Shaikh and O'Donnell, 2017).

Dairy products have several intrinsic fluorophores like tryptophan, fluorescent Maillard reaction products (FMRP), vitamin A, and NADH which could be used as compounds of interest and are widely studied using fluorescence spectroscopy (Andersen and Mortensen, 2008). FFFS coupled with chemometric tools have previously been used to characterize dairy products

(Dufour and Riaublanc, 1997), monitor the structural changes and physico-chemical modification during milk heat treatment and coagulation of milk proteins (Kulmyrzaev et al., 2005; Boubellouta and Dufour, 2008; Blecker et al., 2012), determine the quality of various cheeses during ripening (Karoui et al., 2007), confirm geographic origin of cheeses (Karoui et al., 2005), and monitor storage changes of non-fat dry milk (NFDM) (Liu and Metzger, 2007). The objective of this study was to determine if FFFS coupled with chemometrics could be used as a rapid and non-destructive technique to monitor and predict the effect of protein content and storage time/temperature on the solubility of MPC powders.

Materials and methods

Milk protein concentrate powder samples

MPC powders (n=20) with 4 different protein contents (70, 80, 85, and 90%) were collected from 4 different commercial manufacturers. For simplicity, the powders will be called MPC70, MPC80, MPC85, and MPC90, respectively, indicating the protein content in the powders on the dry basis. In order to generate the MPC powders with different dissolution characteristics, each powder samples were divided into 10 equal parts (one bag each for 5 storage times at 2 temperatures), individually sealed in Whirl-Pak bags (Nasco, CA) and were stored at 2 different temperatures (25 and 40ºC) in an incubator (Percival Scientific, Perry, IA). The powders were analyzed on 0 (control, C), 1, 2, 4, 8, and 12 weeks of storage for color, solubility, dissolution behavior, and FFFS. The strategy of storing the MPC powders (n=20) at 2 different temperatures for 12 weeks resulted in a total of 220 samples (N=220) with different dissolution characteristics.

Color

On each experimental day, the color of MPC powders were determined by Hunter-Lab Mini Scan XE colorimeter (Reston, VA) to assess the changes in color caused by the Maillard reaction during the storage period. The Hunter color values were expressed as L* (whiteness or brightness/darkness), a* (redness/ greenness), and b* (yellowness/blueness). Color measurement was carried out in triplicate and reported as the mean.

Solubility index

MPC solutions of 5% (w/w) concentration were prepared at a dissolution temperature of 40ºC (Hauser and Amamcharla, 2016b) using distilled water and the solubility index of the MPC powders stored at 25 and 40ºC for 0, 1,2,4,8, and 12 weeks were measured based on the total solids in the supernatant obtained by centrifugation (700 × g for 10 min at 25ºC) as described by Anema et al. (2006). The amount of soluble material (σ) in the MPC powders was calculated using Equation 5.1.

$$\sigma = \frac{weight\ of\ dry\ material}{weight\ of\ solution} \times 100 \qquad (5.1)$$

Relative dissolution index (RDI)

The dissolution characteristics of the MPC powders stored at 25ºC and 40ºC for 0, 1, 2, 4, 8, and 12 weeks were evaluated using focused beam reflectance measurement (FBRM) following the method described by Hauser and Amamcharla (2016b). Protein solutions of 5% (w/w) concentration of MPC powders were prepared by dissolving MPC powders in distilled water, maintained at 40ºC. Each experiment was carried out in a 250-mL glass beaker, equipped with an overhead stirrer 4-blade impeller (Caframo, Georgian Bluffs, Ontario) rotating at 400 rpm. The iC FBRM software (version 4.3.391, Mettler-Toledo AutoChem Inc., Columbia, MD) was used to monitor and acquire the data from FBRM. The software program enabled tracking of the

number of particles in the category of <10 μm. The dissolution characteristics of control MPC powders and powders stored at 25ºC and 40ºC for 1, 2, 4, 8, and 12 weeks were monitored using changes in particle counts over time for 30 min. During the dissolution of MPC powders, the counts of fine particles (<10 μm chord length) are expected to increase with time, and hence the fine particle counts were plotted against powder dissolution time. Subsequently, the area under the fine particle count curve was extracted to characterize the powder dissolution. The area under the curve was calculated using the trapezoidal rule. Relative dissolution index (RDI, %) was derived for the MPC powders stored for time t in weeks from the area under the fine particle count of the MPC powder at time t and the area under the fine particle count of the same MPC powder when it was control (t=0). Equation 5.2 was used for calculating the RDI (%).

$$RDI(\%) = \frac{Area\ under\ the\ curve\ for\ the\ sample\ at\ time\ t}{Area\ under\ the\ curve\ for\ the\ sample\ at\ time\ 0} \times 100 \qquad (5.2)$$

FFFS

Front-face fluorescence spectra of all the 220 samples were collected using a Perkin–Elmer LS50B Luminescence spectrometer equipped with the front face accessory. On each experimental day, the MPC powder sample was loaded into a powder sample holder with a quartz window. To obtain the fluorescence spectra, the powder sample holder was then mounted on a front-face accessory fitted to a Perkin-Elmer LS50B spectrometer, maintaining an incidence angle of excitation at 56º. Five scans were performed on each MPC sample to record the fluorescence emission spectra of tryptophan (305 to 450 nm) at an excitation wavelength of 290 nm, Maillard products emission spectra (380 to 480 nm) at an excitation wavelength of 360 nm, and the Maillard excitation spectra in the 260 to 350 nm range at an emission of 410 nm. The slit widths were set at 9.0 and 4.0 nm for excitation and emission, respectively. Each MPC sample was analyzed in triplicate. Therefore, a total of 15 individual spectra were collected for each

sample in the regions described above. FL Data Manager Software (Perkin-Elmer) was used for the spectral data acquisition.

Spectral data analysis

The spectral data were analyzed by the technique of multivariate statistical analysis. All spectral pre-processing was accomplished in the Unscrambler X 10.4.1 software (CAMO Software Inc., Norway). For the pre-processing, spectral scans from each sample at each temperature and storage time were averaged. Subsequently, fluorescence spectra were normalized by area normalization technique available in the Unscrambler X software to reduce the light scattering effects and noise. Principal component analysis (PCA) was then applied to examine the differences between MPC samples stored at various temperatures and time combinations. PCA was helpful in calculating several principal components (PCs) which can give insights into the differences between the samples.

Model development and performance evaluation

The relationship between spectral measurements and solubility were obtained by applying partial least squares regression (PLSR) analysis available in the Unscrambler software. The PLSR uses the 2-block predictive PLSR to model the relationship between 2 matrices, X (the input matrix) and Y (desired output matrix). The fluorescence spectra collected on the MPC powders were related to their respective solubility index and RDI using PLSR. The PLSR models were established for correlating spectral data to solubility index and RDI using the root mean square error of cross-validation (RMSECV; Equation 5.3).

$$RMSECV = \sqrt{\frac{\sum_{i=1}^{n}\left(Y_{pred}-Y_{obs}\right)^2}{n}} \qquad (3)$$

where RMSECV is the root mean square error of cross-validation, Y_{pred} is the predicted value, Y_{obs} is the observed value, and n is the number of samples in the test set.

The accuracy of the PLSR calibration was evaluated based on the residual prediction deviation (RPD). The RPD is defined as the ratio of standard deviation (SD) of the actual measured values to RMSECV (Williams, 1987). In the present study, RPD values <1.5 indicated a very poor model; RPD values between 1.5 and 2 indicated a poor model, RPD between 2 and 2.5 indicated a fair model or predictions which may be used for approximate quantitative predictions; and RPD values between 2.5 and 3.0 and > 3.0 indicated good and very good predictions (Amamcharla and Metzger, 2015).

Results and discussion

As per the certificate of analysis provided by the manufacturer, the composition of MPC powders used in this study is shown in Table 5.1. As the protein content increased from 70.3 to 88.1% (w/w), the lactose content decreased from 16.1 to 0.5% (w/w). The MPC powders used in this study did not exhibit any difference in the levels of fat.

Color

The mean of L*, a*, and b* were used to evaluate the changes in color before and during storage at 25 and 40ºC (Table 5.2). As expected, storage at 40ºC showed a decrease in L* values and an increase in a* and b* values. Also, a similar trend was observed with the increase in protein content from 70 to 90%. The decrease in the L* value shows an increase in brown coloration and decrease in lightness in stored MPC powders. Additionally, the increase in a* and b* values (Table 5.2) also indicated a brown pigment formation in MPC powders. Le et al. (2011) found that MPC80 after storage for 12 weeks (at 25 and 40ºC) also developed similar changes, which they believed are the most sensitive indicators of the effects of storage temperature and time on the progress of the late-stage Maillard reaction during storage.

Solubility index

The solubility index of the MPC powders after storage at 25 and 40ºC for 12 weeks are provided in Figure 5.1A and Figure 5.1B, respectively. The MPC powders stored at 25ºC exhibited a higher solubility index as compared to powders stored at 40ºC. Additionally, the solubility has decreased with the increase in the protein content from 70 to 90%. Previous studies reported that solubility of MPC powders is maximum immediately after production and it decreases with the increase in storage time and temperature (Anema et al., 2006; Fyfe et al., 2011), which agreed with the results from this study. Also, the increase in protein content negatively impacted the solubility (Gazi and Huppertz, 2015).

Relative dissolution index (RDI)

Solubility index method described above measures the status of the MPC powder at the end of the rehydration period (generally 30 min) by selectively removing the undissolved particles by centrifugation. On the other hand, FBRM-based method can provide in-line monitoring capability of powder rehydration process in a comparatively robust manner without the need for sampling or dilution. It has been proved to be a suitable technique for studying the rehydration of MPC powders (Fang et al., 2011). FBRM results suggested that dissolution characteristics of MPC powder were influenced by the protein content and storage temperature. The RDI of the MPC powders before and after storage (1, 2, 4, 8, and 12 weeks) at 25 and 40ºC is provided in Figure 5.2A and Figure 5.2B, respectively. The MPC powders stored at 25ºC exhibited higher RDI as compared to powders stored at 40ºC. Interpretation of FBRM data matches the overall trend observed by Crowley et al. (2015) and Hauser and Amamcharla (2016b). Fang et al. (2011) compared the dissolution rate constant and the final particle size for control and stored MPC. They observed that control MPC powders were the most soluble and

had a high dissolution rate constant and a lower final mean particle size. A comparable approach was used to understand the dissolution behavior of MPC powders in the present study. Additionally, the RDI has decreased with the increase in the protein content from 70 to 90%. The changes in the fine particle counts (<10 µm chord length) of MPC70 and MPC90 from the same manufacturer (control and stored at 40ºC for 1, 2, 4, 8 and 12 weeks) are provided in Figure 5.3A and Figure 5.3B, respectively. MPC80 and MPC85 also exhibited similar trends with increasing storage temperature and time (data not shown). It was observed that fine particle counts increased more rapidly for MPC70 stored at 40ºC as compared to MPC90 stored at 40ºC during dissolution. Additionally, the slow distribution rate of particles establishes the effect of storage temperature/time on the MPC powders. Similar observations were obtained in previous studies (Hauser and Amamcharla, 2016b). Storing the MPC powders at elevated temperatures such as 40ºC resulted in crosslinking networks at the surface of the MPC powders and could be attributed to its poor dissolution characteristics (Anema et al., 2006). The crosslinking networks include interactions between hydrophobic caseins and whey proteins, and thereby hinder the hydration in the MPC powders (Anema et al., 2006; Uluko et al., 2016). As the protein content increased in MPC powders from 70 to 90% (w/w), the MPC90 showed more primary particle aggregates and exhibited more resistance to dispersing in water (Crowley et al., 2015). Also, with the increase in storage temperature the protein-protein aggregations increased, as shown by lesser counts of fines in FBRM. Therefore, composition and storage of MPC powders resulted in powders with diverse physical characteristics.

Table 5.1 Compositional analysis (%, w/w; mean values) of milk protein concentrate (MPC) powders used in this study.

Type	Manufacturer*	Protein (%, w/w)	Fat (%, w/w)	Moisture (%, w/w)	Lactose (%, w/w)	Ash (%)
MPC70 (n=3)	M_1, M_2	70.4	1.3	4.7	16.1	6.4
MPC80 (n=4)	M_1, M_4	81.6	1.1	4.9	6.6	6.3
MPC85 (n=6)	M_1, M_2, M_4	85.7	1.1	4.9	2.6	6.2
MPC90 (n=7)	M_1, M_2, M_3, M_4	88.1	1.1	4.6	0.5	6.3

*Samples with same subscript originate from the same manufacturer.

Table 5.2 The mean values of L*, a*, and b* for the MPC samples received from one of the manufacturer before storage and samples stored at 25 and 40 ºC for 12 weeks[1]

Protein Content	Manufacturer*	Fresh Powders			Powders stored at 25ºC for 12			Powders stored at 40ºC for 12		
		L*	a*	b*	L*	a*	b*	L*	a*	b*
MPC70	M_1	93.65	-0.95	10.62	93.32	-0.45	10.97	91.89	0.05	17.25
MPC80	M_1	92.24	-0.29	10.20	91.39	-0.21	12.49	88.41	0.62	21.7
MPC85	M_1	92.24	-0.34	9.67	91.19	0.08	12.17	89.09	0.42	20.73
MPC90	M_1	92.71	-0.21	9.26	90.12	0.18	12.25	89.41	0.48	18.23

[1]L*, a*, b* color system: L* (0 = black; 100 = white component); a* (+ = red; − = green component); and b* (+ = yellow; − = blue component).
*Samples with same subscript originate from the same manufacture

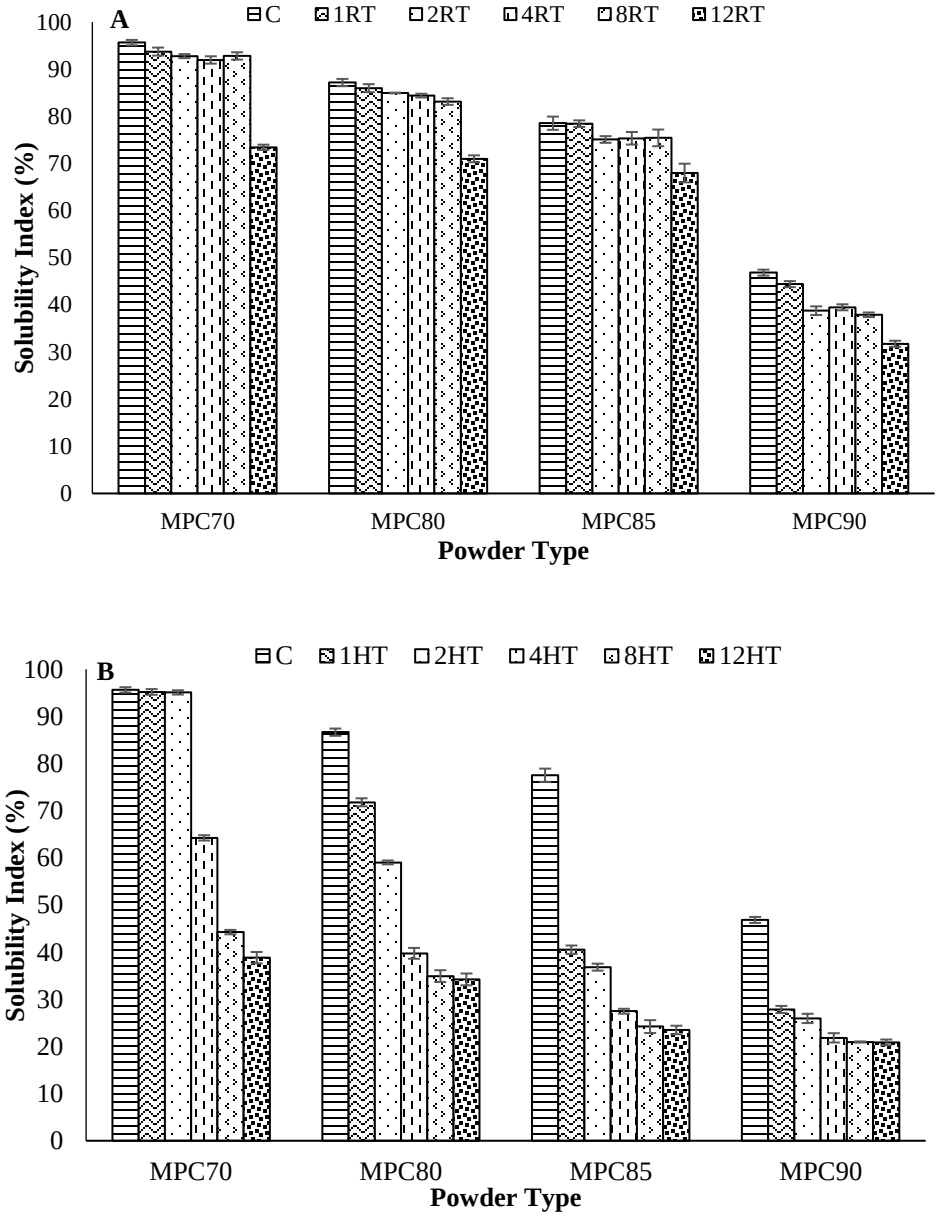

Figure 5.1 Solubility index (%) of selected (obtained from manufacturer M_1) milk protein concentrate (MPC) powders before and during storage at different temperatures (A) 25ºC (RT) and (B) 40ºC (HT) for control (C), 1, 2, 4, 8, and 12 weeks. The numbers in the legend represent the storage time in week.

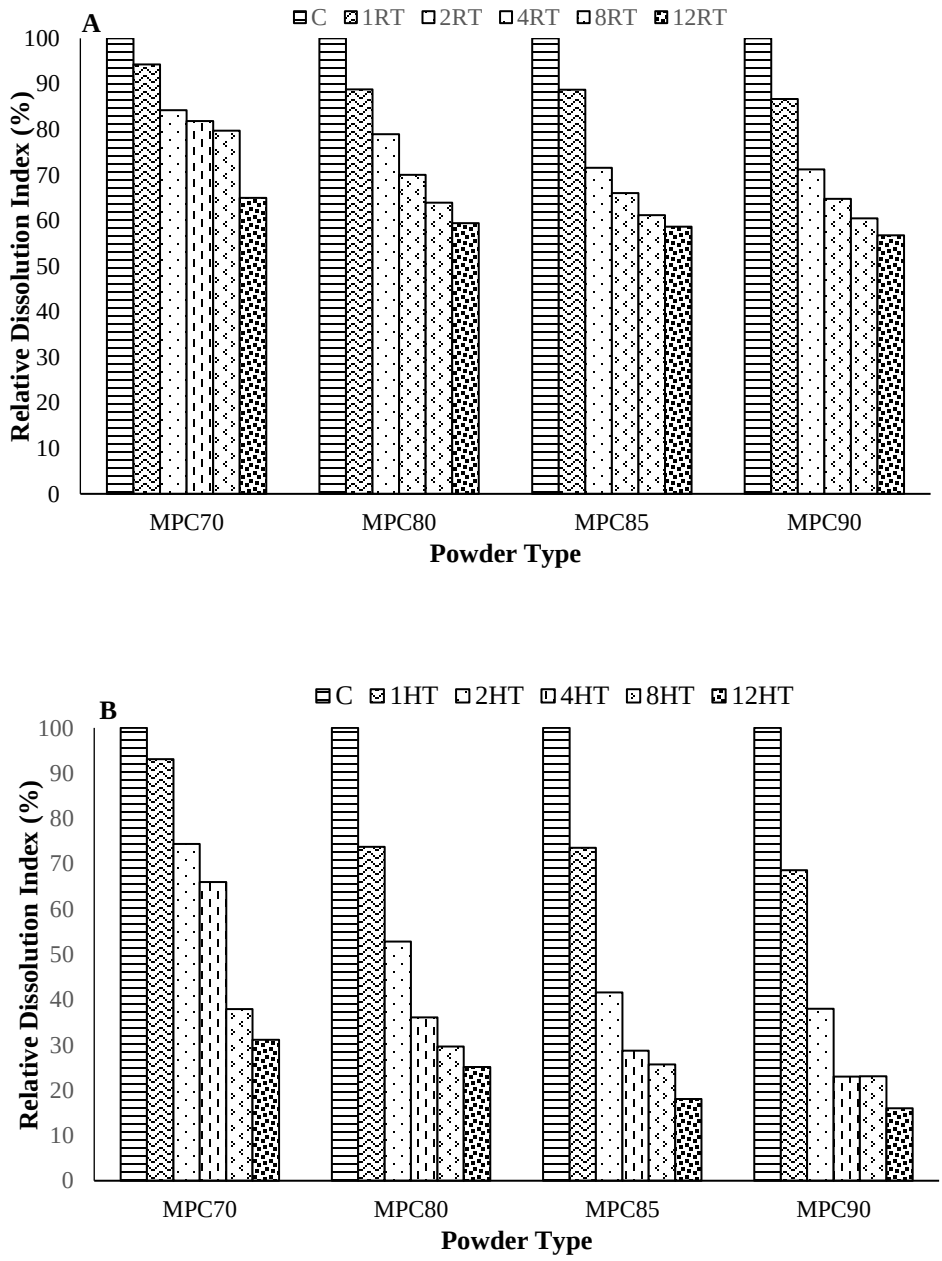

Figure 5.2 Relative dissolution index (%) of selected (obtained from manufacturer M_1) milk protein concentrate (MPC) powders before and during storage at different temperatures (A) 25ºC (RT) and (B) 40ºC (HT) for control (C), 1, 2, 4, 8, and 12 weeks. The numbers in the legend represent the storage time in week.

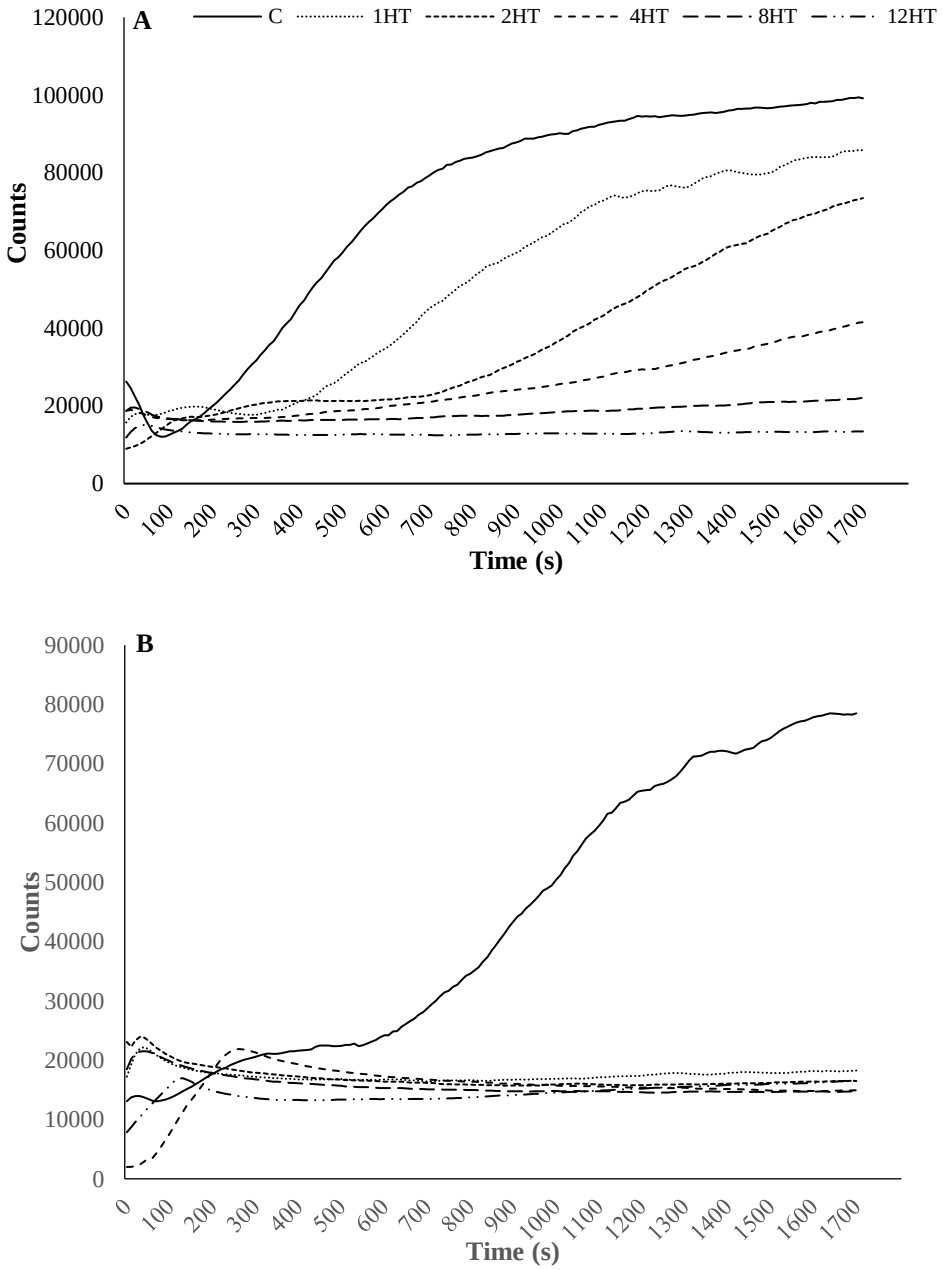

Figure 5.3 Changes in fine (<10 μm) counts obtained from data collected with the focused beam reflectance measurement for milk protein concentrate (MPC) powders (obtained from manufacturer M_2): (A) MPC70; (B) MPC90 stored at 40ºC (HT) for control (C), 1, 2, 4, 8, and 12 weeks. The numbers in the legend represent the storage time in week.

Front-face fluorescence spectra

Tryptophan emission spectra

Figure 5.4-1A, Figure 5.4-1B, Figure 5.4-2A and Figure 5.4-2B show an overlaid plot of the averaged and area normalized emission spectra for tryptophan in MPC70 and MPC90 (before and during storage at 25 and 40ºC for, 1, 2, 4, 8, and 12 weeks). Before storage, the MPC samples with different protein contents from the same manufacturer displayed different fluorescence intensities of the individual tryptophan emission spectra (Figure 5.4-1A and Figure 5.4-2A). Before storage, the tryptophan emission spectra of MPC70 at 25ºC (Figure 5.4-1A) exhibited a tryptophan maximum at around 341.5 nm, whereas for MPC90 at 25ºC, the tryptophan maximum was around 341 nm (Figure 5.4-2A). Evident changes in the tryptophan emission spectra were observed during storage of the MPC powders, especially for the samples stored at 40ºC. The tryptophan emission peaks corresponding MPC70 and MPC90 after storage for 1, 2, 4, 8, and 12 weeks at 40ºC presented a red shift. A decrease in peak intensity and red shift were previously reported for the tryptophan emission spectra of NFDM powders before storage and samples stored at 50ºC for 1, 2, 4, and 8 weeks (Liu and Metzger, 2007). Whereas, the tryptophan emission peaks corresponding to MPC70 and MPC90 after storage for 1, 2, 4, 8, and 12 weeks at 25ºC presented a blue shift. The emission of tryptophan is highly sensitive to its local environment, and the spectral peak shifts demonstrate the protein conformational changes in the MPC powders during storage. MPC80 and MPC85 samples displayed similar trends during storage (data not shown). Spectral shifts in tryptophan emission observed for the MPC powders could be due to the protein-protein association and protein unfolding (Lakowicz, 2006). After 1 week of storage, the tryptophan emission spectra of MPC70 (Figure 5.4-1A) exhibited a tryptophan maximum at around 338 nm at 25ºC. Whereas, for MPC70 stored for 1 week at 40ºC

the tryptophan maximum was around 344 nm (Figure 5.4-1B). Similarly, after 1 week of storage the tryptophan emission spectra of MPC90 at 25ºC (Figure 5.4-2A) exhibited a tryptophan maximum at around 339.5 nm. Whereas, for MPC90 at 40ºC the tryptophan maximum was around 344.5nm (Figure 5.4-2B). The prominent peak around 338 nm in the tryptophan emission spectra was attributed to the presence of tryptophan in NFDM (Liu and Metzger, 2007). For the tryptophan emission spectra of MPC70 and MPC90, a prominent decrease in the peak intensities between 335 and 355 nm was observed with the increase in storage time (Figure 5.4-1B and Figure 5.4-2B), indicating changes in the environment of the tryptophan residues in dairy proteins during storage (Liu and Metzger, 2007).

Maillard emission spectra

An overlaid plot of Maillard emission spectra for MPC70 and MPC90 (before and after storage at 25 and 40ºC for 1, 2, 4, 8, and 12 weeks) are shown in Figure 5.5. MPC80 and MPC85 samples displayed similar trends of changes during storage (data not shown). The Maillard emission spectra show a broad peak from 420 to 450 nm with an emission maximum 435 nm for MPC70 at 25ºC (Figure 5.5-1A). Whereas, for MPC70 at 40ºC the emission maximum was found to be at 438 nm (Figure 5.5-1B). The emission maximum of Maillard emission spectra of MPC90 at 25 and 40ºC was at 435 nm (Figure 5.5-2A) and 438 nm (Figure 5.5-2B), respectively. Advanced Maillard Products (AMP) in milk samples have been reported (Birlouez-Aragon et al., 1998) to excite around 350 nm with emission at 440 nm, which is almost identical to the peak observed in the present study. Previous studies reported that the development of Amadori products and advanced glycosylation end (AGE) products has an emission wavelength in the range of 420 to 450 nm (Matiacevich and Buera, 2006). For the Maillard emission spectra of MPC70 and MPC90, a prominent increase in the peak intensities between 420 to 450 nm was

observed with increase in storage time (Figure 5.5-1B and Figure 5.5-2B). Thus, the peaks shown in Figure 5 correspond to AMP. These variations in the Maillard emission spectra could also be explained by the b* values (Table 5.2). The b* value is a good measure of browning in milk powders because it shows the color change toward yellow and brown (Morales and Van Boekel, 1998). The increase in b* values became noticeable with increasing storage time and temperature, indicating changes in color caused by the Maillard reaction. Similarly, the increase in peak intensities started in all the samples from 1 week of storage (40ºC) and continued to increase until the end of storage period (12 weeks).

Maillard exitation spectra

Overlaid plots of Maillard excitation spectra for MPC70 and MPC90 (before and during storage at 25 and 40ºC for 1, 2, 4, 8, and 12 weeks) are shown in Figure 5.6. MPC80 and MPC85 samples displayed similar trends of changes during storage (data not shown). The Maillard excitation spectra for MPC70 at 25ºC (Figure 5.6-1A), MPC70 at 40ºC (Figure 5.6-1B), MPC90 at 25ºC (Figure 5.6-2A), and MPC90 at 40ºC (Figure 5.6-2B) were in the range of 260 to 350 nm with a peak around 300 and 335 nm. Fluorescence of Maillard products (excitation and emission wavelengths of 347 and 415 nm) have been previously observed in milk systems during the Maillard reaction (Morales et al., 1996; Birlouez-Aragon et al., 2002; Liu and Metzger, 2007).

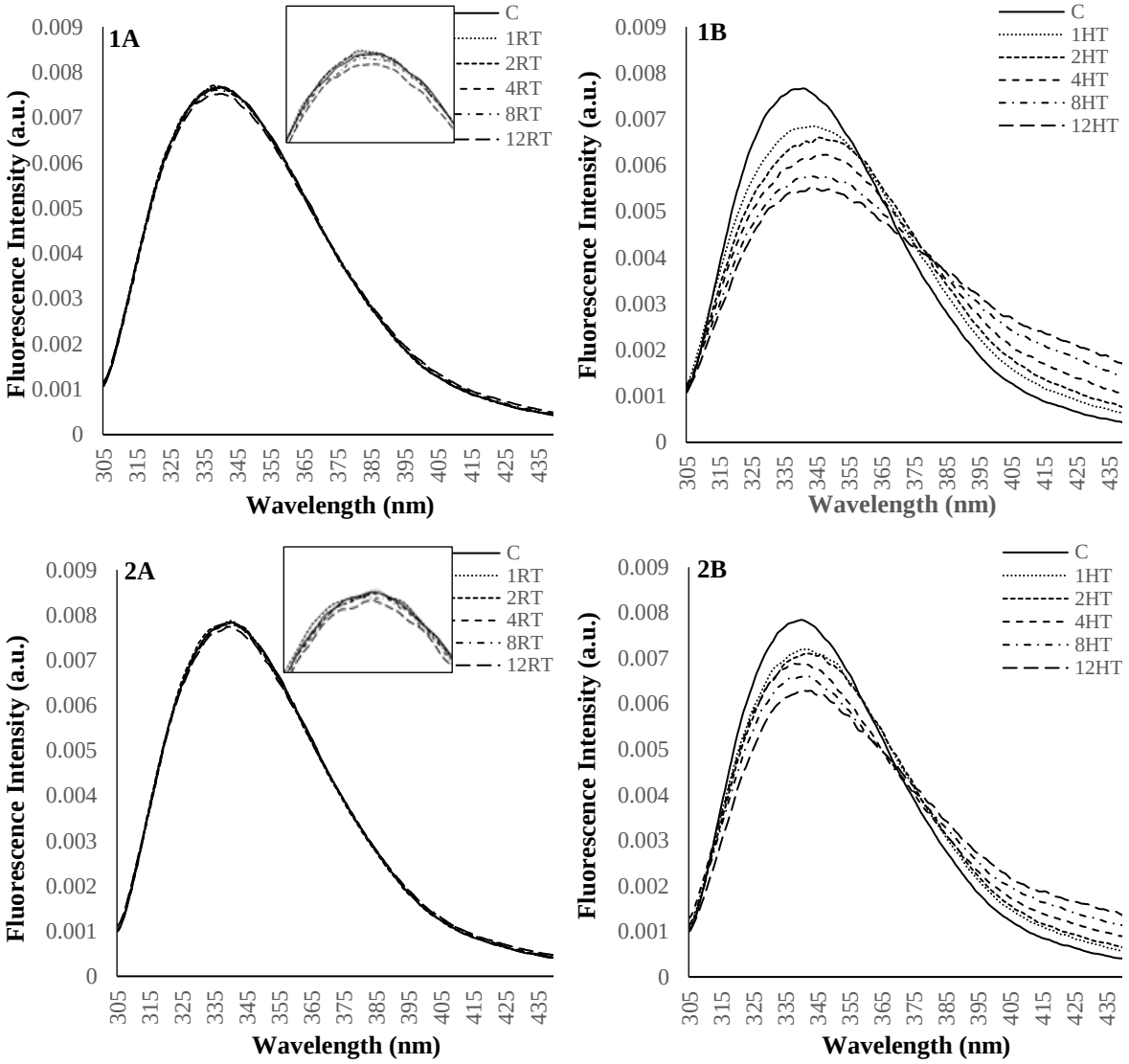

Figure 5.4 Tryptophan emission spectra of (1) MPC70 and (2) MPC90 samples (same manufacturer) before storage and after storage at (A) 25ºC (RT) and (B) 40ºC (HT) of control (C), 1, 2, 4, 8, and 12 weeks. The numbers in the legend represent the storage time of the sample in weeks.

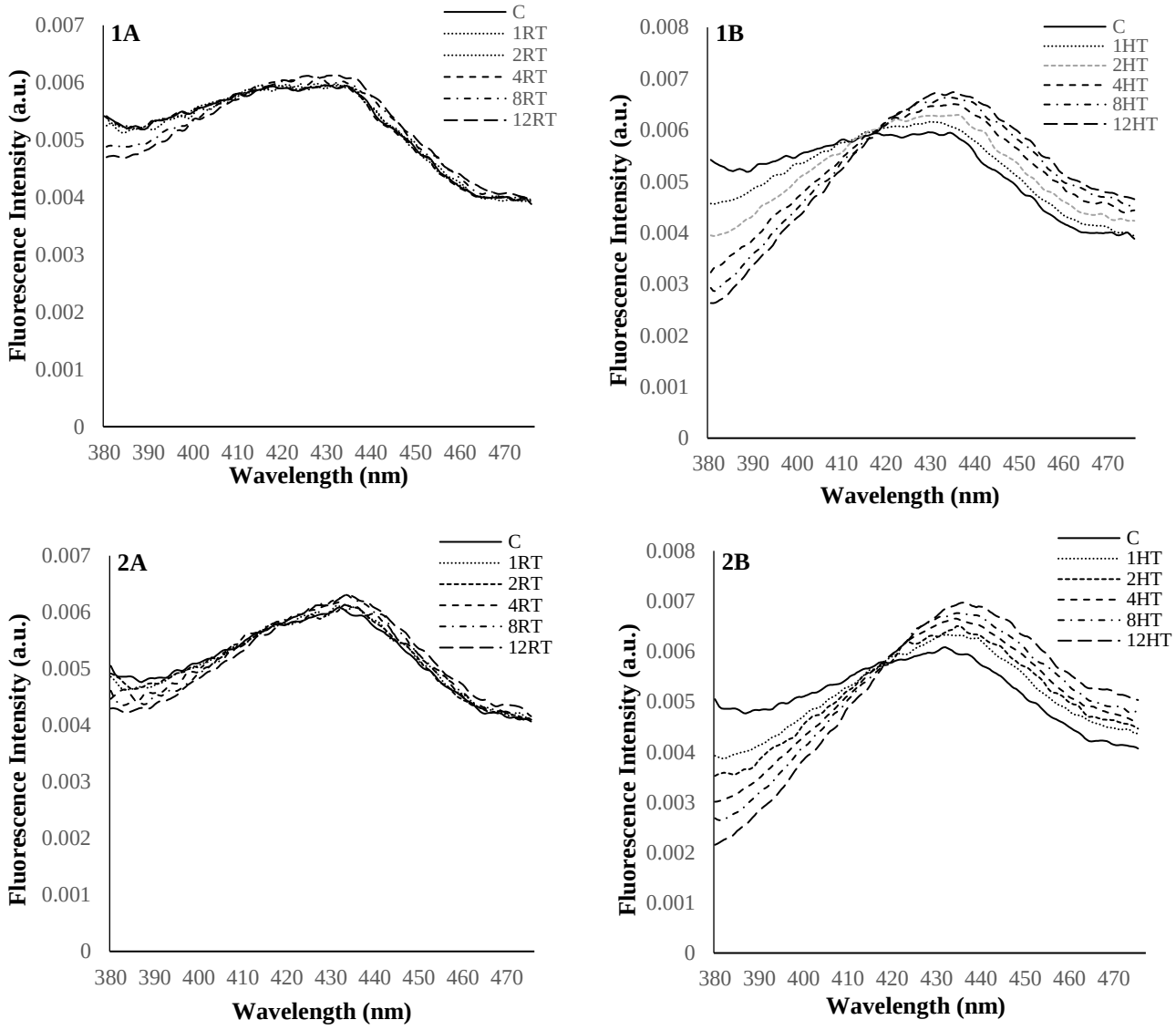

Figure 5.5 Maillard emission spectra of (1) MPC70 and (2) MPC90 samples (same manufacturer) before storage and after storage at (A) 25ºC (RT) and (B) 40ºC (HT) of control (C), 1, 2, 4, 8, and 12 weeks. The numbers in the legend represent the storage time of the sample in weeks.

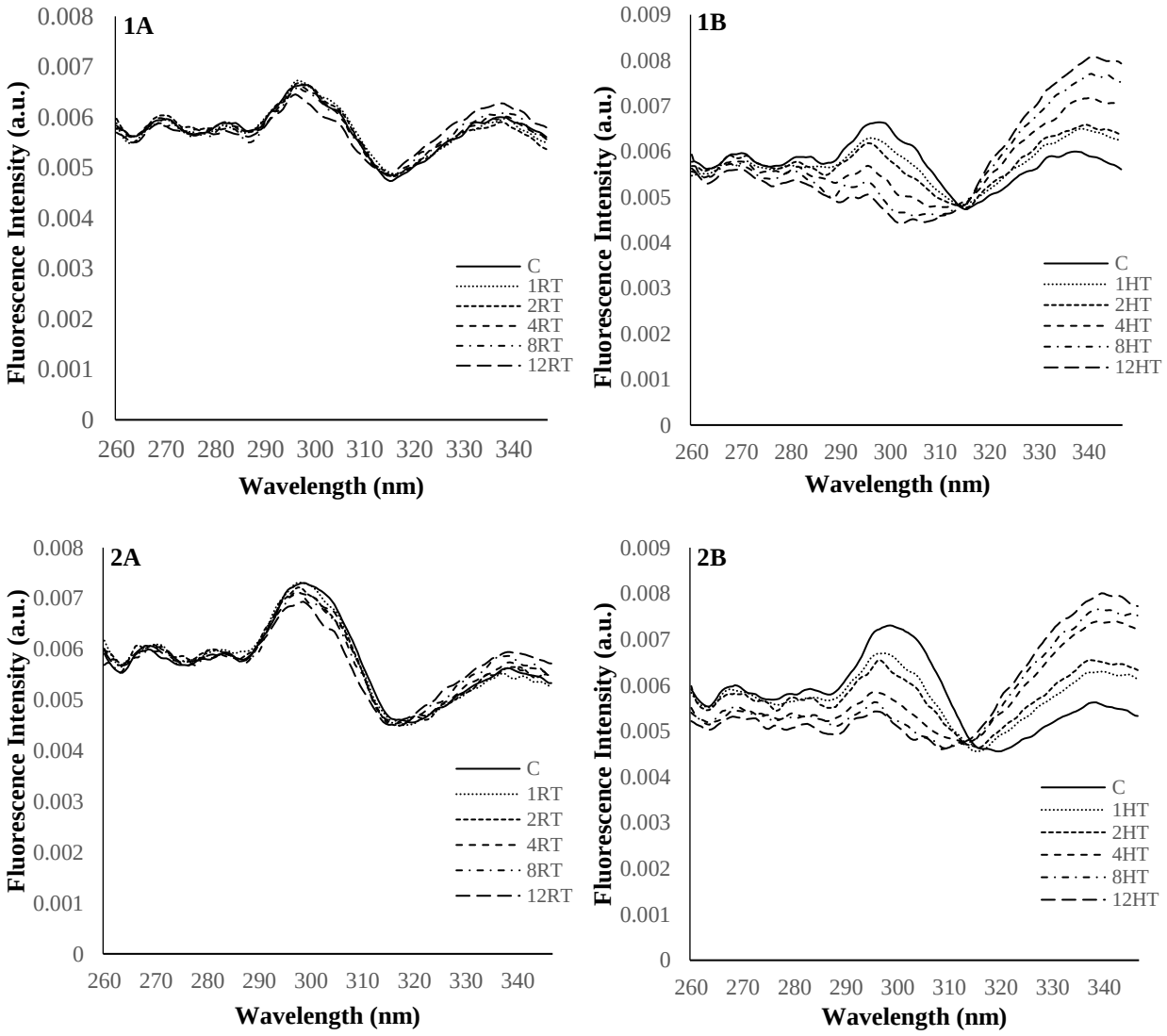

Figure 5.6 Maillard excitation spectra of (1) MPC70 and (2) MPC90 samples (same manufacturer) before storage and after storage at (A) 25ºC (RT) and (B) 40ºC (HT) of control (C), 1, 2, 4, 8, and 12 weeks. The numbers in the legend represent the storage time of the sample in weeks.

Multivariate analysis of MPC powders fluorescence spectra

After storage, the PC-1 accounted for 95% of the total variability and PC-2 accounted for 4% of the total variability. The factor loadings of PC-1 showed a positive peak at 340 nm and a broad negative band at around 380 nm (Figure 5.7A), and the factor loading of PC-2 exhibited a negative maximum at 335 nm and a positive peak at 385 nm. PC-1 and PC-2 described changes in the fluorescence intensity during storage and could be correlated with the changes in the

normalized tryptophan spectra. In the similarity map (Figure 5.7B), storage at 25ºC gave these samples larger PC-1 scores than the samples stored at 40ºC. The tryptophan maximum emission has been previously reported in most studies in the region between 332 and 343 nm (Ntakatsane et al., 2011; Dufour et al., 2001; Kulmyrzaev et al., 2005), depending on the sample composition, origin, processing, and storage conditions. The changes in tryptophan maximum emission wavelength showed changes in the polarity of the tryptophan residues micro-environment (Liu et al., 2005). Therefore, variation in the hydrophobicity of the tryptophan residues in the MPC powders after storage was found among the samples. Dufour and Riaublanc (1997) studied the FFFS tryptophan spectra of raw and heated milk and described how discriminations of the samples are a function of heat treatment. The variation in the tryptophan spectra observed in MPC powders during storage was probably due to the variation in the manufacturing conditions of the MPC powders, such as pasteurization, evaporation, spray-drying conditions, and subsequent storage conditions. Before storage, factor loading of PC-1 showed a broader negative band from 365 to 425 nm compared to the broader positive band from 365 to 425 nm of factor loading of PC-1 after storage, indicating the modification of the tryptophan environment. The variation in composition, processing, and storage conditions in the MPC samples have resulted in changes in the fluorescence intensity and red shift.

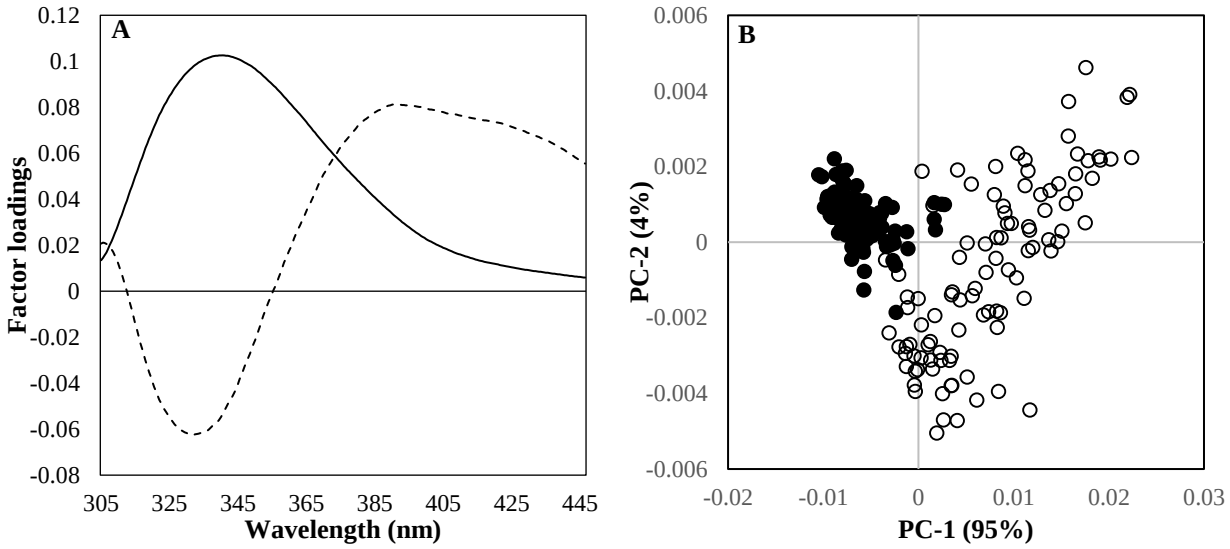

Figure 5.7 Factor loadings of the first two principal components (A) and similarity map (B) of principal component analysis (PCA) made on tryptophan emission spectra of the MPC samples after storage. The solid line in (A) indicate PC-1 and dotted line in (A) indicate PC-2. The open circles in (B) represent samples stored at 25ºC (RT) and solid circles in (B) represent samples stored at 40ºC (HT).

The similarity maps and the factor loadings of the first 2 PC of the Maillard emission data fluorescence data sets are presented in Figure 5.8. The factor loadings plot of PC-1 showed a broad band from 425 to 440 nm, suggesting the presence and variation of Maillard reaction products in the MPC samples, in agreement with Liu and Metzger (2007) and Ntakatsane et al. (2011). They attributed positive band of PC-1 at 430 nm to display the accumulation of AGE products during storage of dairy products. The factor loadings of PC-2 showed a positive band between 380 and 395 nm and the negative band between 385 and 440 nm (Figure 5.8A). Thus, PC-2 describes the contents of pentosidine and cross-linked compounds in the MPC samples (Liu and Metzger, 2007). Additionally, similar factors were accountable for the variation in the samples (MPC80 and MPC85) before storage (data not shown) and their changes during storage. Furthermore, Maillard emission spectra indicated that variation in the types and amounts of Maillard reaction products accumulated during their manufacturing processes depending on protein contents. The PC-1 accounted for 95% of the total variability and PC-2 accounted for 4%

of the total variability. Discrimination of the MPC powders stored at 25 and 40ºC was observed in the similarity maps. In the PCA results of Maillard emission fluorescence (Figure 5.8B), most of the MPC samples stored at 25ºC showed positive PC-1 scores. Whereas, most of the samples stored at 40ºC had negative scores in PC-1. Moreaux and Birlouez-Aragon, (1997) reported maximum emission at 425 nm, and 450 to 460 nm corresponds to intense Maillard reaction of β-LG and lactose, indicating AGE products. The factor loadings plot of PC-2 showed a similar negative peak at 420 nm. Kulmyrzaev and Dufour (2002) observed a shift in the maximum emission wavelength from 416 to 419 nm after excessive heat treatment of the milk. Therefore, PC-1 and PC-2 may describe the presence and variation in the AGE in the MPC powders during storage. Guyomarc'h et al. (2000) have reported that spray drying conditions can influence the level of the Maillard reaction that occurs in NFDM as measured by the amount of lactosylation of milk proteins. In a previous study, Lecle´re and Birlouez-Aragon (2001) used a fluorescence-based method to estimate the heat treatment (60ºC) of milk by measuring the AMP at 330 to 420 nm. They noted that AMP fluorescence increased during heat treatment. In the manufacturing of MPC powders, in addition to the spray-drying process, pasteurization, and evaporation treatments may also influence the Maillard emission spectra. There was an observed difference in the pattern of Maillard excitation data to that of Maillard emission data. For the Maillard excitation spectra, the characteristics of 98% of the data were described by the first 2 components. In Figure 5.9A, the factor loadings of the PC-1 showed a positive peak at 300 nm in opposition to the negative peak at 305 nm in PC-2. The factor loadings of PC-1 showed a positive band between 260 and 315 nm and a negative band between 315 and 340 nm (Figure 5.9A). However, similar noticeable patterns were observed from the Maillard emission and excitation similarity maps, which suggested that the Maillard emission and excitation spectra

might describe the presence of similar Maillard reaction products. The factor loading of PC-2 showed a broad peak from 320 to 340 nm, indicating changes in the intensity of the fluorescence spectra.

Overall, the factor loadings of the PC-1 and PC-2 for the 3 fluorescence spectra of the samples before storage were comparable to the PCA results of the samples during storage. It appears that similar factors are responsible for the variation in the samples before storage and their changes during storage, which indicated that biochemical reactions such as modification of the tryptophan environment and the Maillard reaction occurred during the manufacturing process and subsequent storage of the samples. Therefore, this investigation underlines the potential of FFFS in combination with chemometrics as a fast, nondestructive method for monitoring the storage changes in MPC powders.

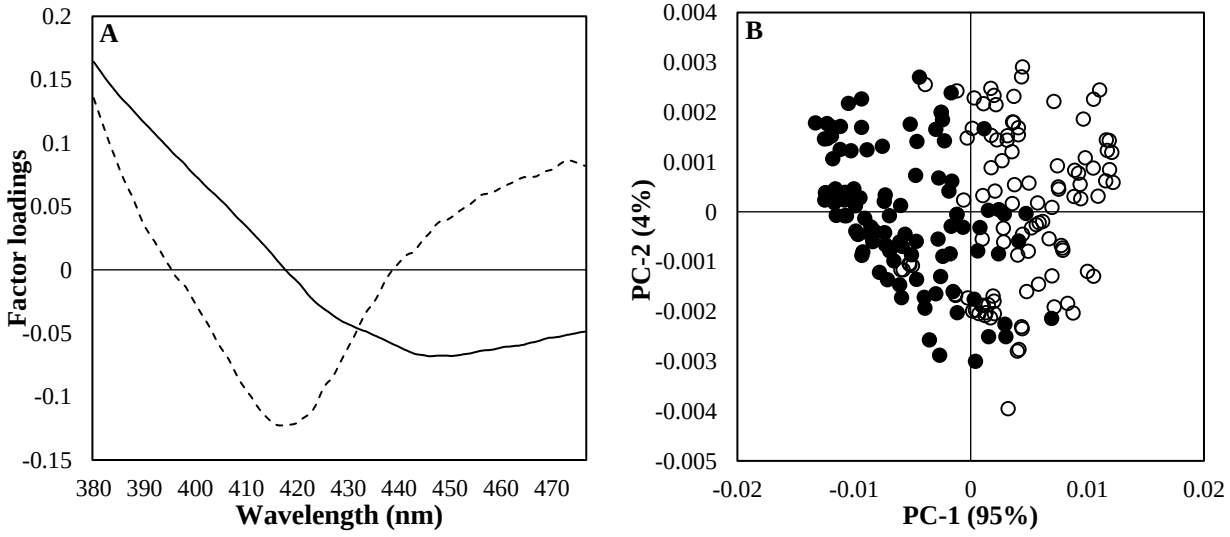

Figure 5.8 Factor loadings of the first two principal components (A) and similarity map (B) of principal component analysis (PCA) made on Maillard emission spectra of the MPC samples after storage. The solid line in (A) indicate PC-1 and dotted line in (A) indicate PC-2. The open circles in (B) represent samples stored at 25ºC (RT) and solid circles in (B) represent samples stored at 40ºC (HT).

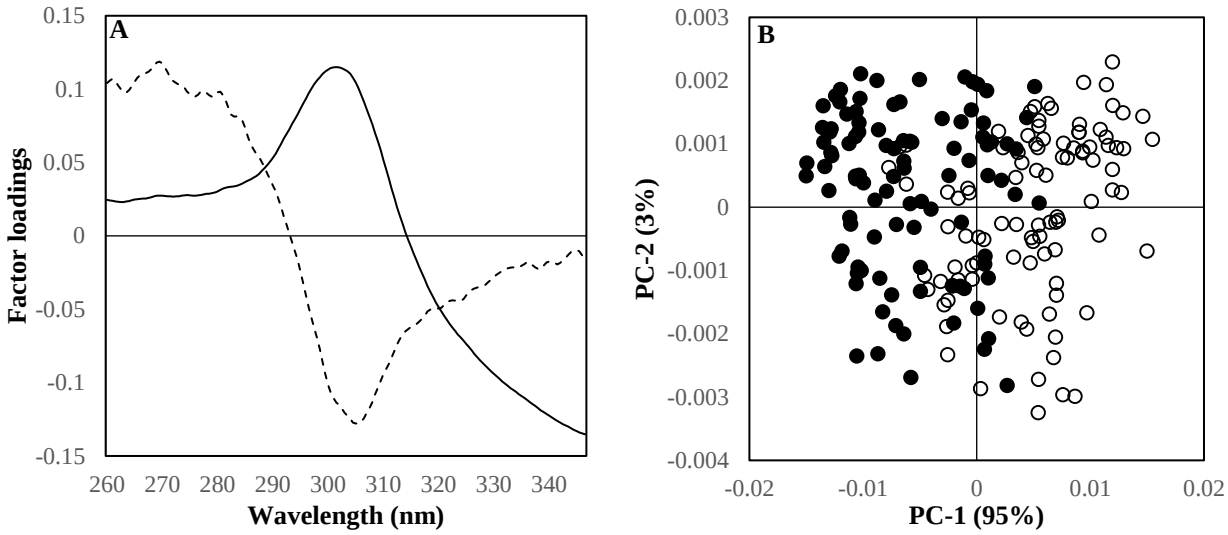

Figure 5.9 Factor loadings of the first two principal components (A) and similarity map (B) of principal component analysis (PCA) made on Maillard excitation spectra of the MPC samples after storage. The solid line in (A) indicate PC-1 and dotted line in (A) indicate PC-2. The open circles in (B) represent samples stored at 25ºC (RT) and solid circles in (B) represent samples stored at 40ºC (HT).

Prediction of solubility index using PLSR

The front-face fluorescence spectra obtained on the MPC samples (N=220) were used to develop a 7-factor PLSR model for prediction of solubility index of MPC powders. Figure 5.10-A, Figure 5.10-B, and Figure 5.10-C show scatter plots between the observed and predicted solubility index obtained for the entire data set. The R^2, RMSECV, and RPD obtained for the dataset (N=220) are provided in Table 5.3. The coefficient of determination (R^2) value for the 3 front-face fluorescence spectra predicted was between 0.77 and 0.85. The RMSECV for the dataset was 12.79, 11.30, and 13.64 for prediction of a spectral data set of tryptophan emission, Maillard emission, and Maillard excitation, respectively. The RPD for data set was 2.16, 2.44, and 2.02 for prediction of a spectral data set of tryptophan emission, Maillard emission, and Maillard excitation, respectively. This indicates that the developed model had good predictability and practical utility. The RPD value desired is greater than 2 for a good calibration and a value less than 1.5 indicates incorrect predictions and an unstable model (Karoui et al., 2006;

Amamcharla and Metzger, 2015). The higher correlation and more robust model for the FFFS spectral data and solubility index values support our theory that FFFS data may be used to measure the solubility index of MPC powders. The chemistry behind this correlation can be explained by the environment-sensitive characteristics of tryptophan and Maillard reaction occurred during the processing and subsequent storage.

Prediction of relative dissolution index using PLSR

The front-face fluorescence spectra obtained on the MPC samples (N=220) were used to develop a 7 factor PLSR model for prediction of RDI values of MPC powders. As the FBRM measurements provide a complete overview of the rehydration process, it was predicted by using PLSR. Figure 5.11-A and Figure 5.11-B show scatter plots between the observed and predicted RDI obtained for the entire data set of tryptophan and Maillard emission spectra. The R^2, RMSECV, and RPD obtained for the dataset are provided in Table 5.3. The R^2 value for the front-face fluorescence spectra predicted was and 0.74 and 0.71 for prediction of a spectral data set of tryptophan emission and Maillard emission, respectively, suggesting that the FBRM measurements (counts <10 μm) could be predicted from the fluorescence spectra. The RMSECV for data set was 12.38 and 13.04 for prediction of a spectral data set of tryptophan emission and Maillard emission, respectively. The RPD for the dataset was 1.98 and 1.88 for the prediction of a spectral data set of tryptophan emission and Maillard emission, respectively. The RPD values of <2 indicated poor PLSR model. However, the model performance could be improved by adapting different pre-processing techniques such as feature selection and using other model algorithms such as multilayer perceptron neural network. Overall, the front-face fluorescence technique provides unique information, which is a real reflection of the dissolution changes of MPC powders.

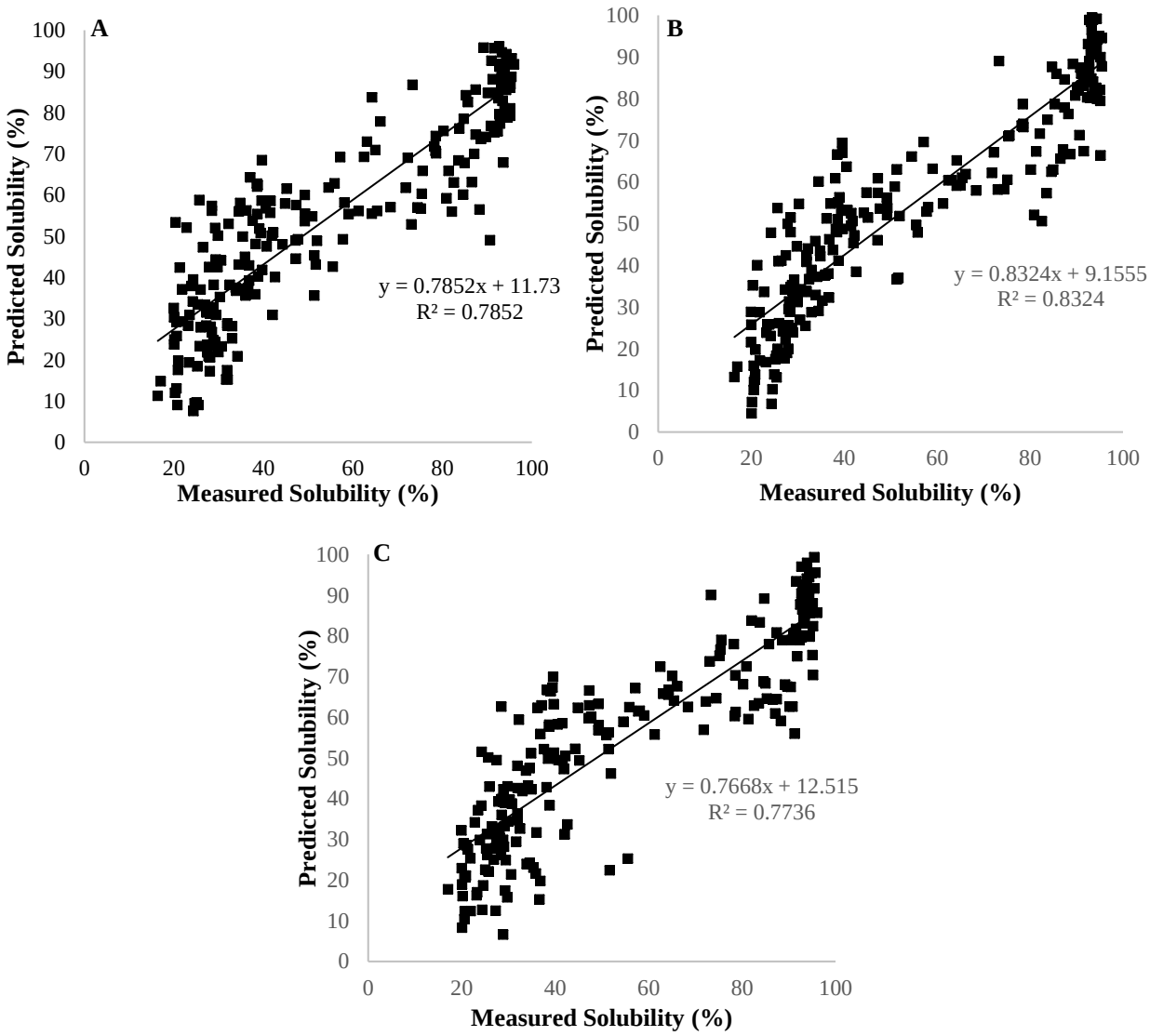

Figure 5.10 Partial least squares prediction model: measured vs. predicted solubility index (%) values plot for a cross-validation prediction of (A) tryptophan fluorescence spectra, (B) Maillard emission spectra, and (C) Maillard excitation spectra for the 7-factor model for the entire data set (n=220).

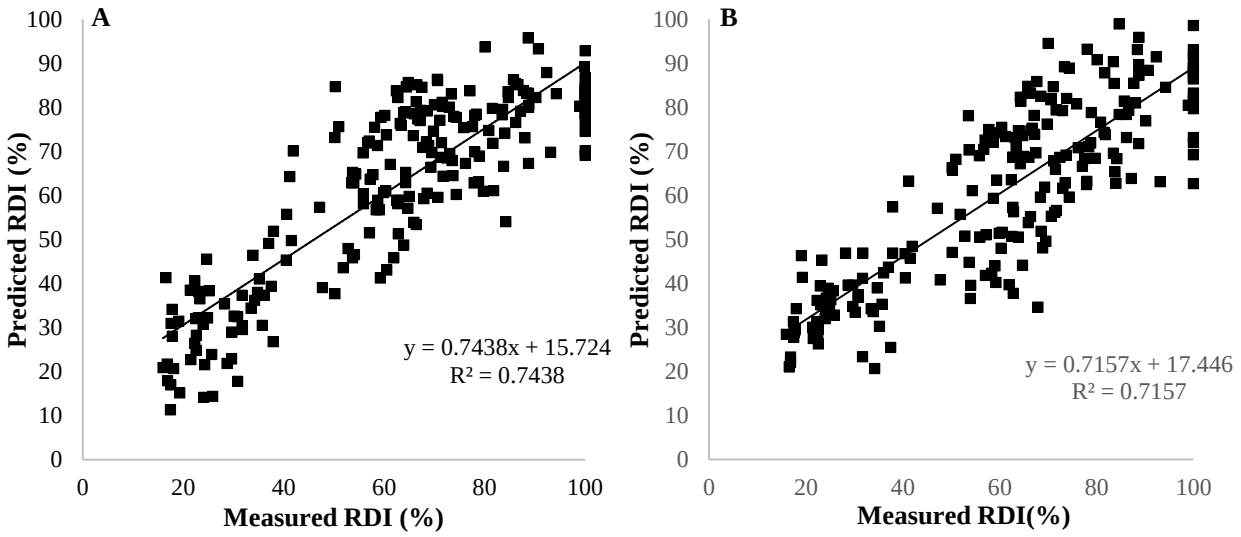

Figure 5.11 Partial least squares prediction model: measured vs. predicted relative solubility index (%) values as obtained from the focused beam reflectance measurement plot for a cross-validation prediction of (A) tryptophan fluorescence spectra and (B) Maillard emission spectra.

Table 5.3 Summary of partial least squares (PLS) predictions for solubility index and relative solubility using front-face fluorescence spectroscopy.

Measure attribute	Spectral attribute	Parameter	PLSR
Solubility index	Tryptophan emission fluorescence spectra	R^2	0.78
		RMSE	12.79
		RPD	2.16
	Maillard emission fluorescence spectra	R^2	0.83
		RMSE	11.30
		RPD	2.44
	Maillard excitation fluorescence spectra	R^2	0.76
		RMSE	13.64
		RPD	2.02
Relative solubility measured from FBRM	Tryptophan emission fluorescence spectra	R^2	0.74
		RMSE	12.38
		RPD	1.98
	Maillard emission fluorescence spectra	R^2	0.71
		RMSE	13.04
		RPD	1.88

Acknowledgments

We thank Midwest Dairy Foods Research Center (St. Paul, MN) for their financial support.

Conclusion

This study demonstrated that FFFS, coupled with chemometrics, has potential as a rapid technique to monitor variation in the MPC powders from different manufacturers and different protein contents. Biochemical reactions, such as modification of the tryptophan environment and Maillard reaction occurred during the manufacturing process of MPC powders and the subsequent storage of the samples at 40ºC have accelerated these reactions. Furthermore, this investigation underlines the potential of FFFS in combination with chemometrics as a fast and nondestructive method that can be applied to MPC powders for monitoring the storage changes. FFFS combined with PLSR was successfully used as a nondestructive technique to predict the solubility and dissolution charectierictics of MPC powders. The PLSR models using solubility index performed slightly better than the models using RDI. The fluorescence spectra of tryptophan and Maillard products were correlated to the MPC solubility index and RDI values. This correlation may be related to changes in the environment of tryptophan and formation of Maillard products because of the changes in the MPC system due to protein content, storage time, and storage temperature of MPC powders. The results suggest that FFFS has the potential to provide rapid, nondestructive, and accurate measurements of solubility characteristics of MPC powders.

References

Agarwal, S., R. L. Beausire, S. Patel and H. Patel. 2015. Innovative uses of milk protein concentrates in product development. J. Food Sci. 80. A23-A29.

Amamcharla, J. K. and L. E. Metzger. 2015. Prediction of process cheese instrumental texture and melting characteristics using dielectric spectroscopy and chemometrics. J. Dairy Sci. 98:6004-6013.

Andersen, C. M., and Mortensen, G. 2008. Fluorescence spectroscopy: A rapid tool for analyzing dairy products. J. Agric. Food Chem. 56:720-729.

Anema, S. G., D. N. Pinder, R. J. Hunter and Y. Hemar. 2006. Effects of storage temperature on the solubility of milk protein concentrate (MPC85). Food Hydrocoll. 20:386-393.

Augustin, M. A., P. Sanguansri, R. Williams and H. Andrews. 2012. High shear treatment of concentrates and drying conditions influence the solubility of milk protein concentrate powders. J. Dairy Res. 79:459-468.

Birlouez-Aragon, I., M. Nicolas, A. Metais, N. Marchond, J. Grenier and D. Calvo. 1998. A rapid fluorimetric method to estimate the heat treatment of liquid milk. Int. Dairy J. 8:771-777.

Birlouez-Aragon, I., P. Sabat, and N. Gouti. 2002. A new method for discriminating milk heat treatment. Int. Dairy J. 12:59-67.

Blecker, C., J. Habib-Jiwan and R. Karoui. 2012. Effect of heat treatment of rennet skim milk induced coagulation on the rheological properties and molecular structure determined by synchronous fluorescence spectroscopy and turbiscan. Food Chem. 135:1809-1817.

Boubellouta, T. and R. Dufour. 2008. Effects of mild heating and acidification on the molecular structure of milk components as investigated by synchronous front-face fluorescence spectroscopy coupled with parallel factor analysis. Appl. Spectrosc. 62:490-496.

Corredig, M. and D. G. Dalgleish. 1999. The mechanisms of the heat-induced interaction of whey proteins with casein micelles in milk. Int. Dairy J. 9:233-236.

Crowley, S. V., B. Desautel, I. Gazi, A. L. Kelly, T. Huppertz and J. A. O'Mahony. 2015. Rehydration characteristics of milk protein concentrate powders. J. Food Eng. 149:105-113.

Dufour, E., M. F. Devaux, P. Fortier, and S. Herbert. 2001. Delineation of the structure of soft cheeses at the molecular level by fluorescence spectroscopy—Relationship with texture. Int. Dairy J. 11:465-473.

Dufour, E., and Riaublanc, A. 1997. Potentiality of spectroscopic methods for the characterisation of dairy products. I. Front-face fluorescence study of raw, heated and homogenised milks. Le Lait. 77:657-670.

Fang, Y., S. Rogers, C. Selomulya and X. D. Chen. 2012. Functionality of milk protein concentrate: Effect of spray drying temperature. Biochem. Eng. J. 62:101-105.

Fang, Y., C. Selomulya, S. Ainsworth, M. Palmer, and X. D. Chen. 2011. On quantifying the dissolution behaviour of milk protein concentrate. Food Hydrocoll. 25:503-510.

Fyfe, K. N., O. Kravchuk, T. Le, H. C. Deeth, A. V. Nguyen and B. Bhandari. 2011. Storage induced changes to high protein powders: Influence on surface properties and solubility. J. Sci. Food Agric. 91:2566-2575.

Gaiani, C., P. Schuck, J. Scher, S. Desobry and S. Banon. 2007. Dairy powder rehydration: Influence of protein state, incorporation mode, and agglomeration. J. Dairy Sci. 90:570-581.

Gazi, I. and T. Huppertz. 2015. Influence of protein content and storage conditions on the solubility of caseins and whey proteins in milk protein concentrates. Int. Dairy J. 46:22-30.

Guyomarc'h, F., F. Warin, D. D. Muir, and J. Leaver. 2000. Lactosylation of milk proteins during the manufacture and storage of skim milk powders. Int. Dairy J. 10:863-872.

Hauser, M. and J. K. Amamcharla. 2016a. Development of a method to characterize high-protein dairy powders using an ultrasonic flaw detector. J. Dairy Sci. 99:1056-1064.

Hauser, M. and J. K. Amamcharla. 2016b. Novel methods to study the effect of protein content and dissolution temperature on the solubility of milk protein concentrate: Focused beam reflectance and ultrasonic flaw detector-based methods. J. Dairy Sci. 99:3334-3344.

Kamal, M. and R. Karoui. 2015. Analytical methods coupled with chemometric tools for determining the authenticity and detecting the adulteration of dairy products: A review. Trends Food Sci. Technol. 46:27-48.

Karoui, R., G. Mazerolles and E. Dufour. 2003. Spectroscopic techniques coupled with chemometric tools for structure and texture determinations in dairy products. Int. Dairy J. 13:607-620.

Karoui, R., Dufour, L. Pillonel, E. Schaller, D. Picque, T. Cattenoz and J. Bosset. 2005. The potential of combined infrared and fluorescence spectroscopies as a method of determination of the geographic origin of emmental cheeses. Int. Dairy J. 15:287-298.

Karoui, R., A. Mouazen, E. Dufour, R. Schoonheydt, and J. Baerdemaeker. 2006. A comparison and joint use of VIS-NIR and MIR spectroscopic methods for the determination of some chemical parameters in soft cheeses at external and central zones: A preliminary study. Eur. Food Res. Technol. 223:363-371.

Karoui, R., Dufour and J. De Baerdemaeker. 2007. Front face fluorescence spectroscopy coupled with chemometric tools for monitoring the oxidation of semi-hard cheeses throughout ripening. Food Chem. 101:1305-1314.

Karoui, R. and C. Blecker. 2011. Fluorescence spectroscopy measurement for quality assessment of food systems—a review. Food Bioproc. Tech. 4:364-386.

Kulmyrzaev, A., and E. Dufour. 2002. Determination of lactulose and furosine in milk using front-face fluorescence spectroscopy. Le Lait. 82:725-735.

Kulmyrzaev, A. A., Levieux, D., and Dufour, R. 2005. Front-face fluorescence spectroscopy allows the characterization of mild heat treatments applied to milk. relations with the denaturation of milk proteins. J. Agric. Food Chem. 53(3), 502-507.

Lakowicz, J. R. 2006. Principles of Fluorescence Spectroscopy. Third Edition. Springer, New York.

Le, T. T., B. Bhandari and H. C. Deeth. 2011. Chemical and physical changes in milk protein concentrate (MPC80) powder during storage. J. Agric. Food Chem. 59:5465-5473.

Lecle´re, J., and I. Birlouez-Aragon. 2001. The fluorescence of advanced Maillard products is a good indicator of lysine damage during the Maillard reaction. J. Agric. Food Chem. 49:4682-4687.

Liu, X. and L. E. Metzger. 2007. Application of fluorescence spectroscopy for monitoring changes in nonfat dry milk during storage. J. Dairy Sci. 90:24-37.

Liu, X., J. R. Powers, B. G. Swanson, H. H. Hill and S. Clark. 2005. Modification of whey protein concentrate hydrophobicity by high hydrostatic pressure. Innov. Food Sci. Emerg. Technol. 6:310-317.

Matiacevich, S. B., and M. P. Buera. 2006. A critical evaluation of fluorescence as a potential marker for the Maillard reaction. Food Chem. 95:423-430.

Mimouni, A., H. C. Deeth, A. K. Whittaker, M. J. Gidley and B. R. Bhandari. 2010. Investigation of the microstructure of milk protein concentrate powders during rehydration: Alterations during storage. J. Dairy Sci. 93:463-472.

Morales, F. J. and M. Van Boekel. 1998. A study on advanced maillard reaction in heated casein/sugar solutions: Colour formation. Int. Dairy J. 8:907-915.

Morales, F. J., C. Romero, and S. Jime´nez-Pe´rez. 1996. Fluorescence associated with Maillard reaction in milk and milk-resembling birlsystems. Food Chem. 57:423-428.

Moreaux, V. and I. Birlouez-Aragon. 1997. Degradation of tryptophan in heated β-lactoglobulin− lactose mixtures is associated with intense Maillard reaction. J. Agric. Food Chem. 45:1905-1910.

Ntakatsane, M. P., X. Q. Yang, M. Lin, X. M. Liu and P. Zhou. 2011. Suitability of fluorescence spectroscopy for characterization of commercial milk of different composition and origin. J. Dairy Sci. 94:5375-5380.

Richard, B., M. Toubal, J. Le Page, G. Nassar, E. Radziszewski, B. Nongaillard, P. Debreyne, P. Schuck, R. Jeantet and G. Delaplace. 2012. Ultrasound tests in a stirred vessel to evaluate the reconstitution ability of dairy powders. Innov. Food Sci. Emerg Technol. 16:233-242.

Shaikh, S. and C. O'Donnell. 2017. Applications of fluorescence spectroscopy in dairy processing: A review. Curr. Opin. Food Sci. 17:16-24.

Strasburg, G. M. and R. D. Ludescher. 1995. Theory and applications of fluorescence spectroscopy in food research. Trends Food Sci. Technol. 6:69-75.

Uluko, H., L. Liu, J. Lv and S. Zhang. 2016. Functional characteristics of milk protein concentrates and their modification. Crit. Rev. Food Sci. Nutr. 56:1193-1208.

Williams, P. C. 1987. Variables affecting near-infrared reflectance spectroscopic analysis. Pages 143-167 in Near-Infrared Technology in the Agricultural and Food Industries. P. Williams and K. Norris, ed. American Association of Cereal Chemists, St. Paul, MN.

Chapter 6 - Conclusions

Milk protein concentrate (MPC) powders are used as dairy ingredients in numerous food product formulations including beverages, high protein bars, ice cream, cheese, etc. to improve the nutritional, sensory, and functional properties of the finished product. However, there is a lack of fundamental understanding of the bulk flow and shear characteristics of MPC powders, especially its impacts during storage. Morphological and flow properties of MPC powders were investigated as a function of protein content and storage temperature. Knowledge of these characteristics is necessary for the design of handling and processing equipment and to understand their behavior during storage. Flowability of MPC powders having protein contents of 70, 80, and 90% (w/w) stored at 25 and 40ºC for 12 weeks were measured and characterized using the FT4 powder rheometer. The storage temperature and protein content significantly ($P < 0.05$) influenced the flowability of MPC powders. The higher protein concentration (80 and 90 %, w/w) of MPC powders and higher storage temperature (40ºC) have influenced the morphological characteristics such as circularity and elongation and consequently influenced their flow behavior. Dynamic flow tests indicated that MPC powders with high protein content displayed higher permeability. Shear tests confirmed that samples stored at 25ºC were more flowable than samples stored at 40ºC. Also, the higher protein content samples showed poor shear flow behavior. The results indicated that MPC powders stored at 25ºC had lesser cohesiveness and better flow characteristics than MPC powders stored at 40ºC.

The use of MPC powders is sometimes limited or reduced by their poor dissolution characteristics due to the formation of an inter-linked network of casein micelles at particle surfaces during processing and storage. Additionally, current methods available for characterizing the solubility of MPC powders are time-consuming, subjective, require expensive

equipment, and skilled operators. Therefore, front-face fluorescence spectroscopy (FFFS) based method was developed for the determination of rehydration behavior of MPC powders. The decrease in solubility index and relative dissolution index (RDI) displayed storage changes, and results indicated that the solubility of the MPC decreased as the storage time and temperature increased. Partial least square regression (PLSR) models were developed using the fluorescence spectra of tryptophan and Maillard products to predict the reference solubility index and RDI of MPC powders. The residual prediction deviation was >2 for solubility index and ~2 for RDI, indicating a potential practical utility of the statistical prediction models. FFFS coupled with PLSR could be a useful tool for the nondestructive measurement of functional properties in MPC powders. Future research with the FFFF can focus on using multilayer perceptron neural network to capture non-linear input/output relationships to develop a prediction model.

In the last decade, notable advances have been made in the examination of rehydration and flow characteristics in MPC powder, enabling improved understanding about reasons of their poor rehydration and impaired flow behavior. However, the specific explanations for factors influencing these properties of MPC powders are still evolving. Therefore, more mechanistic insights and systematic research are still needed to understand the influence of composition, processing, and storage conditions on MPC powders.

Appendix A – FT4 powder rheometer

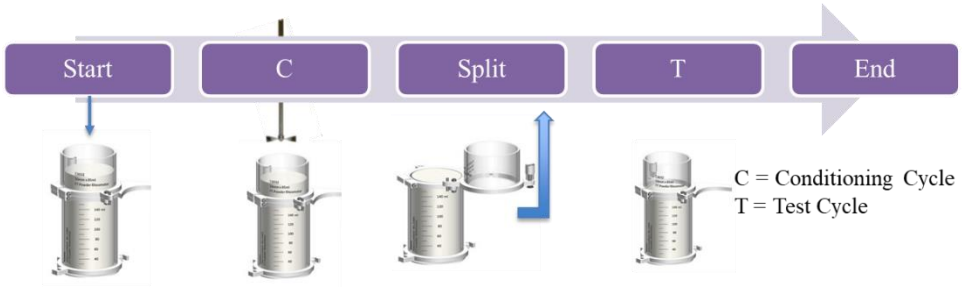

Figure A.1 Test sequence of flow measurement.

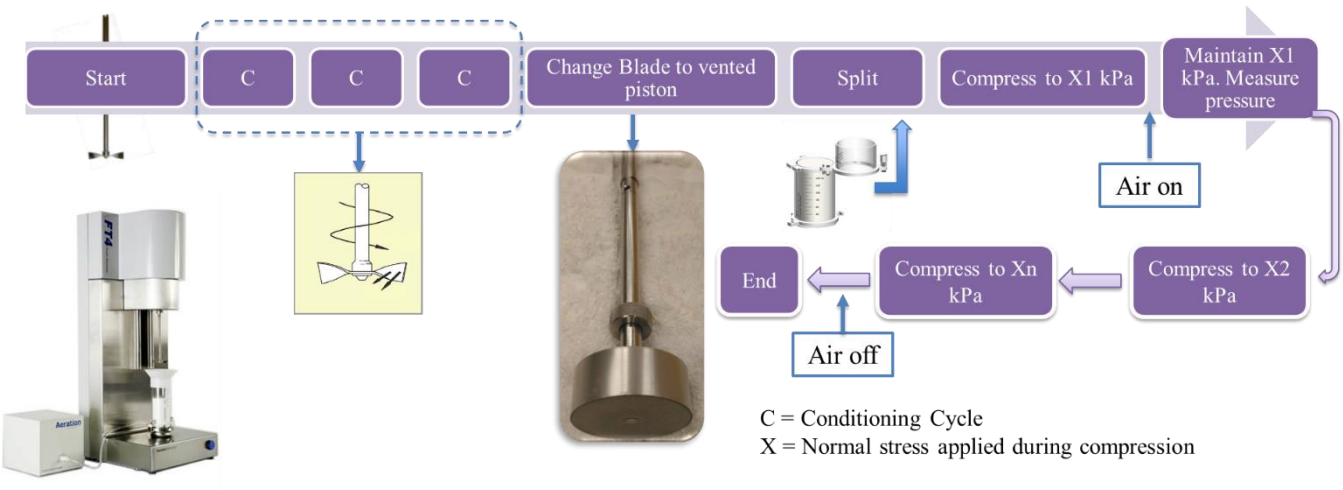

Figure A.2 Test sequence of permeability measurement.

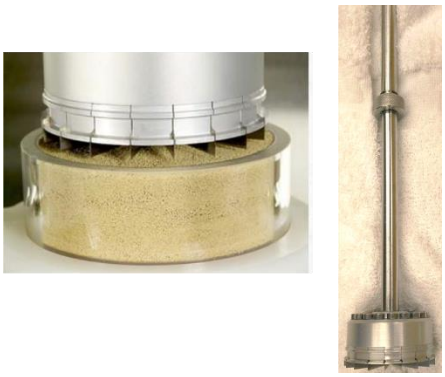

Figure A.3 Shear head for shear cell test.

Appendix B - SAS code for chapter 4

Solubility index (Sol)
Basic flow energy (BFE)
Stability index (SI)
Flow rate index (FRI)
Specific energy (SE)
Unconfined yield strength (UYS)
Cohesion (CH)
Angle of internal friction (AIF)
Flow function coefficient (FF)
Wall friction angle (WFA)
Circle equivalent diameter (CED)
High sensitivity circularity (HSC)
Elongation (EL)
Convexity (CX)

```
/*A. Only for 25C */
data onet;
input Lot$ Type$ Rep$ Sol BFE SI FRI SE UYS CH AIF FF WFA CED HSC EL CX;
datalines;
1      70    1      88.28 522.42      0.995912    1.535105    18.87028
       2.5825605   0.586780346 34.601805   6.0623275   25.17677    13.45 0.872
       0.2   0.992
2      70    2      90.01 497.77      1.096019    1.505209    18.97897
       2.57126605  0.5771235   34.511703   6.065215    25.16677    13.58 0.877
       0.192 0.992
3      80    1      78.2  700.1 0.9708293   1.526301    22.64437    2.698123
       0.63827125  34.96065667 5.91542233  24.76938667 17.18 0.873 0.187 0.988
4      80    2      80.21 690.08      0.984485    1.626029    25.64393
       2.53971233  0.623823633 34.970318   5.931442233 24.66938667 16.94 0.875
       0.186 0.988
5      90    1      51.39 929.21      0.9463021   1.7365854   24.09842
       3.120583667 0.752214267 40.38654    5.242435667 24.25094333 22.85 0.831
       0.227 0.981
6      90    2      50.11 932.3 0.9490278   1.701341    24.77325    3.13058
       0.7523031   40.37763333 5.342435667 24.28509433 22.85 0.831 0.227 0.981

;
run;
proc print data=onet;
run;
proc glimmix data=onet;
* GLIMMIX for everything else;
class Type;
model Sol = Type/solution;
lsmeans Type/ pdiff adjust=tukey cl plot=meanplot(ascending cl);
output out=residuals residual=residual predicted=predicted;
run;
proc glimmix data=onet;
* GLIMMIX for everything else;
class Type;
```

```
model BFE = Type/solution;
lsmeans Type/cl pdiff adjust=tukey plot=meanplot(ascending cl);
output out=residuals residual=residual predicted=predicted;
run;

proc glimmix data=onet;
* GLIMMIX for everything else;
class Type;
model SI = Type/solution;
lsmeans Type/ pdiff adjust=tukey cl plot=meanplot(ascending cl);
output out=residuals residual=residual predicted=predicted;
run;
proc glimmix data=onet;
* GLIMMIX for everything else;
class Type;
model FRI = Type/solution;
lsmeans Type/ pdiff adjust=tukey cl plot=meanplot(ascending cl);
output out=residuals residual=residual predicted=predicted;
run;
proc glimmix data=onet;
* GLIMMIX for everything else;
class Type;
model SE = Type/solution;
lsmeans Type/ pdiff adjust=tukey cl plot=meanplot(ascending cl);
output out=residuals residual=residual predicted=predicted;
run;
proc glimmix data=onet;
* GLIMMIX for everything else;
class Type;
model UYS = Type/solution;
lsmeans Type/ pdiff adjust=tukey cl plot=meanplot(ascending cl);
output out=residuals residual=residual predicted=predicted;
run;
proc glimmix data=onet;
* GLIMMIX for everything else;
class Type;
model CH = Type/solution;
lsmeans Type/ pdiff adjust=tukey cl plot=meanplot(ascending cl);
output out=residuals residual=residual predicted=predicted;
run;
proc glimmix data=onet;
* GLIMMIX for everything else;
class Type;
model AIF = Type/solution;
lsmeans Type/ pdiff adjust=tukey cl plot=meanplot(ascending cl);
output out=residuals residual=residual predicted=predicted;
run;
proc glimmix data=onet;
* GLIMMIX for everything else;
class Type;
model FF = Type/solution;
lsmeans Type/ pdiff adjust=tukey cl plot=meanplot(ascending cl);
output out=residuals residual=residual predicted=predicted;
run;
proc glimmix data=onet;
* GLIMMIX for everything else;
class Type;
```

```
model WFA = Type/solution;
lsmeans Type/ pdiff adjust=tukey cl plot=meanplot(ascending cl);
output out=residuals residual=residual predicted=predicted;
run;
proc glimmix data=onet;
* GLIMMIX for everything else;
class Type;
model CED = Type/solution;
lsmeans Type/ pdiff adjust=tukey cl plot=meanplot(ascending cl);
output out=residuals residual=residual predicted=predicted;
run;
proc glimmix data=onet;
* GLIMMIX for everything else;
class Type;
model HSC = Type/solution;
lsmeans Type/ pdiff adjust=tukey cl plot=meanplot(ascending cl);
output out=residuals residual=residual predicted=predicted;
run;
proc glimmix data=onet;
* GLIMMIX for everything else;
class Type;
model EL = Type/solution;
lsmeans Type/ pdiff adjust=tukey cl plot=meanplot(ascending cl);
output out=residuals residual=residual predicted=predicted;
run;
proc glimmix data=onet;
* GLIMMIX for everything else;
class Type;
model CX = Type/solution;
lsmeans Type/ pdiff adjust=tukey cl plot=meanplot(ascending cl);
output out=residuals residual=residual predicted=predicted;
run;

/*B. Compare both 20C and 40C */
data twot;
input Lot$ Type$ Temp$ Rep$ Sol BFE SI FRI SE UYS     CH AIF FF WFA CED HSC
EL CX;*Composition*;
datalines;
1      70    25    1      88.28 522.42       0.995912    1.535105    18.87028
       2.5825605   0.586780346 34.601805   6.0623275   25.17677    13.45 0.872
       0.2   0.992
2      70    25    2      90.01 497.77       1.096019    1.505209    18.97897
       2.57126605  0.5771235   34.511703   6.065215    25.16677    13.58 0.877
       0.192 0.992
3      70    40    1      38.82 522.13       1.014405    1.542751    18.41004
       2.792785    0.61419285  36.28373    5.729603    24.999485   14.12 0.888
       0.178 0.991
4      70    40    2      39.82 502.92       1.089497    1.439659    18.27676
       2.6802511   0.621328385 36.294835   5.730123    24.899485   14.12 0.893
       0.177 0.991
5      80    25    1      78.2  700.1 0.9708293   1.526301    22.64437
       2.698123    0.63827125  34.96065667 5.91542233  24.76938667 17.18 0.873
       0.187 0.988
6      80    25    2      80.21 690.08       0.984485    1.626029    25.64393
       2.53971233  0.623823633 34.970318   5.931442233 24.66938667 16.94 0.875
       0.186 0.988
```

```
7       80      40      1       31.68   607.36          0.9235415       1.580815        21.43836
        2.971405        0.73193805      37.625605       5.151509        24.477585       14.71 0.893
        0.171 0.992
8       80      40      2       33.63   627.38          1.04549         1.624467        22.57268
        2.982115        0.72283805      37.634713       5.161509        24.457585       15.41 0.891
        0.172 0.991
9       90      25      1       51.39   929.21          0.9463021       1.7365854       24.09842
        3.120583667     0.752214267     40.38654        5.242435667     24.25094333     22.85 0.831
        0.227 0.981
10      90      25      2       50.11   932.3   0.9490278       1.701341        24.77325
        3.13058         0.7523031       40.37763333     5.342435667     24.28509433     22.85 0.831
        0.227 0.981
11      90      40      1       24.61   720.3   0.9928277       1.7205233       23.87152
        3.3549325       0.82669531      41.335633       4.94056         23.875725       19.63 0.877
        0.178 0.988
12      90      40      2       23.77   724.61          0.9620942       1.7297424       23.98403
        3.1348122       0.816768411     41.364525       4.8914814       23.8275725      19.73 0.882
        0.185 0.988

;
run;
proc print data=twot;
run;
proc glimmix data=twot;
* GLIMMIX for everything else;
class Type Temp;
model Sol = Type Temp Type*Temp/solution;
lsmeans Type Temp Type*Temp/cl plot=meanplot(ascending cl);
output out=residuals residual=residual predicted=predicted;
run;
proc glimmix data=twot;
* GLIMMIX for everything else;
class Type Temp;
model BFE = Type Temp Type*Temp/solution;
lsmeans Type Temp Type*Temp/cl plot=meanplot(ascending cl);
output out=residuals residual=residual predicted=predicted;
run;
proc glimmix data=twot;
* GLIMMIX for everything else;
class Type Temp;
model SI = Type Temp Type*Temp/solution;
lsmeans Type Temp Type*Temp/cl plot=meanplot(ascending cl);
output out=residuals residual=residual predicted=predicted;
run;
proc glimmix data=twot;
* GLIMMIX for everything else;
class Type Temp;
model FRI = Type Temp Type*Temp/solution;
lsmeans Type Temp Type*Temp/cl plot=meanplot(ascending cl);
output out=residuals residual=residual predicted=predicted;
run;
proc glimmix data=twot;
* GLIMMIX for everything else;
class Type Temp;
model SE = Type Temp Type*Temp/solution;
lsmeans Type Temp Type*Temp/cl plot=meanplot(ascending cl);
output out=residuals residual=residual predicted=predicted;
```

```
run;
proc glimmix data=twot;
* GLIMMIX for everything else;
class Type Temp;
model UYS = Type Temp Type*Temp/solution;
lsmeans Type Temp Type*Temp/cl plot=meanplot(ascending cl);
output out=residuals residual=residual predicted=predicted;
run;
proc glimmix data=twot;
* GLIMMIX for everything else;
class Type Temp;
model CH = Type Temp Type*Temp/solution;
lsmeans Type Temp Type*Temp/cl plot=meanplot(ascending cl);
output out=residuals residual=residual predicted=predicted;
run;
proc glimmix data=twot;
* GLIMMIX for everything else;
class Type Temp;
model AIF = Type Temp Type*Temp/solution;
lsmeans Type Temp Type*Temp/cl plot=meanplot(ascending cl);
output out=residuals residual=residual predicted=predicted;
run;
proc glimmix data=twot;
* GLIMMIX for everything else;
class Type Temp;
model FF = Type Temp Type*Temp/solution;
lsmeans Type Temp Type*Temp/cl plot=meanplot(ascending cl);
output out=residuals residual=residual predicted=predicted;
run;
proc glimmix data=twot;
* GLIMMIX for everything else;
class Type Temp;
model WFA = Type Temp Type*Temp/solution;
lsmeans Type Temp Type*Temp/cl plot=meanplot(ascending cl);
output out=residuals residual=residual predicted=predicted;
run;
proc glimmix data=twot;
* GLIMMIX for everything else;
class Type Temp;
model CED = Type Temp Type*Temp/solution;
lsmeans Type Temp Type*Temp/cl plot=meanplot(ascending cl);
output out=residuals residual=residual predicted=predicted;
run;
proc glimmix data=twot;
* GLIMMIX for everything else;
class Type Temp;
model HSC = Type Temp Type*Temp/solution;
lsmeans Type Temp Type*Temp/cl plot=meanplot(ascending cl);
output out=residuals residual=residual predicted=predicted;
run;
proc glimmix data=twot;
* GLIMMIX for everything else;
class Type Temp;
model EL = Type Temp Type*Temp/solution;
lsmeans Type Temp Type*Temp/cl plot=meanplot(ascending cl);
output out=residuals residual=residual predicted=predicted;
run;
```

```
proc glimmix data=twot;
* GLIMMIX for everything else;
class Type Temp;
model CX = Type Temp Type*Temp/solution;
lsmeans Type Temp Type*Temp/cl plot=meanplot(ascending cl);
output out=residuals residual=residual predicted=predicted;
run;

/*C. Only for 40C */
data onet;
input Lot$ Type$ Rep$ Sol BFE SI FRI SE UYS     CH AIF FF WFA CED HSC EL CX;
datalines;
1      70    1      38.82 522.13       1.014405    1.542751    18.41004
       2.792785    0.61419285  36.28373    5.729603    24.999485   14.12 0.888
       0.178 0.991
2      70    2      39.82 502.92       1.089497    1.439659    18.27676
       2.6802511   0.621328385 36.294835   5.730123    24.899485   14.12 0.893
       0.177 0.991
3      80    1      31.68 607.36       0.9235415   1.580815    21.43836
       2.971405    0.73193805  37.625605   5.151509    24.477585   14.71 0.893
       0.171 0.992
4      80    2      33.63 627.38       1.04549     1.624467    22.57268
       2.982115    0.72283805  37.634713   5.161509    24.457585   15.41 0.891
       0.172 0.991
5      90    1      24.61 720.3 0.9928277   1.7205233   23.87152    3.3549325
       0.82669531  41.335633   4.94056     23.875725   19.63 0.877 0.178 0.988
6      90    2      23.77 724.61       0.9620942   1.7297424   23.98403
       3.1348122   0.816768411 41.364525   4.8914814   23.8275725  19.73 0.882
       0.185 0.988

;
run;
proc print data=onet;
run;
proc glimmix data=onet;
* GLIMMIX for everything else;
class Type;
model Sol = Type/solution;
lsmeans Type/ pdiff adjust=tukey cl plot=meanplot(ascending cl);
output out=residuals residual=residual predicted=predicted;
run;
proc glimmix data=onet;
* GLIMMIX for everything else;
class Type;
model BFE = Type/solution;
lsmeans Type/cl pdiff adjust=tukey plot=meanplot(ascending cl);
output out=residuals residual=residual predicted=predicted;
run;

proc glimmix data=onet;
* GLIMMIX for everything else;
class Type;
model SI = Type/solution;
lsmeans Type/ pdiff adjust=tukey cl plot=meanplot(ascending cl);
output out=residuals residual=residual predicted=predicted;
run;
proc glimmix data=onet;
```

```
* GLIMMIX for everything else;
class Type;
model FRI = Type/solution;
lsmeans Type/ pdiff adjust=tukey cl plot=meanplot(ascending cl);
output out=residuals residual=residual predicted=predicted;
run;
proc glimmix data=onet;
* GLIMMIX for everything else;
class Type;
model SE = Type/solution;
lsmeans Type/ pdiff adjust=tukey cl plot=meanplot(ascending cl);
output out=residuals residual=residual predicted=predicted;
run;
proc glimmix data=onet;
* GLIMMIX for everything else;
class Type;
model UYS = Type/solution;
lsmeans Type/ pdiff adjust=tukey cl plot=meanplot(ascending cl);
output out=residuals residual=residual predicted=predicted;
run;
proc glimmix data=onet;
* GLIMMIX for everything else;
class Type;
model CH = Type/solution;
lsmeans Type/ pdiff adjust=tukey cl plot=meanplot(ascending cl);
output out=residuals residual=residual predicted=predicted;
run;
proc glimmix data=onet;
* GLIMMIX for everything else;
class Type;
model AIF = Type/solution;
lsmeans Type/ pdiff adjust=tukey cl plot=meanplot(ascending cl);
output out=residuals residual=residual predicted=predicted;
run;
proc glimmix data=onet;
* GLIMMIX for everything else;
class Type;
model FF = Type/solution;
lsmeans Type/ pdiff adjust=tukey cl plot=meanplot(ascending cl);
output out=residuals residual=residual predicted=predicted;
run;
proc glimmix data=onet;
* GLIMMIX for everything else;
class Type;
model WFA = Type/solution;
lsmeans Type/ pdiff adjust=tukey cl plot=meanplot(ascending cl);
output out=residuals residual=residual predicted=predicted;
run;
proc glimmix data=onet;
* GLIMMIX for everything else;
class Type;
model CED = Type/solution;
lsmeans Type/ pdiff adjust=tukey cl plot=meanplot(ascending cl);
output out=residuals residual=residual predicted=predicted;
run;
proc glimmix data=onet;
* GLIMMIX for everything else;
```

```
class Type;
model HSC = Type/solution;
lsmeans Type/ pdiff adjust=tukey cl plot=meanplot(ascending cl);
output out=residuals residual=residual predicted=predicted;
run;
proc glimmix data=onet;
* GLIMMIX for everything else;
class Type;
model EL = Type/solution;
lsmeans Type/ pdiff adjust=tukey cl plot=meanplot(ascending cl);
output out=residuals residual=residual predicted=predicted;
run;
proc glimmix data=onet;
* GLIMMIX for everything else;
class Type;
model CX = Type/solution;
lsmeans Type/ pdiff adjust=tukey cl plot=meanplot(ascending cl);
output out=residuals residual=residual predicted=predicted;
run;
```